Functional and Molecular Characterisation of Mesenchymal Stem Cells Derived From Bone Marrow and Dental Tissues

Danijela Menicanin

Mesenchymal Stem Cell Research Group
Bone and Cancer Research Laboratory
Division of Haematology
Hanson Institute
Institute of Medical and Veterinary Sciences
SA Pathology

and

Colgate Australian Clinical Dental Research Centre
School of Dentistry
Faculty of Health Sciences
University of Adelaide

A thesis submitted to the University of Adelaide
for the degree of Doctor of Philosophy
June 2010

Chapter 1:

Introduction

1. Introduction

1.1. Stem Cells

The defining features of stem cells include a capacity to self renew, undergo extensive proliferation and the potential to reproducibly differentiate into functional cells indicative of several different lineages. To date, three types of stem cells have been identified; embryonic stem cells, adult stem cells and more recently, through genetic manipulation, induced pluripotent stem cells. Embryonic stem cells (ESC) are totipotent cells derived from the early mammalian embryo and as such have the ability to proliferate extensively and differentiate into cells with features of all three embryonic germ layers [1-3]. Induced pluripotent stem cells (iPSC) are ESC-like cells, comparable to ESC in terms of their morphology, gene expression profiles, proliferation and differentiation capacities [4, 5]. Although ESC and iPS cells have immense potential in cell based therapeutic applications, there are numerous challenges and limitations associated with their use. Other than the ethical considerations in relation to derivation, maintenance and manipulation of ESCs [6, 7], major obstacles associated with their use include difficulty in controlling directed differentiation and inhibition of growth. Furthermore, ESCs and iPSCs both carry tumour-producing properties which result in formation of teratomas, hence raising a significant safety challenge in the use of these cells for regenerative medicine [8, 9]. Adult, somatic or postnatal stem cells reside amongst differentiated cells within a number of organs in the body where they play a role in tissue maintenance, renewal and repair. Whilst these cells exhibit limited proliferation and differentiation potential, they are easily accessible, immunocompatible and are not associated with ethical issues in relation to their use.

1.1.1. Adult Stem Cells Derived From Bone Marrow

Bone marrow consists of three main cellular systems, haematopoietic, endothelial and stromal [10]. These systems are derived from at least three different stem cell populations present in the bone marrow: haematopoietic stem cells (HSCs) that give rise to blood cells; endothelial precursor cells, known as angioblasts; and different stromal populations derived from bone marrow stromal/stem cells (BMSC) [11-13]. HSCs have been successfully isolated and clinically applied for the treatment of various haematological disorders. The therapeutic potential of angioblasts has also been explored for treatment of

cardiovascular disease [14]. It has been shown that angioblasts, or endothelial progenitor cells, have the capacity to differentiate into endothelial lineage cells *in vitro*, and to incorporate into active sites of neovascularisation in animal models [14]. The possible clinical applications of angioblasts can be divided into neo-vascularisation of ischemic tissue or endothelialisation of denuded endothelium and vascular grafts [15].

In 1974, Patt and Maloney assessed bone marrow regenerative programs using a mechanically depleted medullary cavity of rabbit femurs as an experimental model [16]. They found that the reconstruction of bone marrow involves an initial period of reorganisation followed by a prolonged period of haemic cell repopulation, with completion of the process occurring several weeks post marrow depletion. Several well-defined transitions identified in this process were, formation of granulation tissue, emergence of connective tissue and vasculature and finally transient invasion of the cavity by trabecular bone to restore the sinusoidal marrow. It was thought that undifferentiated stromal cells played a major role in initiating the regenerative processes. Furthermore, it was realised that stem cells of stromal origin were responsible for the regeneration of the marrow matrix, whilst giving support to haematopoietic stem cells responsible for the support and maintenance of haematopoietic activity [16]. Following on from studies by Friedenstein and Kuralesova, this work supported the concept of the co-existence of haematopoietic and stromal stem cells as independent lines of precursors, working together to regenerate the bone marrow microenvironment [17,18]. Traditionally, BMSC have been studied based on their pivotal role in the formation of the haematopoietic microenvironment (HME) that supports and regulates HSC that give rise to leukocytes and erythrocytes. BMSC provide physical support for HSC by giving rise to supportive stroma that constitutes the HME, including production of matrix molecules, expression of ligands for surface molecules expressed by cells of haematopoietic lineage and activation of leukocyte cell adhesion molecule, as well as secretion of cytokines important for HSC differentiation [19-22].

More recently, interest in BMSC has arisen because of their potential therapeutic applications [23]. Whilst it is clear that BMSCs have great potential in cell based tissue engineering applications, some of the technical issues which need to be addressed in future research include identification and isolation of optimal precursor cell types, establishment

of optimal growth and differentiation conditions *in vitro* and design of biocompatible delivery vehicles for the *in vivo* transplantation of BMSC [24].

1.1.2. Mesenchymal Stem Cells (MSCs)

Mesenchymal stem cells (MSCs) are a heterogeneous mix of progenitors, where subset populations are capable of differentiating into cells of mesodermal (adipocytes, osteoblasts, chondrocytes, tenocytes, skeletal myocytes and visceral stromal cells) [12, 13, 25-28], ectodermal (neurons, astrocytes) [29] and endodermal (hepatocytes) [30] origins. MSC demonstrate a lower developmental potential and shorter life span [31] than totipotent embryonic stem cells, which have the ability to proliferate indefinitely *in vitro* and the potential to differentiate into all cell types present in the body [32, 33].

Clonogenic bone marrow derived, plastic adherent cells were first referred to as colony-forming unit fobroblast (CFU-F) by Friedenstein [34, 35], and were later termed bone marrow stromal cells and stromal precursor cells, and mesenchymal stem cells [36]. To address the inconsistency in nomenclature and account for the biologic properties of multipotential, clonogenic, plastic adherent cells derived from various stromal tissues, the committee for the International Society for Cellular Therapy has clarified that the use of acronym MSC may be applied to both, multipotent mesenchymal stromal cells (fibroblast-like, plastic adherent cells, regardless of their tissue of origin) and mesenchymal stem cells (cells that meet specific stem cell criteria) [37, 38].

Initial studies identified clonogenic MSCs from bone marrow aspirates, spleen and thymus [34, 35]. Subsequent studies have identified MSC-like cells from trabecular bone, periosteum, articular cartilage, synovium, synovial fluid, skeletal muscle, adipose tissue [39], tendons, blood [40], blood vessels, dental tissues [24, 41], umbilical cord vasculature [42], placental tissue [43, 44] fetal tissues [45, 46] and skin [47]. However, the developmental relationship between these different MSC-like populations has yet to be determined. Additionally, mesenchymal precursors have been derived through controlled differentiation of human ESCs [48-51] and human iPS cells [52].

Figure 1.1 A Hypothetical Diagram of the Cellular Differentiation Hierarchy of the Stromal System (adapted from Friedenstein *Exp Haematology 1978*).

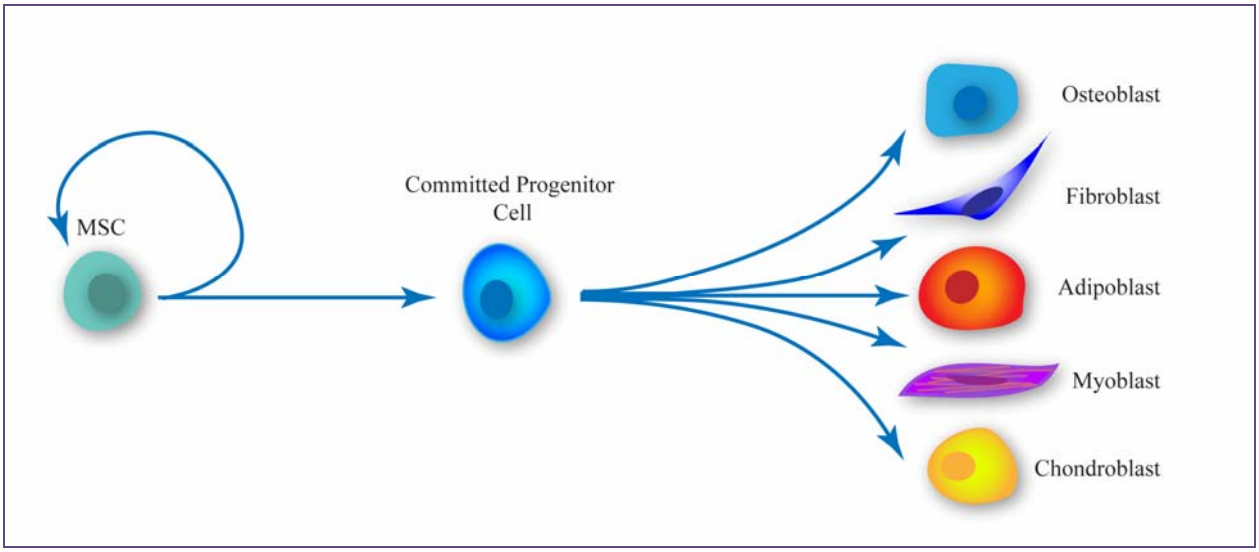

1.1.2.1. Isolation and Identification of BMSCs

BMSCs are isolated from bone marrow cells by utilising their capacity to adhere to plastic and undergo clonogenic growth *in vitro* (CFU-F: colony forming unit-fibroblastic). Furthermore, these cells exhibit the ability for extensive proliferation in culture, maintain the expression of specific cell surface marker proteins and demonstrate the potential to differentiate into multiple cell lineages [12, 53]. Initial isolation techniques, based on plastic adherence, generated significant heterogeneity within the MSC populations and introduced contamination with other cell types, hence other methods of selection were necessary to isolate well characterised MSC subpopulations. In order to achieve this, immunophenotypic features characterising these cells were utilized in the development of selection and isolation protocols. MSC surface expression profiles were investigated to identify unique markers to distinguish subsets within these cell populations.

A study by Simmons and Torok-Storb (1991) reported the generation of a novel murine IgM monoclonal antibody marker, STRO-1, that identifies a cell surface antigen expressed by stromal elements in human bone marrow including CFU-F forming cells, whilst not reacting with committed HSC and blood progenitor cells [54]. A study by Gronthos *et al* showed that cells positive for STRO-1 are capable of differentiating into functional osteoblasts and as such are termed osteoprogenitors. They also showed that approximately 50% of the CFU-F examined showed the capacity to differentiate into cells of adipogenic

as well as osteogenic lineage [55]. Subsequent studies have determined that STRO-1^+ BMSCs demonstrate the potential to differentiate into multiple stromal cell lineages including, smooth muscle cells, myelosupportive stroma, adipocytes, osteoblasts and chondrocytes [12, 56, 57]. Moreover, MSCs derived from bone marrow and dental pulp tissues were found to express CD146 [58], a cell adhesion molecule previously detected on smooth muscle cells, endothelial cells, myfibroblasts and Schwann cells [59]. Shi and Gronthos used an antibody to CD146 in combination with STRO-1 to isolate and purify a distinct population within bone marrow and dental pulp derived MSCs [58]. Correspondingly, Sacchetti and colleagues demonstrated high levels of CD146 expression in clonogenic cell populations derived from human bone marrow. Their study illustrated that CD146 identified all *ex vivo* assayable CFU-Fs which, upon further characterisation, exhibited extensive self-renewal capacity and multipotency [60].

Moreover, Gronthos and colleagues isolated a highly clonogenic population of MSC derived from the bone marrow, using STRO-1 and an antibody directed against CD106/VCAM-1 [12], a vascular cell adhesion molecule previously reported to be constitutively expressed by marrow stromal tissue [54, 61]. Similar studies isolated clonogenic murine BMSC based on their expression of CD106 and other markers [62]. Earlier studies demonstrated that stroma-initiating cells (SIC) residing in the mouse bone marrow were present in the lineage negative (Lin^-) sub-population [63]. Further investigation of Lin^- cell fraction was based on the expression studies of various markers including c-fms (M-CSF (macrophage - colony stimulating factor) receptor) [64, 65], c-kit (receptor for stem cell factor)[66] and VCAM-1[67]. These results highlighted enrichment of SICs in the Lin^-c-fms^+c-kit^{low}VCAM-1^+ populations [62].

The expression of D7-FIB, a marker of human fibroblasts, was identified in human mesenchymal progenitor cells derived from the bone marrow and used in the isolation of cells that exhibited oseto-, adipo- and chondrogenic differentiation potential [68].
Studies conducted by Deschaseaux and colleagues identified that primate and human mesenchymal precursor cells isolated from the bone marrow express CD49a, a molecule of the α1-integrin subunit of the very late antigen (VLA) integrin, and further showed that BMSCs isolated using CD49a exhibited properties of STRO-1 positive cells [69, 70]. Furthermore, Gronthos *et al* showed that clonogenic BMSC are present in the CD49a,$CD29^+$/STRO-1^{bright} fraction of human bone marrow [71].

Following on from previous isolation of CD105 (endoglin) positive cells, that exhibited capacity to form bone and cartilage *in vivo* [72], Kastrinaki *et al* confirmed that BMSCs expressing CD105, generally present on endothelial cells, represent a population enriched in immature stem cells [73]. However, endoglin, an ancillary TGF-β receptor, is also present on HSC, as demonstrated by Chen and colleagues who showed that the endoglin$^+$ cell fraction contains all long term repopulating (LTR) HSCs in mouse bone marrow. They further suggested that, due to its high specificity, endoglin may be used as a HSC marker to obtain near-homogenous populations of LTR-HSCs in enrichment protocols of cells isolated from mouse bone marrow [74].

Gronthos *et al* identified a novel monoclonal antibody, STRO-3, which recognises a unique epitope found on the extracellular domain of tissue non specific alkaline phosphatase that co-expressed with STRO-1 [75]. This antibody was used to isolate a population of human mesenchymal precursor cells of high proliferative potential with the ability to differentiate into bone, cartilage and adipose lineages [75]. More recently, a monoclonal antibody reagent, STRO-4, which recognises cell surface protein Hsp90β has been identified as a potential selection agent of ovine and human mesenchymal precursor cells with extensive proliferative potential and tri-potential differentiation capacity [76]. In addition to the above mentioned studies, BMSC have been found to express CD10, CD13 CD44, CD71, CD73 (ecto 5'nucleotidase), CD90 (Thy-1), CD166 (ALCAM), ICAM and others [68, 77-82].

1.1.2.2. Adult MSC-like Cells Derived from Dental Tissues

The human tooth is composed of various mineralised components (enamel, dentin and cementum), and a fibrous pulp tissue formed during development as a result of reciprocal interactions between the dental epithelium and neural crest cell-derived ectomesenchyme. This process is initiated by the dental epithelium and includes five distinct morphological stages: bud, cap, bell, crown and root [83-88]. The tooth supporting structure, the periodontium, is comprised of the periodontal ligament, cementum, and alveolar bone which begins to form at the bell stage [89, 90]. Together the tooth and the periodontium form a functional unit, embedded in the alveolar bone of the maxilla or the mandible [89].

Following tooth development, periodontal and dental tissues with the exception of enamel, exhibit limited regenerative or reparative capacity [91] which is thought to be mediated by the presence of multipotent progenitor cells that are capable of differentiation into functional, lineage specific cells [92-95].

In dental structures, MSC-like cells have been obtained from the dental pulp of adult and exfoliated deciduous teeth as well as periodontal ligament [24, 41, 96]. Characterisation of cells residing in dental pulp and periodontal ligament tissues has shown that these cells exhibit similar features to that described for BMSCs [24, 41, 96], by their potential to differentiate into mineral and fat producing cells. Furthermore, dental pulp derived cells exhibit the capacity to form dentin-pulp-like structures *in vivo* [97], whilst cells derived from the periodontal ligament exhibited the potential to generate cementum/PDL-like tissue [41] (**Figure 1.2**). Based upon these findings dental pulp and periodontal ligament derived stem cells are now being considered as candidate cell types to be used in various tissue engineering approaches for the regeneration of dental structures.

1.1.2.2.1. Isolation and Identification of MSC-like Cells Derived from Dental Pulp

Dental pulp is a fibrous connective tissue occupying the central portion of the root enclosed by dentin (**Figure 1.3**). It has a major role in the support of dentin and participates in dentin formation as well as housing the nerves and the blood vessels of the tooth [98, 99]. Dental pulp is involved in regenerative responses to injury caused by dental caries, attrition, abrasion, erosion, trauma, dental restorative procedures and materials [100-106]. The response reaction largely results in hard tissue formation mainly as focal deposition of tertiary dentine matrix beneath the site of injury. This process consequently leads to an increase of the distance between the injury site and the pulpal cells and formation of a protection barrier as well as a hard tissue base for subsequent restoration. In cases of mild tooth injury, odontoblasts are able to survive the challenge and are stimulated to produce a reactionary dentine matrix focally at the pulp-dentine interface beneath the injury site [107]. However, in cases of severe tooth injury, odontoblasts directly beneath the injury site may die and immature odontoblast-like pulp cells may differentiate and secrete the reparative dentine matrix [108]. Clinically, it is considered that both the reactionary and the reparative response are present during different stages of injury and repair process [109].

Figure 1.2 Developmental Potential of MSCs Derived from the Bone Marrow, Dental Pulp and Periodontal Ligament Tissues *In Vivo*.

BMSCs exhibit the capacity to form bone/marrow structures *in vivo*. DPSCs exhibit the potential to generate dentin-pulp like-complexes, whilst PDLSCs exhibit the capacity to form cementum/PDL-like structures *in vivo* [24, 41].

Figure 1.2

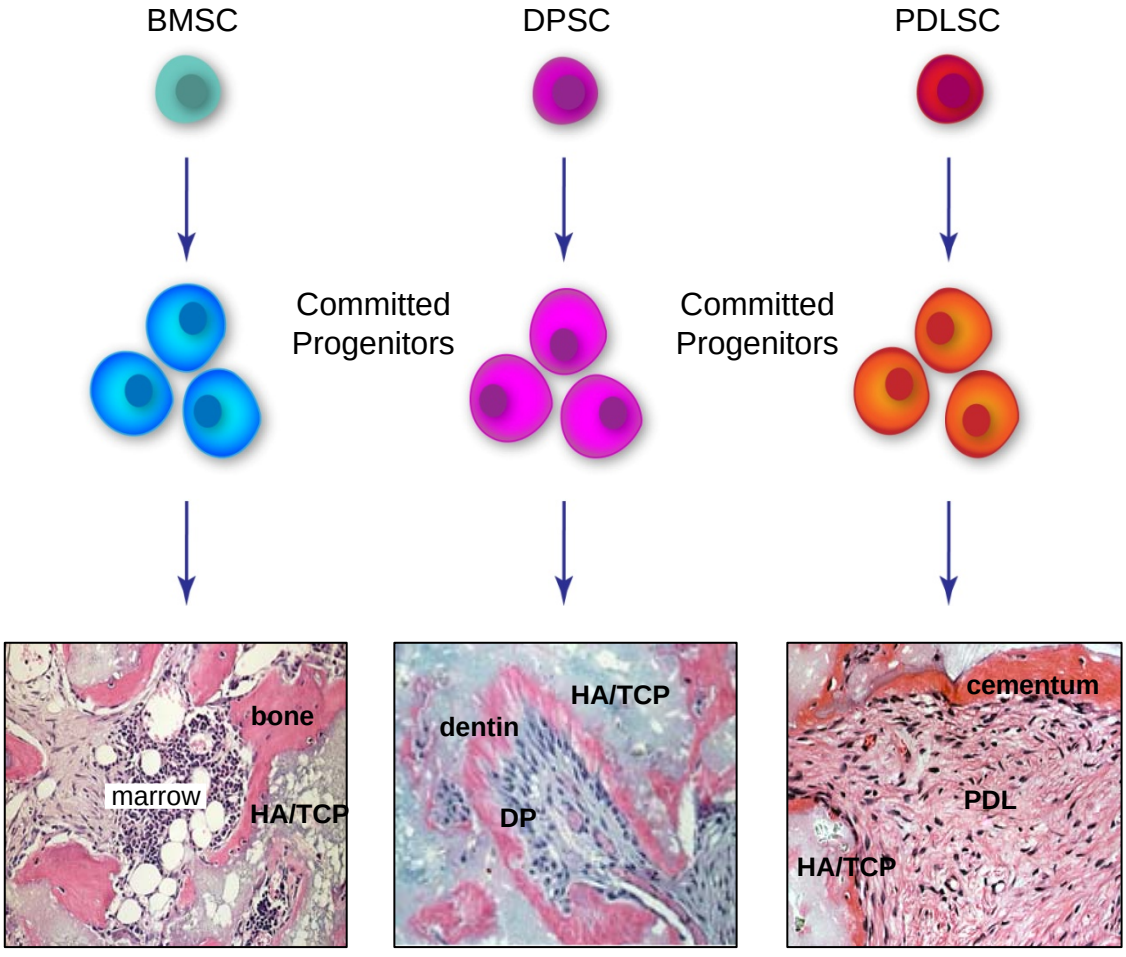
BMSC
DPSC
PDLSC
Committed Progenitors
Committed Progenitors
bone
marrow
HA/TCP
HA/TCP
dentin
DP
cementum
PDL
HA/TCP

Structurally, dental pulp is composed of cellular, neuronal, vascular and matrix components. The extracellular matrix is principally composed of fibrous components such as type I and III collagens as well as nonfibrous matter including proteoglycans and other macromolecules. Histologically, there are four distinguishable zones comprising the odontoblastic zone, a cell-free zone, a cell rich zone and the pulp core, characterised by the presence of major vessels and nerves of the pulp. The cells types predominantly present in the pulp are fibroblasts, odontoblasts, macrophages and undifferentiated mesenchymal cells [98, 99]. In the past it was considered that the role of fibroblasts in the pulp was to form and maintain collagen and other components of the extracellular matrix, whereas the undifferentiated odontogenic precursor cells were considered the source pool from which other pulp cells are derived [99].

Gronthos and colleagues examined whether adult dental pulp tissue contains a population of multi-potential cells similar to that described for BMSCs. Their findings showed that these cells exhibited features of BMSCs, including CFU-F formation, high proliferation and regenerative potential, and as such were termed dental pulp stem cells (DPSCs) [24]. The identification of DPSCs involved comparative analysis of cells from the dental pulp and BMSCs using cell culturing for colony forming efficiency, immunohistochemistry, histochemistry, transplantation, reverse transcription PCR and *in situ* hybridisation [24]. This study found that the number of proliferating cells as well as the frequency of colony-forming cells was significantly higher in DPSCs when compared to BMSCs. Furthermore, immunohistochemical analysis showed that the two cell populations exhibited similar expression profiles for markers associated with endothelium, smooth muscle, bone, and fibroblasts [24]. In parallel experiments, the gene expression profiles were compared between DPSC and BMSC using cDNA microanalysis [110]. These studies showed a similar gene expression profile for many genes, including those encoding for collagen type III and type IV, noncollagenous extracellular matrix components, several cell adhesion molecules and various growth factors. Non-collagenous extracellular matrix components included osteopontin, osteonectin, matrix-gla protein, decorin, biglycan and alkaline phosphatase, whilst the cell adhesion molecules included VCAM-1, CD44, integrins $\beta_{1,}$ $\alpha_{v2,}$ $\alpha_{v,}$ and β_3 [110]. Many of these molecules are known to influence the process of dentinogenesis [111, 112] and are associated with the initiation of mineralisation and bone homeostasis [71, 113-118]. Similarly, the growth factors included, IGF-1, PDGF, FGF-2,

TGF-β1, BMP-2, BMP-4 and BMP-7 are considered strong promoters of osteogenesis and formation of mineralised bone extracellular matrix [119-122], and are involved in tooth morphogenesis [121, 123, 124]. Shi and Gronthos showed that DPSC isolated by immunoselection, using the BMSC markers, STRO-1 and CD146, are pericyte-like confirmed by their expression of alpha smooth muscle actin, the pericyte antigen, 3G5 and their localisation to the perivascular regions around blood vessels in human pulp [58].

1.1.2.2.2. Isolation and Identification of MSC-like Cells Derived from Periodontal Ligament

The periodontium is considered the supporting tissue of the tooth and consists of root cementum, periodontal ligament, and alveolar bone [125, 126] (**Figure 1.3**). Periodontal ligament, which is a physically small part of the periodontium, is functionally important in tooth support, proprioception and regulation of alveolar bone volume. The main features of periodontal ligament are rapid matrix turnover and ability to adapt to alterations of mechanical loading which in combination with presence of heterogenous cell populations allows for dynamic and strong connections between teeth roots and bone, in spite of considerable force levels of mastication [127, 128]. The ability of periodontal ligament to remodel and allow for tooth movement is particularly important in maintenance of the periodontium [128]. Periodontal ligament has a very high turnover rate, and is mainly composed of fibrous elements, largely constituted by type I and III collagen, and the cell populations present in the healthy state of the tissue include fibroblasts, myofibroblasts, endothelial cells, epithelial cells, nerve cells, osteoblasts and cementoblasts [129, 130].

Studies have previously described a rare population of cells identified as ‘progenitor cells’ which exhibit some of the classical cytological features of stem cells [130]. The presence of these progenitor cells is supported by the limited regeneration occuring within this part of the periodontium as seen in the early phases of periodontal disease. It has been postulated that MSCs are recruited and activated following damage to the periodontium, where they undergo terminal differentiation into ligament forming cells or mineral forming cementoblasts, which both act to secure the connections between the cementum and the adjacent alveolar bone [131, 132]. However, the origin and ontogeny of these progenitor cells remains largely unknown.

Figure 1.3 A Schematic Diagram Detailing the Anatomy of an Adult Tooth.

The crown of the tooth is covered by hard, acellular, inert tissue, termed enamel. The enamel is supported by dentin which forms the bulk of the tooth. Dental pulp is enclosed by dentin and located in the central part of the tooth. This fibrous connective tissue houses the nerves and blood vessels of the tooth. The root of the tooth is covered by hard, bone-like tissue, termed cementum. Cementum functions to anchor periodontal ligament fibres to the tooth. Periodontal ligament, situated between the tooth and the alveolar bone, holds a vital role in connecting the tooth to the jaw.

Figure 1.3

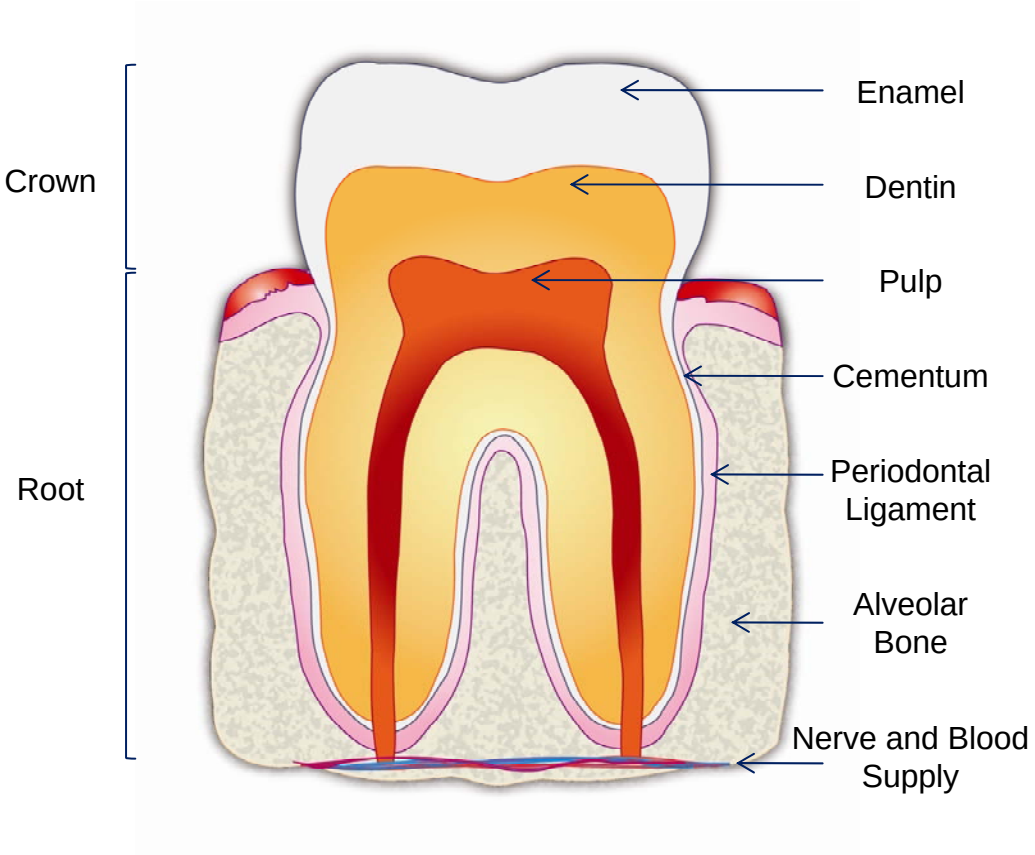
Crown
Root
Enamel
Dentin
Pulp
Cementum
Periodontal Ligament
Alveolar Bone
Nerve and Blood Supply

In order to identify putative periodontal ligament stem cells, various techniques used to characterise BMSC and DPSC were employed including cell culture, magnetic and fluorescence activated cell sorting, immunohistochemistry, RT-PCR, western and northern blot analyses [41]. When plated under the same growth conditions as described for BMSCs and DPSCs, PDL derived cells were found to generate clonogenic adherent cell colonies, where the incidence of fibroblastic colony forming unit (CFU-F), was greater than that reported for BMSCs and DPSCs. Therefore, these cells were termed periodontal ligament stem cells, PDLSCs. Further characterisation studies found that PDLSCs expressed the cell surface molecules STRO-1 and CD146/MUC18, early BMSC markers as well as scleraxis, a tendon-specific transcription factor [41]. PDLSCs were also found to be derived from perivascular niches as described for MSC isolated from human bone marrow, dental pulp and adipose tissues, due to their common expression of STRO-1/CD146 [41, 58, 133, 134]. Collectively, these studies imply that MSC populations derived from different tissues share a similar perivascular origin.

The level of expression of scleraxis by PDLSCs, which was higher than that in BMSCs and DPSCs, suggests that PDLSCs may exhibit unique properties to other MSCs [41, 135]. This was supported by differentiation assays used to asses the ability of PDLSCs to undergo cementoblastic/osteoblastic and adipogenic differentiation, which resulted in calcium accumulation and development of lipid laden fat cells *in vitro* [41]. Transplantation of *ex vivo* expanded PDLSCs into immunocompromised mice validated the ability of these cells to form functional cementoblast-like cells and cementum/PDL-like tissue *in vivo* [41, 135]. Furthermore, transplantation of isolated human periodontal ligament stem cells into surgically created periodontal defects of immunodeficient rats was performed to assess the ability of these cells to contribute in periodontal tissue repair. These experiments showed that PDLSCs exhibited a potential role in regeneration of periodontal tissues, however, further studies in large animal models are still required to demonstrate the therapeutic capacity of these stem cells [41].

1.2. The Use of MSC in Tissue Engineering

Due to their accessibility, high growth capacity and multi-potential, MSCs hold great promise for tissue regeneration in clinical applications. However, some of the technical

issues that need to be overcome, include identification and isolation of appropriate precursor cell types, establishment of optimal growth and differentiation conditions *in vitro* and efficient modes of delivery for the successful transplantation of MSCs [24]. Tissue engineering is considered an alternative approach to current treatments that may help alleviate the shortcomings of more conventional therapeutic options or lack of effective treatment regimes. The essential components for generating effective cellular based therapeutic strategies include, a population of multi-potential progenitor cells, presence of signalling molecules/inductive morphogenic signals and a conductive extracellular matrix scaffold or appropriate delivery system [89, 136, 137]. One major obstacle that limits the clinical use of MSCs is the lack of the ability of investigators to define the initial cell preparations and the heterogeneity of the starting cell population which may result in poor reproducibility of therapeutic outcomes, which clearly requires further characterization of these different cell populations [138].

1.2.1. Efficacy of MSC in Regenerating Calcified Tissues

1.2.1.1. Regenerative Potential of BMSCs *in vivo*

The bone forming capacity of BMSC has been well documented and thoroughly reviewed [139-145]. Collectively, these reviews have focused on the regenerative potential of BMSC in bone defects in small and large animal models.

The *in vivo* osteogenic capacity of BMSCs was primarily assessed by subcutaneous transplantation of cultured BMSC into the dorsal surface of two month old SCID mice in combination with hydroxyappatite/tricalcium (HA/TCP) phosphate carrier particles [53]. Histological examination of the harvested transplants demonstrated extensive networks of blood vessels and fibrous tissue and formation of new bone. The cellular material in the newly formed bone tissue *in vivo* was confirmed to be of human origin by *in situ* hybridisation using the human specific *Alu* gene sequence [12]. In their pioneering studies, Bruder *et al* assessed the reparative potential of BMSCs in osseous tissues of large animals [146]. The use of BMSCs to repair critical-sized segmental femoral bone defects in a canine model demonstrated good bone formation and healing at the defect site following implantation of BMSCs. Uniform and substantial amount of new bone was noted throughout the defects implanted with BMSCs, which was integrated with the surrounding

host bone [146]. In contrast, at the time of assessment, those implants that did not contain BMSCs were mostly filled with fibrous tissue. These findings were confirmed in a later study by Brodke and colleagues, where a canine femoral defect model was used to show that enrichment of graft materials with BMSC resulted in efficient repair of criticial-sized defects [147]. Marcacci *et al* initially developed an ovine model of a critical sized bone defect where they demonstrated the capacity of hydroxyapatite bone ceramics to induce bone healing [148]. In subsequent studies they introduced the application of BMSCs in combination with a hydroxyapatite scaffold, and this experimental approach resulted in an improvement in the amount of bone formation and stiffness of the BMSC loaded implant [149]. Similarly, a study of BMSC implantation into osteoperiosteal defects in sheep conducted by Viateau and colleagues determined that new bone was formed in all of the defects treated with implants containing BMSCs [150] and thus confirmed findings of previously published work [151, 152]. Other studies also used autologous BMSC but with porous β-tricalcium phosphate to repair critical-sized bone defects in goats, that became fully load-bearing [153]. More recently, Liu *et al* demonstrated that implantation of autologous BMSCs into segmental bone defects of goat tibia led to tissue repair within an eight week period [154]. BMSCs in combination with porous nano-hydroxyapatite/collagen composite scaffold reinforced with chitin fibres, formed new bone lacunae and bone cells, indicative of new bone formation present within the scaffold [154]. Many other studies have assessed and confirmed the ability of BMSCs to regenerate bone in different animal models [155-159].

In a clinical setting, Quarto and colleagues reported on the ability of autologous BMSC to repair long bone defects in humans [160]. Limb function was recovered in all three patients that had BMSCs loaded hydroxyapatite scaffolds implanted into the defect sites of large bone defects. Abundant callus formation and good integration of the implant with the host bone was observed two months post surgery [160].

Previous work by Dorotka and colleagues confirmed the potential of BMSCs in regeneration of cartilage in an ovine chondral defect model [161]. Similarly, Mrugala *et al* used autologous implantation of BMSC onto a chitosan-based scaffold to treat cartilaginous lesions of sheep joints [162]. Nine weeks after the surgery, defects that were treated with BMSCs presented with glossy white repaired tissue which was integrated with the surrounding cartilage [162]. In addition, Quintavalla *et al* used fluorescent labelling of

BMSCs to monitor the ability of these cells to survive and contribute to tissue repair *in vivo* [163]. MSCs derived from goat bone marrow were labelled using a CMTMR (5-(((4-chloromethyl)benzoyl)amino)-tetramethylrhodamine) dye, loaded onto gelatine sponges and implanted into osteochondral defects created in articular sites in goats. They showed that labelled BMSC retained their osteogenic and chondrogenic potentials *in vitro* and that implanted cells remained in the defect site and maintained their viability during the first 2 days post implantation. However, analysis performed at 7 and 14 days post implantation demonstrated an extensive loss of implanted MSCs. Moreover, gelfoam containing MSCs was located at the border of condylar defects and fragments of implanted constructs were noted in marrow spaces, away from the original defect site. Experimental evaluation based on one set of conditions and use of one type of biomaterial were the major limitations of this study, however the investigators provide a protocol for tracking and monitoring MSCs used in cell-based tissue regenerative applications [163]. Murphy *et al* investigated the capacity of goat derived BMSCs in regeneration of knee joints post traumatic osteoarthritis (OA) inductive injury [164]. In this caprine model, OA was induced by unilateral medial meniscectomy and transaction of the anterior cruciate ligament was performed. At 6 weeks post BMSC implantation, development of meniscal-like repair tissue in treated knee joints was observed and this finding was associated with detainment of degenerative changes related to the ontogenesis of OA [164].

1.2.1.2. Regenerative Potential of DPSC *in vivo*

Previous studies have shown that human DPSCs isolated from primary transplants are capable of undergoing self-renewal through their capacity to form dentin-pulp-like structures following secondary transplantation *in vivo* [97]. Further research by other groups has shown that a population of DPSC-like cells is capable of differentiating into living autologous bone tissue (LAB) *in vitro* and lamellar bone following implantation into immunocompromised rats. Immunofluorescence examination showed that LAB was largely positive to markers for fibrous bone tissue including fibronectin, collagen I and III, bone sialoprotein (BSP), bone-specific alkaline phosphatase (BALP), osteonectin and osteocalcin [165]. However, the origin of the cells that gave rise to the ectopic bone *in vivo* was not determined in these studies. Additionally, it was confirmed that DPSC, similar to BMSCs, have the potential to differentiate into cells of adipogenic and neurogenic lineages [97]. These features classify DPSCs as multipotent adult stem cells making them attractive for therapeutic use in regenerative endodontics and other tissues [166].

Zhang *et al* assessed the differentiation/maturation potential of DPSC towards odontogenic, adipogenic and myogenic lineages [167]. In this study, DPSC were incubated in required induction media prior to being subcutaneously implanted into mice. The rationale for this experiment was to identify the potential of DPSC without the stimulation and guidance of the surrounding microenvironment, hence an atypical environment was chosen as an adequate implantation site [167]. The findings of this study indicated that DPSC maintained a limited potential to differentiate into odontogenic, adipogenic and myogenic lineages in aberrant surrounding environment [167].

More recently, Yamada and colleagues assessed the potential of DPSC in bone regeneration, in a study where autologous DPSC/platelet rich plasma scaffolds were implanted into bone defects created in mandibles of adult hybrid dogs [168]. New bone formation with a tubular pattern and abundant formation of vasculature was observed eight weeks after implantation in cavities containing DPSC. This newly generated bone tissue consisted of woven and lamellar bone tissue. In parallel experiments the comparable ability of BMSC and deciduous tooth stem cells (DTSC) for regeneration of bone tissues, in this canine defect model, was observed [168].

The potential of DPSC in repair of bone defects in humans has been tested in a clinical study [169]. The aim of this study was to treat alveolar bone defects routinely associated with extraction of impacted, unerupted or partially erupted wisdom teeth. At the time of wisdom tooth extraction, autologous DPSC, previously obtained from upper molar teeth of these patients, were combined with a collagen sponge scaffold and implanted into the site of the extracted teeth to prevent post-operative alveolar bone loss. The results of this trial indicated that autologous bone regeneration was achieved, as this procedure led to optimal bone repair with the restoration of periodontal tissue in the desired area [169].

1.2.1.3. Regenerative Potential of PDLSC *in vivo*

It has been previously shown that PDL cells have the potential to form connective tissue resembling periodontal ligament *in vivo*. A study by Lang *et al* used a miniature pig model for autologous re-implantation of dental roots lined with PDL cells to test the potential of tissue regeneration [170]. The results showed connective tissue formation around the PDL-

roots and orientation of the fibre bundles within four weeks of implantation. Twelve weeks post implantation the root surfaces were covered by organised connective tissue resembling periodontal ligament and oriented fibre bundles were attached to alveolar bone and root, penetrating the bone and root surfaces in the same way as Sharpey's fibres [170]. In addition, their subsequent studies showed the potential of *ex vivo* expanded alveolar bone cells (ABCs) to induce regeneration in periodontal defects, using the minature pig model [171]. Histological analysis confirmed marked cementum and bone formation in dental defects containing ABCs during the early stages of wound healing. In contrast, a fibrous structure resembling periodontal ligament was formed after 30 days post transplantation, whereas the formation of new attachment with oriented fibre bundles anchored both in the cementum layer and in the newly formed bone was observed at 90 days post transplantation [170, 171].

Recently, a study by Sonoyama and colleagues explored the potential for reconstruction of a functional tooth in miniature pigs [172]. They used a combination of two types of cells, stem cells from root apical papilla (SCAP) and PDLSCs to show the potential of this combination in regeneration of root/periodontal tissue. The implant used in this study was constructed of a root shaped HA/TCP block, loaded with SCAP, which contained an inner post channel space to allow for the subsequent installation of the porcelain crown. Prior to implantation this construct was coated with Gelfoam containing PDLSCs. Following extraction of the lower incisor, the site was cleaned to ensure removal of all periodontal ligament tissues and the implant was inserted into the extraction socket and sutured. The surface of the constructed implant was surgically re-opened at three months post implantation and a porcelain crown resembling a miniature pig incisor was inserted and cemented into the preformed site in the implant. Four weeks post installation of the crown, CT and histological analysis confirmed regeneration of the root/periodontal structure. This study showed the efficacy of using a multi-stem cell approach (SCAP and PDLSCs) to mimick a bio-physiological root/periodontal reconstruction. Moreover, this study resulted not only in regeneration of both of the tissues, but demonstrated a significantly improved compressive strength of the newly formed bio-roots when compared to that of previous HA/TCP carriers. Therefore, this proof-of-concept study demonstrated the potential for use of two distinct autologous stem cell populations in conjunction with artificial dental crowns in functional tooth regeneration [172].

MSCs isolated from periodontal ligament tissues of miniature pigs exhibit the capacity to form bone, cementum and periodontal ligament in autologous transplantation into alveolar defects of a preclinical periodontitis model [173]. In this study periodontitis-associated defects were generated in the periodontium to create a typical and stable model of periodontitis in a large animal model. One month post induction of the disease, GFP-labelled PDLSCs were transplanted into the bone defects and assessment of tissue regeneration was performed twelve weeks after transplantation. The findings of this study indicated that PDLSC combined with HA/TCP played a significant role in periodontal tissue regeneration as the presence of GFP^+ differentiated osteoblasts was detected in newly formed periodontal bone. More recently, Kim and colleagues used a canine peri-implant defect model to make a comparative assessment of the regenerative potential of BMSC and PDLSC in regeneration of alveolar bone [174]. The experimental protocol involved transplantation of autologous BMSC and PDLSC on HA/TCP carriers and cell free HA/TCP controls in surgically created peri-implant saddle like defects. The findings of this pilot study indicated that both populations of MSCs showed a comparable potential involvement in the regeneration of alveolar bone and were more effective than HA/TCP controls that did not contain MSCs [174].

In a clinical study, the potential of periodontal ligament progenitors (PDLP) was assessed for the reconstruction of periodontal intrabony defects in three patients [175]. PDLP are progenitor cells derived from the periodontal ligament, isolated using crude isolation techniques compared to the previously characterised PDLSCs. Retrospective comparison of PDLP to PDLSCs demonstrated that, although PDLP exhibited the phenotype of MSC-like cells, these cells may be more committed than PDLSC as their osteogenic and adipogenic differentiation capacity was reduced *in vitro* [175]. However, PDLP presented elevated cell migratory properties *in vitro* and the two cell types exhibited comparable capacities to form Sharpey's fibres in a mouse model of periodontal ligament tissue regeneration [175]. In these experiments autologous PDLPs, mixed with bone grafting material, were implanted into deep periodontal pockets and the patients were monitored over the course of 3, 6, 12, 26, 32, 42 and 72 months. The findings of this study demonstrated that two out of three patients, that had undergone surgical evaluation of tissue regeneration exhibited reasonable regain of healthy tissue. Accordingly, the third patient assessed in this study presented with decreased tooth movement and probing depth, decreased gingival recession and stable improvement of attachment gain [175]. This

investigation concluded that the use of autologous PDLPs in cell based surgical treatment for periodontitis may be used in effective regenerative dentistry.

1.3. Heterogeneity within MSC Populations – A Challenge in Therapeutic Cell Based Applications

MSCs act as an attractive candidate for therapeutic use, however there are numerous challenges associated with the use of MSCs in cell based therapy. Their clinical application is highly uncertain due to lack of knowledge and understanding of critical processes involved in maintaining the potency of these cells. The heterogeneity present within MSC populations accounts for the compromised and undefined profiles of these cells. This is presented in terms of morphological variability, inconsistency in levels of proliferation and differentiation potentials, as well as differences in patterns of gene and protein expression profiles of the individual cell population subsets [176, 177-179]. The studies that have addressed the issue of heterogeneity within MSC populations and looked at differences between CFU-F clones at gene and protein levels were limited in their approaches. The understanding of molecular mechanisms vital to proliferation, differentiation, engraftment and homing of MSC is essential in order to expand the potential clinical applications of these cells.

1.4. Gene Expression Profiling of MSCs

The sequencing of the human genome has provided the basic structural information for all human genes [180, 181]. This knowledge, combined with the emergence of high density array technology, allows the assessment of global patterns of gene expression by simultaneously screening thousands of genes from an array comparing multiple experimental samples. The application of microarray analysis allows for the testing of differential gene expression patterns between multiple samples of interest in order to identify major genomic differences and unique biological markers specific to the target cell population [182]. The pace and direction of biomedical research is now fundamentally changing due to the development of high-throughput screening techniques. Gene expression array technologies are currently being used in studies examining complex multigenic processes by analysing a large number of interacting genes. These studies aim to gain a greater understanding of the relationship of multiple gene families and the nature of their interactions in different biological systems [183, 184]. Advances in molecular

genetics and genomic profiling have led to the identification of many candidate molecular biomarkers or classifier genes for predicting the unique phenotypic features of a given cell population [185, 186]. Genomic profiling has also been used in large-scale industry initiated projects and undertaken to apply genomic studies in the discovery of new diagnostic and therapeutic targets [183]. Numerous studies have taken place to examine and define MSCs and their progeny based on gene expression profiling.

1.4.1. Gene Expression Profiling of MSCs During Osteogenic Differentiation

Bone formation is known to occur through the activation of key transcriptional regulators such as RUNX2 and OSTERIX, that orchestrate the differentiation of MSCs into functional bone forming cells known as osteoblast [187-189]. However, the complex molecular signalling pathways involved in this process are only now starting to be elucidated [190]. In one study, Kulterer and colleagues examined the gene expression profiles of MSCs following long-term cell cultivation or during osteogenic differentiation *in vitro* [191]. This study showed no significant change in gene expression profiles during long-term cell expansion under normal growth conditions. These findings were supported by the observation that MSCs maintained their undifferentiated phenotype and retained their capacity for osteogenic differentiation at early and late cell passages [191]. However, MSCs exhibited three distinct stages of osteogenic development at the molecular level, following osteogenic induction. Using large-scale expression profiling of clinical samples, gene clusters were associated with distinct stages of proliferation, matrix maturation and mineralization during the development of the osteoblast phenotype [191]. In particular, ID4, CRYAB and SORT1 were identified as late markers of osteogenesis (**Table 1.1**). ID4 is a member of the ID (inhibitor of DNA binding) transcription factor family. The members of this family have been shown to play a key role in the differentiation processes and are involved in cell cycle control [192-195]. The other members of the ID family ID1, ID2 and ID3 have previously been identified as early targets of osteogenic factors such as BMP2, BMP6 and BMP8 [196]. A specific role for CRYAB (crystallin-αB), a small heat shock protein, widely expressed in many tissues and organs [197], is not completely understood however, the up-regulation of CRYAB suggests its involvement in osteogenic differentiation [191]. SORT1 (sortillin 1) represents a multi-ligand type I receptor, which binds a number of unrelated ligands that participate in a large range of cellular activities

Table 1.1 A List of Highly Expressed Genes in MSCs During Differentiation Processes.

Gene Symbol	**Gene Name**	**Lineage of Differentiation**	**Reference**
ZNF145	zinc finger and BTB domain containing 16	early osteogenesis /chondrogenesis/adipogenesis	[222]
FKBP5	FK506 binding protein 5	early osteogenesis /chondrogenesis/adipogenesis	[222]
ID4	inhibitor of DNA binding 4, dominant negative helix-loop-helix protein	late osteogenesis	[191]
CRYAB	Crystallin-αB	late osteogenesis	[191]
SORT1	Sortillin 1	late osteogenesis	[191]
DPT	Dermatopontin	osteogenesis / chondrogenesis	[200, 222]
HRH1	Histamine receptor H1	osteogenesis	[200, 206]
OMD	osteomodulin	osteogenesis	[222]
APOD	apolipoprotein D	osteogenesis	[222]
ADAMTS-1	ADAM metallopeptidase with thrombospondin type 1 motif, 1	adipogenesis	[206]
ADAMTS-4	ADAM metallopeptidase with thrombospondin type 1 motif,4	adipogenesis / late chondrogenesis	[206, 213]
LPL	lipoprotein lipase	adipogenesis	[222]
FABP4	fatty acid binding protein 4, adipocyte	adipogenesis	[222]
PDK4	pyruvate dehydrogenase kinase, isozyme 4	adipogenesis	[222]
ACDC	adiponectin, C1Q and collagen domain containing	adipogenesis	[222]
CCN3/NOV	nephroblastoma overexpressed gene	Chondrogenesis	[213]
CCN4/WISP1	WNT1 inducible signaling pathway protein 1	Chondrogenesis	[213]
CCN5/WISP2	WNT1 inducible signaling pathway protein 2	Chondrogenesis	[213]
ADAMTS-5	ADAM metallopeptidase with thrombospondin type 1 motif, 5	Late chondrogenesis	[213]
COL10A1	collagen, type X, alpha 1	chondrogenesis	[222]

[198]. Earlier studies by Maeda *et al* showed that SORT1 promotes extracellular matrix maturation and is differentially expressed during osteogenic differentiation [199].

Using a different approach, a report by Pochampally and colleagues described the use of microarray analysis to identify candidate molecules for new downstream targets of transcription factor vitamin D receptor (VDR) [200], which has previously been identified as one of the drivers of osteoblast differentiation processes [201]. This was achieved by mining the microarray data generated from the genomic profiling of MSCs during osteogenic differentiation for genes that were co-expressed with osteocalcin, a known downstream target for the VDR transcription complex. Two candidate target genes dermatopontin (DPT) and histamine receptor (HRH1) were identified (**Table 1.1**), and were found to be regulated by the VDR during osteogenic differentiation of MSCs, based on promoter binding and activity assays [200]. HRH1 and DPT were found to be downstream targets of VDR, and over-expression of VDR induced expression of DPT and HRH1 in an osteosarcoma cell line, where as inhibitors of DPT and HRH1 decreased osteogenic differentiation of MSCs [200]. Together, these studies further our knowledge of the genomic regulation of bone formation, by identifying potential downstream targets of osteogenenic transcription factors. However, functional studies are still required to determine the precise role of each of these genes during osteogenesis.

1.4.2. Gene Expression Profiling of MSCs During Adipogenic Differentiation

The fibroblasts and adipocytes present in the bone marrow microenvironment provide the cytokines and extracellular matrix proteins required for the maturation and proliferation of hematopoietic stem cells [202-205]. Due to the complexity of the bone marrow organ, the functional role of bone marrow adipocytes has yet to be properly defined. Characterization of the developmental pathways that mediate MSC differentiation into mature adipocytes is now helping define the role of adipose tissue in bone and blood cell homeostasis. One study employed microarray analysis to examine gene expression profiles of MSCs associated with their potential to form adipogenic tissue [206]. This study demonstrated initiation of adipogenesis occured early following induction by detecting mRNA expression of several adipogenesis markers, including LPL, PPARγ2 and aP2 genes. Furthermore, an additional 82 genes were found to be upregulated by fivefold or greater, and 31 genes were observed to be downregulated twofold or greater between the gene

expression profiles of MSCs and their differentiated progeny. The differentially expressed genes were grouped into several categories based on their sub-cellular location and function including cell membrane proteins/antigens, cell matrix proteins, structure proteins, nuclear proteins, binding protein/receptors/channel, signal transduction/growth control, metabolism/enzymes and unclassified genes. Some of the genes that were significantly upregulated during adipogenesis include IGF2, IGFBP2 and GPX3, previously recognised markers of differentiated adipocytes [207]. Several genes that hold specific roles in lipid metabolism, including APOD, CYP1B1, PPAP2B, CES2, OBRGRP and HE1, were also found to be highly expressed in differentiated MSCs [208, 209]. ADAM proteins contain a disintegrin and a matrix metallloproteinase (MMP) domain, which has the dual function of cleavage/release of cell surface proteins and remodelling of the extracellular matrix (ECM) [210]. Previous studies have shown that ADAMTS1 and ADAMTS4 are involved in ECM degradation [211], and Hung *et al* reported an upregulation of gene expression for ADAMTS1 and ADAMTS4 during adipogenesis (**Table 1.1**) [206]. Expectedly, several surface molecules associated with MSCs such as integrin β1 (CD29), CD44 and CD105 showed a decrease in expression after differentiation [206]. Furthermore, several other genes found to be downregulated during adipogenesis were associated with different lineages, including OSF2 (osteogenic lineage), LICAM, CDH2, TUBA3, TUBB, HXB and PRPH (neurogenic lineage) and TAGLN2, P63, CLIC4, IGFBP3 and KRT19 (myo- or epithelial lineage). The investigators suggested that initiation and progression of adipogenesis is associated with the loss of a multi-potential phenotype and transition away from other lineages [206]. It is anticipated that further studies using gene silencing techniques would be useful for identifying distinct genes critical for switching the developmental program towards adipogenic differentiation.

1.4.3. Gene Expression Profiling of Cells Undergoing Chondrogenic Differentiation

Whilst MSC-like populations are classically characterized by their capacity to develop into bone and adipose tissues and their myelosupportive properties, these populations also demonstrate the potential to develop into functional chondrocytes, responsible for forming the components of the extracellular matrix in cartilage [13, 33, 212, 213]. However, there are relatively few reports demonstrating the capacity of *ex vivo* expanded human MSCs to generate hyaline cartilage to any significant extent following transplantation *in vivo*. Therefore, further characterization of the developmental pathways that promote chondrogenesis using genomic profiling will increase our understanding of this process and aid in the manipulation of MSC populations for cartilage related tissue engineering applications.

In a comparative study of gene expression patterns between MSCs and dedifferentiating primary chondrocytes, Goessler *et al* identified distinct molecular changes during the developmental process of chondrogenic differentiation [214]. This group of researchers observed characteristic differences in the mRNA expression of integrins and integrin-associated proteins involved in the cellular processes of differentiation, adhesion and migration, when comparing dedifferentiating primary chondrocytes to differentiating MSCs [214]. The integrins are heterodimeric glycoproteins composed of an α and a β subunit forming a family of cell surface receptors that play a major role in the mediation of the cell-ECM interactions associated with structural and functional changes in surrounding tissue [215, 216]. These molecules have been shown to have a major role in MSC attachment to extracellular matrix proteins [71]. The data obtained by Goessler *et al* showed that the fibronectin receptor, integrin α5β1 was downregulated by MSCs during chondrocyte differentiation. Conversely, an upregulation in integrin α5β1 gene was noted during the dedifferentiation of human chondrocytes, identifying this integrin as a potential marker of undifferentiated fibroblastoid cells [214]. In another study, Djouad *et al* reported the gene expression of several ADAM proteins and two ADAMTS (ADAMTS-4 and ADAMTS-5) molecules, at the late stage of chondrogenesis (**Table 1.1**). The involvement of ADAMTS (ADAM with thrombospondin type 1 motif) molecules has previously been reported in aggrecan breakdown during endochondral ossification [217]. Expression of ADAMTS-5 was shown to be increased by Wnt/β-catenin signalling which was shown to

regulate chondrocyte phenotype, maturation and function in a developmentally regulated manner [218]. Djouad and colleagues postulated that, even though the role of the ADAM molecules in the process of chondrogenesis is not well understood, the interaction of these proteins with integrins, proteoglycans (PGs) and ECM proteins may create a microenvironment favouring differentiation of a chondrocytic phenotype [213].

To elucidate the micro-environmental signals involved in chondrogenic differentiation of MSCs, Djouad *et al* analysed gene expression data generated from MSCs at varying time points during chondrogenic induction *in vitro* [213]. This study showed an increase in the expression of CCN3, CCN4 and CCN5 in MSCs after undergoing chondrogenesis (**Table 1.1**). CCN proteins are secreted, cysteine-rich regulatory proteins that through their interaction with growth factors help mediate cell proliferation and differentiation, particularly in bone and cartilage [219]. However, previous research has shown that CCN5 can act as a growth-arrest-specific gene and can inhibit proliferation, invasiveness and motility of vascular smooth muscle cells [220]. Similarly, CCN proteins may modulate MSC proliferation during the course of the differentiation process [213].

These studies confirmed expression of different ECM or membrane associated molecules in MSCs and chondrocytes that are involved in attachment and cell migration, such as various PGs, collagens, MMPs, CCN proteins, chemokines and their receptors, ADAM proteins, cadherins and integrins. However, it remains to be determined how these molecules are regulated by TGFβ family members and their receptors which are known to promote chondrogenic differentiation *in vitro*, and have also been shown to be differentially expressed during MSC differentiation and chondrocyte dedifferentiation [221].

1.4.4. Comparison of Gene Expression Patterns of MSCs Derived from Different Tissues During Differentiation

In order to understand the processes that govern initial commitment and further differentiation of MSCs into various lineages, Liu and colleagues compared the gene expression profiles of bone marrow and adipose derived MSCs during their differentiation toward osteogenic, chondrogenic and adipogenic lineages [222]. This study identified a set of genes commonly upregulated at early and late stages during differentiation toward

all three lineages in both bone marrow and adipose derived MSCs. The top candidate genes, commonly up-regulated during differentiation into all three lineages, included ZNF145 and FKBP5 (**Table 1.1**). Previous studies have shown that ZNF145 plays an important role in early osteoblastic differentiation as an upstream regulator of CBFA1 [223], and therefore, may be vital to general initiation of MSC differentiation. Previous studies examining FKBP5 have focused on its role in modulating signals from glucocorticoid receptor steroid and hormone receptors [224]. However, the FKBP5 homolog, PAS-1 in *Arabidopsis* plays a critical role in growth and development [225]. Liu *et al* showed that overexpression of FKBP5 in bone marrow and adipose derived MSCs accelerated their differentiation into all three lineages, whereas FKBP5 knockdown resulted in retardation of cellular differentiation. Therefore, it appears that FKBP5 plays an important role in the early stages of the differentiation process of MSCs.

Additinally, the level of dermatopontin, one of the non-collagenous components of the ECM which has role in the maintenance of ECM architecture and modification of cell behaviour [226], and collagen 10A1 expression was increased during early chondrogenesis for both bone marrow and adipose derived MSCs. However, a marked increase in the expression of these two genes in late chondorgenesis was observed only in bone marrow derived MSCs (**Table 1.1**) [222]. In early adipogenesis, an increase in expression of LPL, FABP4, PDK4 and ACDC was observed in both cell types and the levels of these genes were upregulated in late adipogenesis, particularly in adipose derived MSCs. OMD and APOD levels were increased in both cell types during osteogenesis with these genes showing a marked increase in the bone marrow derived MSC population **(Table 1.1)**. These studies have identified potential gene sets that mark the stages of early commitment and differentiation into all three lineages, and late-differentiation genes which may be crucial in terminal differentiation for specific cell types [222].

Wagner and colleagues, in their study of genomic profiling, compared gene expression patterns of MSC-like cells derived from bone marrow, adipose tissue and umbilical cord with non-multipotent fibroblasts. The primary aim of this study was to analyse the reproducibility of generating different MSCs under standardised conditions. The study also compared the molecular genetic profiles of MSCs derived from different ontogenic sources to identify commonly expressed genes in all preparations of MSCs to aid in the

discovery of novel MSC markers [138]. Overall, the study identified differentially upregulated **(Table1.2)** and downregulated genes common to MSCs in comparison to fibroblast cell preparations. Wagner *et al* concluded that a panel of markers, rather than a single gene, is essential in the identification of mulitpotent MSCs [138].

Tsai *et al* hypothesised that MSCs derived from different origins would most likely exhibit unique genomic profiles, but would also express a subset of common genes [227]. This study compared genomic profiles of MSCs isolated from adult bone marrow, amniotic fluid, amniotic membrane and umbilical cord blood. They further contrasted the MSC genomic profiles to those of foetal brain, heart, lung, liver, kidney and muscle. The study demonstrated that gene expression profiles in individual MSCs remained stable during *ex vivo* expansion and subculture, and that each MSC population exhibited a unique signature genomic profile. In addition, the different postnatal MSC populations shared a common, core genomic profile distinct from that of foetal organs [227]. Using highly stringent criteria, 48 genes were identified that were differentially upregulated **(Table 1.3)** and 11 genes that were downregulated, common to MSCs. Some of the upregulated genes include those involved in plasmin-related extracellular matrix remodelling (CD44, collagen II, IGF-2, PLAU, PLAUR, SERPINE 1 and TIMP1), cytoskeletal regulation (ACTN1, ARPC1B, Cav1, Cav2, CDKN1, PLAU, PLAUR and SERPINE 1), chemokine regulation and adhesion (ACTN1, ARPC1B, Cav1, Cav2, CDKN1A, PLAU, PLAUR, SERPINE-1 and thrombospondin 1), plasmin activation (PLAU and TFPI-2) and TGF-β receptor signalling (Cav1, Cav2, CDKN1A, SMURF and SERPINE1). Other genes that were significantly upregulated in all MSCs population in comparison to fetal organs included genes involved in metabolism regulation; NQO1 (NADH dehydrogenase), LOXL2 (metabolism of arginine), PLOD2 (metabolism of lysine), SMURF2 (metabolism of tryptophan), NNMT (NAD metabolism) and NT5E (nucleotide and NAD metabolism). MSC upregulated genes involved in regulation of intracellular signal transduction included KDELR3, involved in both cAMP and protein kinase A signalling, and RGS4, which drives G proteins into their inactive GDP-bound forms. This study suggests that the potential roles of each of the MSCs populations may be determined based on their gene expression patterns. It was proposed that MSCs derived from amniotic fluid may initiate the interaction with the uterus by upregulating oxytocins and thrombin receptors, whereas amniotic membrane MSCs may play a role in homeostasis of fluid and electrolytes by

Table 1.2 A List of Highly Expressed Genes, Common to Bone Marrow, Adipose Tissue and Umbilical Cord Derived MSCs Populations in Comparison to Fibroblast Cell Populations [138].

Gene Symbol	**Gene Name**
	Extracellular Matrix
ECM2	Extracellular Matrix Protein 2
FN1	Fibronectin 1
GPC4	Glypican 4
CSPG2	Chondroitin sulfate proteoglycan 2
LTBP1	Latent TGFβ binding protein 1
	Cell Signalling
DDIT4	DNA-damage-inducible transcript 4
TM4SF1	Transmembrane 4 superfamily member 1
AGTR1	Angiotensin II receptor, type I
	Cell Growth/Development
MIG-6	Mitogen-inducible gene 6
URB	Steroid-sensitive gene 1
	Transcription Regulatory Protein
ID1	Inhibitor of DNA binding 1
NFIB	Nuclear factor I/B
DSIPI	Delta sleep-inducing peptide
HOXA5	Homeobox protein HOX-A5
HOXB6	Homeobox protein HOX-B6
DLGAP1	Discs, large homolog-associated protein 1

Table 1.3 A List of Genes Highly Expressed (> 8 fold) by MSCs Derived from the Bone Marrow, Amniotic Fluid, Amniotic Membrane and Cord Blood in Comparison to Foetal Organs [227].

NOTE:
This table is included in the print copy of the thesis held in the University of Adelaide Library.

regulating networks of endothelin, neprilysin, bradykinin receptor and atrial natriuretic peptide. It was also postulated that cord blood MSCs may be involved in the innate immune system, as the neonatal defence against earliest encountered pathogens and that bone marrow derived MSCs may be an important source for all blood lineages and bone formation [227].

A study by Shi *et al* focused on the characterization of the gene expression patterns of MSC like cells found in dental pulp tissue (DPSCs) compared to that of bone marrow derived MSCs [110]. They used a cDNA microarray platform representative of 4000 known human genes and demonstrated that a comparison of the two cell types showed a similar gene expression profile for many of the represented genes. Commonly expressed genes included those encoding for collagen type III and type IV, noncollagenous extracellular matrix components, several cell adhesion molecules and various growth factors. Non-collagenous extracellular matrix components included osteopontin, osteonectin, matrix-gla protein, decorin, biglycan and alkaline phosphatase, whilst the cell adhesion molecules included VCAM-1, CD44, integrins $\beta_{1,}$ $\alpha_{v2,}$ $\alpha_{v,}$ and β_3 [110]. Many of these molecules are known to influence the process of dentinogenesis [111, 112] and are associated with the initiation of mineralization and bone homeostasis [71, 113-118]. Similarly, growth factors including IGF-1, PDGF, FGF-2, TGF-β1, BMP-2, BMP-4 and BMP-7, are considered strong promoters of osteogenesis and formation of mineralized bone extracellular matrix [119-122], and are involved in tooth morphogenesis [121, 123, 124]. A number of differentially expressed genes were identified following comparisons of the gene expression patterns of the two MSC-like populations. It was observed that collagen type XVIII α1 (COLL 18 α1), insulin-like growth factor-2 (IGF-2), discordin domain tyrosine kinase (DDR2), NAD(P)H menadione oxidoreductase (NMOR1), homolg 2 of *Drosophila* large disc (DLG2) and cyclin-dependent kinase 6 (CDK6) were highly expressed in DPSCs. On the other hand, levels of expression for genes including insulin-like growth factor binding protein-7 (IGFBP-7) and collagen type I α2 (COLL 1 α2) were higher in the bone marrow derived MSCs when compared to DPSCs [110].

Overall, these studies identify potential markers that may be used to isolate and purify immature MSC from an array of heterogeneous cell populations. Furthermore, they provide data on potential genomic indicators essential to specific differentiation pathways

and as such may be used as tools in guided/induced lineage specific differentiation of MSCs

1.5. Summary

Extensive knowledge of the biological processes involved in tissue repair is vital in developing a stem cell based approach for tissue regeneration. It is of great importance to determine the nature and the phenotype of the cells involved and to understand their molecular regulation during the repair process in order to achieve favourable clinical outcomes. Recent advances in genomic profiling of MSCs allows for genetic characterization, manipulation and modification of the cells or their growth conditions in order to obtain the most optimal cell population to use for this purpose. Today's technology of genomic profiling and fast improvements of the microarray technology provide rapid and reliable data sets that define vital processes involved in MSC growth survival and development. The capacity of MSC to readily differentiate into multiple lineages offers an ideal model to identify key molecular switches involved in MSC lineage commitment using gene expression profiling, where current technological advances are now heading towards the use of high-throughput sequencing of transcriptomes. Furthermore, there are numerous issues still to be addressed in order to achieve effective and sustained therapeutic dental structure regeneration, such as optimal stem cell populations and dose, as well as the use of appropriate biomaterials, in order for this approach to facilitate a positive impact on the clinical management of disease in dental structures.

1.6. Project Aims

Building on from the hypothesis that BMSCs, DPSCs and PDLSCs contain heterogeneous populations of progenitor cells, including a minor subset of multi-potential cells, the general focus for this PhD project was based on the functional and genomic characterisation of clonal MSCs derived from bone marrow, dental pulp and periodontal ligament tissues which exhibit unique capacities to form different calcified tissues including mature bone, dentin and cementum *in vivo,* respectively. It was anticipated that key global factors involved in cellular proliferation and differentiation could be identified by characterising the developmental stages of different MSC-like clonal populations.

Therefore this approach could lead to the identification of novel MSC markers and may also greatly improve the current understanding of fundamental cellular processes involved during stem cell maintenance, growth and development.

In our approach to investigate our hypotheses we aimed to:

- Identify long-lived, multi-potential BMSCs, DPSCs and PDLSCs by comparing the growth and differentiation potential of different clonal cell lines.
- Assess the unique gene expression profile and identify specific markers of multi-potential BMSC, DPSC and PDLSC clones.

Determine the functional significance of these markers in the context of stem cell survival, growth and development.

Chapter 2:

Materials and Methods

2. Materials and Methods

2.1. Subjects

Bone marrow (BM) aspirates were obtained from the posterior iliac crest of normal adult volunteers (20-35 years old) following informed consent, according to procedures approved by the ethics committee of the Royal Adelaide Hospital, South Australia, (Protocol No. 010516). Normal human impacted molars were collected from healthy volunteers between 15 and 19 years of age with informed consent, according to procedures approved by the Human Ethics Committee of the University of Adelaide, South Australia, (Protocol No. H-57-2003).

2.2. Cell Culture

2.2.1. Cell Culture Media

2.2.1.1. α-MEM + additives

- α-MEM (Sigma-Aldrich, St. Louis, MO, USA)
- 10% FCS (Thermo Electron, Melbourne, VIC, Australia)
- 50 U/mL, 5 µg/mL Penicillin, Streptomycin (Sigma-Aldrich, St. Louis, MO, USA)
- 1 mM Sodium Pyruvate (SAFC**,** Lenexa, KS, USA)
- 100 µM L-ascorbate-2-phosphate (Novachem, Melbourne, VIC, Australia)
- 2 mM L-Glutamine (SAFC, Lenexa, KS, USA)

2.2.1.2. DMEM + additives

- DMEM (JRH Biosciences, Lenexa, KS, USA)
- 10% Hyclone FCS (JRH Biosciences, Lenexa, KS, USA)
- 50 U/mL, 5µg/mL Penicillin, Streptomycin (Sigma-Aldrich, St. Louis, MO, USA)
- 10 mM HEPES (Sigma-Aldrich, St. Louis, MO, USA)
- 1 mM Sodium Pyruvate (SAFC, Lenexa, KS, USA)
- 2 mM L-Glutamine (SAFC, Lenexa, KS, USA)

2.2.1.3. Mineralisation Media

- α-MEM (Sigma-Aldrich, St. Louis, MO, USA)
- 5% FCS (Thermo Electron, Melbourne, VIC, Australia)

- 50 U/mL, 5µg/mL Penicillin, Streptomycin (Sigma-Aldrich, St. Louis, MO, USA)
- 1 mM Sodium Pyruvate (SAFC, Lenexa, KS, USA)
- 100 µM L-ascorbate-2-phosphate (Novachem, Melbourne, VIC, Australia)
- 2 mM L-Glutamine (SAFC, Lenexa, KS, USA)
- 10^{-7} M dexamethasone phosphate (Hospira Australia)
- 1.8 mM inorganic phosphate, KH_2PO_4, (BDH Chemicals, Poole, UK)

2.2.1.4. Adipogenic Media

- α-MEM (Sigma-Aldrich, St. Louis, MO, USA)
- 5% FCS (Thermo Electron, Melbourne, 15-011-0500V)
- 50 U/mL, 5µg/mL Penicillin, Streptomycin (Sigma-Aldrich, St. Louis, MO, USA)
- 1 mM Sodium Pyruvate (SAFC, Lenexa, KS, USA)
- 100 µM L-ascorbate-2-phosphate (Novachem, Melbourne, VIC, Australia)
- 2 mM L-Glutamine (SAFC, Lenexa, KS, USA)
- 0.5 µM hydrocortisone (Sigma-Aldrich, St. Louis, MO, USA)
- 60 µM indomethacin (Sigma-Aldrich, St. Louis, MO, USA)
- 0.5 mM IBMX (3-Isobutyl-1-methyl-xanthine) (Sigma-Aldrich, St. Louis, MO, USA)

2.2.1.5. Chondrogenic Media

- DMEM (JRH Biosciences, Lenexa, KS, USA)
- 50U/mL, 5µg/mL Penicillin, Streptomycin (CSL, 85101)
- 1 mM Sodium Pyruvate (SAFC, Lenexa, KS, USA)
- 100 µM L-ascorbate-2-phosphate (Novachem, Melbourne, VIC, Australia)
- 2 mM L-Glutamine (SAFC, Lenexa, KS, USA)
- rhTGFβ3 (PeproTech, Rocky Hill, NJ, USA)

2.2.1.6. LB media

- 10g / L Tryptone Peptone (Becton Dickinson, Sparks, MD, USA)
- 5g / L Yeast Extract (Becton Dickinson, Sparks, MD, USA)
- 10g / L NaCl (Sigma-Aldrich, St. Louis, MO, USA)

2.2.1.7. SOC media

- 2.0% Tryptone Peptone (Becton Dickinson, Sparks, MD, USA)
- 0.5% Yeast Extract (Becton Dickinson, Sparks, MD, USA)
- 10 mM NaCl (Sigma-Aldrich, St. Louis, MO, USA)
- 2.5 mM KCl (BDH Chemicals, Australia)
- 10 mM $MgCl_2$-$6H_2O$ (Merck, Kilsyth, VIC, Australia)
- 10 mM Glucose (Merck, Kilsyth, VIC, Australia)

2.2.2. Cell Culture Buffers

2.2.2.1. HBSS

- Hanks balanced salt solution (JRH Biosciences, Lenexa, KS, USA)

2.2.2.2. 1xPBS

- MilliQ water (Media production unit, IMVS)
- 10% PBS Phosphate Buffered Saline, calcium and magnesium free (Sigma-Aldrich, St. Louis, MO, USA)

2.2.2.3. HHF Buffer

- HBSS
- 5% FCS (Thermo Electron, Melbourne, VIC, Australia)
- 50 U/mL, 5 µg/mL Penicillin, Streptomycin, (Sigma-Aldrich, St. Louis, MO, USA)

2.2.2.4. Blocking Buffer

- HHF Buffer
- 5% normal human serum (Red Cross, SA, Australia)

2.2.2.5. MACS Buffer

- 1xPBS
- 1% BSA (SAFC, Lenexa, KS, USA)
- 5 mM EDTA (Merck, Kilsyth, VIC, Australia)
- 0.01% sodium azide

2.2.3. Cell Culture Conditions

All cell culture protocols were conducted in a Class II laminar flow hood (Top Safe 1.2, Bio Air, Siziano, Italy). Cells cultured for expansion were maintained in MCO-18AIC Sanyo CO_2 incubators (Sanyo Oceania, North Ryde, NSW, Australia), at 37^oC, 5% CO_2 in a humidified environment. Eppendorf 5810 centrifuge (Eppendorf South Pacific, North Ryde, NSW, Australia) was used for centrifugation of cell suspensions during expansion.

2.2.4. Isolation of BMSCs using Magnetic Activated Cell Sorting

This MSC isolation method was based on the protocol described by Associate Professors Gronthos and Zannettino [228]. Following informed consent, approximately 40 mL of human bone marrow (BM) was aspirated from the posterior iliac crest of healthy young volunteers. The samples were then diluted with an equal volume of blocking buffer, mixed well and strained through a 70 µm cell strainer (Becton Dickinson Biosciences, San Jose, CA, USA). BMMNC were isolated using lymphoprep separation medium (Nycomed Pharma AS, Oslo, Norway) by the process of density gradient separation. 3 mL of lymphoprep was transferred into 14 mL polystyrene tubes and was gently overlayed with 8 mL of BM/HFF mixture and centrifuged at 800 *g* for 30 minutes with no break. This was sufficient to separate out the mononuclear layer which was then transferred to fresh 14 mL polypropylene centrifuge tubes and washed in 10 mL HHF twice by centrifugation at 800 *g* for 7 minutes at 4^oC. Following washing, the cells were resuspended in α-MEM + additives, pooled and counted using a haemocytometer as described in **Section 2.2.8.** Following counting, cells were resuspended in 500 µL of mouse anti-human STRO-1 supernatant [54] per 5 x 10^7 cells and incubated on ice for 1 hour with occasional agitation. Cells were then washed twice in HHF and resuspended in 0.5 mL HHF containing biotinylated goat anti-mouse IgM (Southern Biotechnology Associates, Birmingham, UK) and incubated at 4^oC for 45 minutes. Following 3 washes in MACS buffer the cells were resuspended in 450 µL of MACS buffer to which 50 µL of streptavidin microbeads (Miltenyi Biotec, Bergisch Gladbach, Germany) was added (10 µL of microbeads/10^7 cells in 90 µL MACS buffer). The mixture was incubated on ice for 15 minutes before being washed once in ice-cold MACS buffer and then loaded onto a mini MACS column (Miltenyi Biotec, MS column). Cells bound to the STRO-1 antibody were attached to the magnetised matrix of the column. The column was washed three times with 500 µL MACS buffer to remove any non-specifically bound STRO-1 negative cells. The column

was removed from the magnetic field and the STRO-1 positive cells were collected by flushing the column with 1 mL of MACS buffer. The STRO-1 positive cells were then cultured as described in **Section 2.2.6.**

2.2.5. Isolation of DPSCs and PDLSCs using DynaBead Cell Sorting

DPSCs and PDLSCs were isolated from DP and PDL cell populations as previously described [58]. Periodontal ligament was gently removed from the middle third of the tooth root surface using forceps and a surgical blade in a 10 cm tissue culture dish containing 10 mL HHF buffer. The tooth was crushed, dental pulp exposed and dissected into smaller pieces in a 10 cm tissue culture dish containing 10 mL HHF buffer. The HHF buffer containing DP and PDL tissue was transferred into individual 14 mL round bottom polypropylene tubes and centrifuged at 400 *g* for 10 minutes at 4ºC. DP and PDL tissues were resuspended and digested in a solution of 1 mL Type I collagenase (3 mg/mL) and 1 mL dispase II (4 mg/mL) for 1 hour at 37^{o}C. An excess volume of HHF buffer was added to the digested tissue to neutralize enzyme activity and the suspension was strained through a 70 µm Falcon cell strainer to remove undigested tissue from the liberated DP and PDL cells. The cell suspensions were pelleted by centrifugation at 400 *g* for 10 minutes at 4ºC, and resuspended in 2 mL of HHF.

Dynal bead cell sorting was performed on single cell suspensions of dental pulp and periodontal ligament as previously described [58]. Briefly, following counting each cell suspension was incubated in 500 µL mouse anti-human STRO-1 antibody [41] for 1 hour on ice. Following two washes in HHF, the cells were incubated with rat-anti mouse IgM conjugated Dynabeads (Dynal Biotech, Oslo, Norway) at four beads per cell on a rotary mixer at 4^{o}C for 2 hours. The cells were washed twice in HHF and resuspended in 3 mL of HHF. STRO-1 positive cells were isolated with Dynal MPC-1 magnetic particle concentrator (Dynal Biotech, Oslo, Norway) according to the manufacturer's recommendations and were then cultured as described in **Section 2.2.6.**

2.2.6. Culture of Human MSC

Primary immunoseloected BMSC, DPSC and PDLSC cultures were established in α-MEM + additives. Cells were plated at 5x10^{3} cells/ cm^{2} into 10 cm culture dishes and maintained in a CO_2 incubator for 10 to 14 days. Individual colonies were isolated using colony rings and expanded into individual vessels for further cultivation, as previously described [53,

97]. Briefly, single cell derived colonies obtained from primary cultures of BMSC, DPSC and PDLSC populations were seeded at $8x10^3$ cells/cm^2 and allowed to expand to approximately 90% confluency. To harvest and further expand the cells, they were washed in HBSS, and treated with 0.05% trypsin/EDTA (SAFC, Lenexa, KS, USA) for 3 minutes. HHF was added to neutralise trypsin activity and cell suspensions were centrifuged at 800 *g* for 5 minutes at 4°C. Cells were reseeded at $8x10^3$ cells/cm^2, for further expansion. This process was repeated six times or until desired cell numbers were obtained.

2.2.7. Culture of Adherent retroviral HEK 293T Packaging Cell Line

Cells were cultured in T^{75} tissue culture flasks in DMEM + additives. These cells were cultured at a density of 80-90% confluence. When cells reached required confluence they were split to be used in experiments or reseeded (5×10^3 cells per cm^2) for further expansion.

2.2.8. Counting Cells

Washed cells were resuspended in 1 mL of appropriate media. From this cell suspension, 10 µL was removed for counting. Depending on the estimated (using a microscope) cell number, a dilution factor between two and ten was used to count cells. Freshly isolated BMMNC were counted in white cell fluid (2% acetic acid in distilled H_2O) which preferentially lyses erythrocytes due the presence of acetic acid. All other cell types were counted using trypan blue dye exclusion, by diluting cells in 0.4% (w/v) trypan blue (Sigma-Aldrich, St. Louis, MO, USA) to detect living cells. To obtain an accurate cell number at least 100 cells were counted using a haemocytometer.

2.2.9. Cryopreservation of Cells

Cells were cryopreserved in FCS containing 10% (v/v) of dimethyl sulfoxide (DMSO; BDH AnalaR® Merck, Kilsynth, Victoria, Australia). Immediately prior to freezing, 1 mL of pre-prepared, cold FCS 20% DMSO solution was added drop wise to ~1×10^6 cells in 1 mL of FCS on ice. 1 mL of the cell suspensions at were then pipetted into 2 mL cryoampoules (Greiner Bio-One, Frickenhousen, Germany) and transferred into a Mr Frosty cryopreservation container (C1562 Freezing Container, Nalgene, USA) before being placed into a -80°C freezer for at least 4 hours. The Mr Frosty freezing container

ensures the cells are cooled at the appropriate rate of 1^{o}C per minute. After 4 hours the cryoampoules were then transferred to liquid nitrogen for extended storage at -196°C.

2.2.10. Thawing of Cryopreserved Cells

Cells were removed from liquid nitrogen (-196^{o}C) and immediately thawed in a 37^{o}C bath. Once thawed, the cell suspensions were immediately transferred to a 14 mL spin tube containing 11 mL of appropriate growth media. This preparation was centrifuged at 800 *g* for 7 minutes at 4^{o}C. Cell pellets were then resuspended in 10mL of appropriate growth media and plated at a density of 8 x 10^3 cells / cm^2.

2.3. Functional Analysis of Clonal BMSC, DPSC and PDLSC Populations

2.3.1. Proliferation Studies

2.3.1.1. BrdU Incorporation Proliferation Assay

BMSC, DPSC and PDLSC were plated at 1x10^3 and 2x10^3 cells per cm^2 in 96-well plates and cultured in αMEM+additives. Following 2 and 4 days of culture, 10 µl of 1/100 dilution of BrdU labelling reagent (10 mM 5-bromo-2-deoxyuridine, Roche, Manheim, Germany) was added to each well and the cells were re-incubated for an additional 24 hours to detect cells in S-phase. The medium was then aspirated and the cells were fixed for 30 minutes by adding 200 µl of FixDenat fixative solution (Roche, Manheim, Germany) to each well. Following fixation, 100 µl of anti-BrdU-POD working solution (monoclonal antibody from mouse-mouse hybrid cells (clone BMG 6H8) conjugated with peroxidise) (Roche, Manheim, Germany) was added to each well and the cells were incubated for 90 minutes at room temperature. The antibody conjugate was removed and the cells were washed three times with 1xPBS. Following the washes, 100 µl of TMB substrate solution (tetramethyl-benzide Roche, Manheim, Germany) was added to each well and the cells were incubated for 25 minutes at room temperature. Finally, 25 µl of 1 M H_2SO_4 stop solution was added to each well and the absorbance at 450 nm was measured using a microtitre plate reader (BioTek Instruments, Winooski, VT, USA).

2.3.1.2. WST-1 Proliferation Assay

BMSC, DPSC and PDLSC were plated at $1x10^3$ and $2x10^3$ cells per cm^2 in 96-well plates and cultured in αMEM + additives. Following 3 and 5 days of culture, the relative number of viable, metabolically active cells per well was detected by the quantification of mitochondrial dehydrogenase activity via the formation of formazan from WST-1 concentration (4-[3-(4-Iodophenyl)-2-(4-nitrophenyl)-2H-5-tetrazolio)-1,3-benzene disulphonate) (Roche, Manheim, Germany) following the manufacturer's instructions. The media were aspirated and 100 µL volumes of 10% WST-1 solution in phenol red-free c-DMEM (v/v) was added to each test well and to empty wells (for background determination). The cells were incubated at 37°C in humidified CO_2 for 120 min for colour to develop. The optical density of the medium was then read at 540 nm using a microtitre plate reader (BioTek Instruments, Winooski, VT, USA).

2.3.1.3. Assessment of Population Doublings

Single cell-derived colonies obtained from primary cultures of BMSC, DPSC and PDLSC populations were seeded at $8x10^3$ cells/cm^2 and allowed to expand to approximately 90% confluency before being harvested by trypsin/EDTA (JRH Biosciences, Lenexa, KS, USA) treatment. Representative cell samples for each clone were passaged at a seeding density of $8x10^3$ cells/cm^2 into 24 well plates until they had reached *in vitro*-cellular senescence. Cell counts were performed at each passage and population doublings were calculated using the formula ($\log_2$ final cell number/ $\log_2$ seeding cell number). The final population doubling value for each colony was represented as the sum of population doubling values obtained at each passage. The population doubling times per cell passage were calculated using the formula: Generation time = (log2 x days in culture) / (log final cell number – log seeding cell number).

2.3.2. Differentiation Assays

2.3.2.1. Assessment of Osteogenic Differentiation Potential

In vitro mineralization was induced as previously described [12, 55]. Briefly, BMSC, DPSC and PDLSC were seeded at $8x10^3$ cells per cm^2 in 24 well plates and were cultured in mineralization media for 28 days with media changes twice weekly. At 28 days the wells were washed in 1xPBS and fixed with 10% Neutral Buffered Formalin (Fronine Laboratory Supplies, Lomb Scientific, Taren Point, NSW, Australia) for 1 hour. Mineral

deposition was identified by Alizarin Red staining, 2% Alizarin Red S (Sigma-Aldrich Inc., St. Louis, MO, USA) in RO water.

For quantitative assessment, BMSC, DPSC and PDLSC were seeded at $8x10^3$ cells per cm^2 in 96 well plates and cells were cultured in mineralization induction media for 28 days with media changes twice weekly. At 28 days the wells were washed three times with 1xPBS and the mineralised matrix was dissolved in 100 µL of 0.6 M HCl (Merck, Kilsyth, VIC, Australia) for 1 hour at room temperature. The dissolved mineral solution was then transferred to 96-well microtitre plates and calcium levels were quantitated by the Cresolphthalein Complexone assay (Thermo Electron Corporation, Melbourne, VIC, Australia). Briefly, 5 µL of supernatants were transferred to single wells of a fresh microtitre plate. A calcium chloride (calcium/phosphorous combined standard (Sigma Aldrich, St. Louis, MO, USA)) standard curve was also established in triplicate. Equal volumes of reagent A (cresolphthalein complexone 0.10 mmol/L, 8-hydroxyquinoline 5.2 mmol/L, polyvinylpyrrolidine 0.07 mmol/L) and reagent B (2-amino-1-methylpropanol 260 mmol/L) were mixed and 200 µL were added per well. The plates were incubated at room temperature for 2 minutes and the absorbance was read at 540 nm on a microplate reader (EL808 Ultra, BIO-TEK Instruments, Winooski, VT, US).

Following dissolution of the mineral with HCl, the wells were washed with 1xPBS and the cells were digested with 100 µL of proteinase K (100 µg/mL) (Invitrogen, Carlsbad, Canada) for 2 hours at room temperature or overnight at 4°C. The cells were then triturated thoroughly to ensure complete disruption of the cells, 50 µL volumes were transferred to a white 96-well microtitre plate (Costar, Corning, New York, NY, USA). DNA content per well was then determined using the Hoescht assay.

2.3.2.2. Hoescht DNA Assay

DNA content was measured using Hoescht 33258 dye as a surrogate marker of cell number. Diluted Hoescht 33258 solution was made by mixing equal volumes of 4 M sodium chloride (Sigma-Aldrich, St. Louis, MO, USA) and 0.1 sodium phosphate (Sigma-Aldrich, St. Louis, MO, USA), and adding Hoescht 33258 dye (Sigma-Aldrich, St. Louis, MO, USA) at 2 µg/mL. Salmon sperm DNA (Sigma-Aldrich, St. Louis, MO, USA) was diluted in RO water to a 1 mg/mL stock solution. The stock DNA solution was diluted in sodium chloride/sodium phosphate solution to final concentrations of 50 µg/mL, 25

µg/mL, 12.5 µg/mL, 6.25 µg/mL, 3.12 µg/mL and 1.56 µg/mL and these were used to establish the standard curve for the assays. 150 µl of diluted Hoescht 33258 solution was added to the samples and DNA standards in white microtitre plates. The plates were gently agitated then fluorescence was then measured using a fluorescence spectrometer (LS 55, Perkin Elmer Instruments, Boston, MA, USA) with an excitation wavelength of 350 nm, an emission wavelength of 450 nm and a slit width of 2.5 nm.

2.3.2.3. Assessment of Adipogenic Differentiation Potential

Adipogenesis was induced as previously described [12, 13, 229]. BMSCs, DPSCs and PDLSCs were seeded at $8x10^3$ per cm^2 in 24 well plates and were cultured for 28 days in the presence of adipogenic media with media changes twice a week. At 28 days the wells were washed three times with 1xPBS and cells were fixed in 10% Neutral Buffered Formalin for 1 hour at room temperature. Oil Red O staining solution was made by dissolving 0.5g of Oil Red O stain (MP Biomedicals, Solon, OH) in 100 mL of isopropanol (Ajax Finechem, Taren Point, NSW, Australia) and further diluted 1.5:1 in RO water. Formation of lipid-laden fat cells was determined by Oil Red O staining.

For quantitative assessment, BMSC, DPSC and PDLSC were seeded at $8x10^3$ per cm^2 in 96 well plates and were cultured for 28 days in the presence of adipogenic media with media changes twice a week. At 28 days the wells were washed three times with 1xPBS, then fixed in 10% Neutral Buffered Formalin for 1 hour at room temperature and stained with Oil Red O for 2 hour at room temperature. The plates were allowed to dry, before adding 100µL of 100% isopropanol to each well. Following a 10 minute incubation at room temperature, the extracted dye was transferred to new 96 well plates and the absorbance was measured at 490nm using a plate reader.

2.3.2.4. Assessment of Chondrogenic Differentiation Potential

Chondrogenesis was induced as previously described [230]. Briefly, $1x10^6$ BMSC, DPSC and PDLSC were resuspended in DMEM media, centrifuged at 600 *g*, at 4^oC for 5 minutes to form cell pellets. The cell pellets were cultured for 28 days in chondrogenic induction media ± TGFβ3 with media changes twice weekly. At 28 days, pellet cultures designated for histological assessment were fixed in 10% Neutral Buffered Formalin at 4^oC overnight. Pellet cultures designated for RT-PCR analysis were washed 3 times in 1xPBS and RNA extraction and cDNA synthesis were performed as described as described in **Section**

2.4.1., 2.4.2. and **2.4.4.** RT-PCR analysis was employed, as described as described in **Section 2.4.5.** to assess the levels of expression of AGGRECAN, COLLAGEN II and COLLAGEN X.

For quantitative assessment of glycosaminoglycan (GAG) production, BMSC, DPSC and PDLSC were seeded at $5x10^4$ per well of 96-well plates in αMEM + additives. Following overnight adhesion, the cultures were treated with 10 ng/mL TGFβ3. After 48 hours, treatment media were replaced with 100 µL of media containing 1 µCi $^{35}SO_4$ (sulphur-35 radionuclide) (ParkinElmer Life Sciences, Boston, MA, USA) and the plates were incubated at 37°C in 5% CO_2 overnight. To prepare papain digest solution at the final concentration of 20 U/mL, 62.1 mg of papain (Papain from Carica Papaya, 3.1 U/mg) (Sigma-Aldrich, St. Louis, MO, USA) was dissolved in 333 µL of 3 M sodium acetate (Sigma-Aldrich, St. Louis, MO, USA), 48 µL of 0.5 M EDTA (Ethylenediamenetetraacetic acid) (Chem Supply, Gilman, SA, Australia), 1 mL of 200 mM of N-acetyl-L-cysteine (Sigma-Aldrich, St. Louis, MO, USA) and 8.619 mL of RO water. The matrix was then digested at 65°C for 2 h with 100 µL of 20 U/mL papain digest solution. Cetylpyridinium chloride solution was made by dissolving 1 g of cetylpyridinium chloride monohydrate (Sigma-Aldrich, St. Louis, MO, USA) in 16 mL of ethanol and further dilution this solution in 24 mL of RO water. Glycosaminoglycans were precipitated by the addition of 40 µL of cetylpyridinium chloride solution followed by 5 minutes of mixing. CSA solution was made by dissolving 50 mg of Chondroitin sulfate A (Sigma-Aldrich, St. Louis, MO, USA) in 10 mL of RO water. CSA solution (10 µL) was then added, as a carrier, and the plate was mixed for a further 5 minutes. The precipitated proteins were then transferred to a glass fibre filter (Packard Bioscience Company, Meriden, CT, USA) using a cell harvester (Packard Filtermate Harvester, Packard Bioscience Company, Meriden, CT, USA). The membranes were dried for at least 2 hours before adding 25 µL Microscint™ (PerkinElmer Life and Analytical Sciences, Boston, MA, USA) per well where the amount of $^{35}SO_4$-labelled GAG per well was measured using a TopCount NXT Microplate Scinitillation & Luminescence counter (Perkin Elmer Life and Analytical Sciences, Downers Grove, IL, USA). In replicate cultures, cells were digested in 100 µL papain digest solution (100 U/mL) at 65°C for 6 hours. 50 µL of the cell lysate suspension was then transferred to a white microtitre plate and DNA content was measured using Hoecht 33258 dye, as described in **Section 2.3.2.2**.

Glycosaminoglycan levels were then normalised to DNA content to determine relative GAG production per cell.

2.3.2.5. Histological Assessment

Fixed chondrocyte pellets were processed, embedded and sectioned at 5 µm at the histology laboratory in the department of Neuroscience, Hanson Institute, Adelaide, SA, Australia. Sections were de-paraffinised through incubations in 2 changes of xylene (Ajax Finechem, Taren Point, NSW, Australia) 3 changes of absolute ethanol (Merck, Kilsyth, VIC, Austrlia) and a final wash in RO water. To neutralise endogenous peroxidase activity the sections were incubated in 0.5% H_2O_2 (Ajax Finechem, Taren Point, NSW, Australia) (v/v) in methanol (Chem Supply, Gillman, SA, Australia) for 30 minutes and non-specific binding was blocked by incubating sections with 3% (v/v) normal goat serum in 1xPBS for 1 hour at RT. Sections were then incubated overnight with either an isotype-matched, non-binding control monoclonal antibody (1B5, IgG1) or the anti-collagen II monoclonal antibody type II, (MAB1330) (Chemicon International, Temecula, CA) used at 1 in 100 dilution in 3% (v/v) normal goat serum in 1XPBS. Wash buffer was made by adding 50 mM Tris-HCl (Sigma-Aldrich, St. Louis, MO, USA) and 0.1% Tween-20 (Sigma-Aldrich, St. Louis, MO, USA) in RO water. Slides were then washed three times with wash buffer and bound antibody was revealed using the Dako EnVision+® Kit (Dako, Glostrup, Denmark). The sections were incubated with the Peroxidise-Labelled Polymer (Dako, Glostrup, Denmark) for 30 minutes, then washed with wash buffer and incubated with the DAB Substrate-Chromogen (Dako, Glostrup, Denmark) solution for 5-10 minutes. Sections were counterstained briefly with haematoxylin (ProSciTech, Turingowa Central, QLD, Australia) and mounted in DePex mounting media (BDH Chemicals, Poole, UK).

2.3.3. Flow-Cytometric Analysis

To characterise the immunophenotype of *ex vivo* expanded BMSC, DPSC and PDLSC, flow cytometric analysis was used to measure the expression of mesenchymal and non-mesenchymal stem-cell associated surface markers. Adherent ex vivo expanded BMSC, DPSC and PDLSC were washed once with HBSS and liberated by enzymatic digestion by the addition of 3 mL of 0.05% Trypsin/EDTA solution per T^{75} culture flask for 5 minutes at 37ºC. The single cell suspension was then washed twice in HHF buffer. Cell count and assessment of viability was performed as described in **Section 2.2.8.** BMSC, DPSC and PDLSC were resuspended for immunolabeling in 500 µL blocking buffer and incubated on

ice for approximately 30 minutes to reduce the possibility of Fc receptor-mediated binding of antibodies. Individual FACS tubes containing 2 x 10^5 cells were incubated with appropriate primary murine monoclonal antibodies specific to mesenchymal stem cell-associated markers, haemopoietic, non-mesenchymal stem cell-associated markers and isotype-matched controls. at a concentration of 20 µg/mL for 1 hour on ice. The list of these antibodies is outlined in **Table 2.1**. The cells were washed twice in 1 mL of HHF and incubated with secondary detection reagent; goat anti-mouse IgG- or goat anti-mouse IgM-PE (PE) (Phycoerythrin) conjugated antibody (1:50, Southern Biotechnology, Birmingham, AL, USA) for 45 minutes on ice. The cells were then washed in 1 mL of HHF and fixed in 500 µL of FACS Fix solution. Analysis was performed on a fluorescence-activated cell sorter fitted with a 250 MW argon laser (Beckman Coulter Cytomics FC500, using CXP Cytometry List Mode Data Acquisition and Analysis Software version 2.2 (Beckman Coulter, Miami, FL, USA)).

Table 2.1 List of Antibodies

[1]Name	Isotype	Source
1B5	IgG_1	Prof. L.K Ashman (University of Newcastle, Australia)
1D4.5	IgG_{2a}	Prof. L.K Ashman (University of Newcastle, Australia)
1A6.12	IgM	Prof. L.K Ashman (University of Newcastle, Australia)
Alk Phos B/L/K	IgG_1	ATCC
CD14	IgG_2	Beckman Coulter
CD34	IgG_1	Beckman Coulter
CD44	IgG_1	[78]
CD45	IgG_1	Beckman Coulter
CD73	IgG_1	Becton Dickinson
CD90	IgG_1	Becton Dickinson
CD105	IgG_1	Becton Dickinson
CD106	IgG_1	[12]
CD146	IgG_{2a}	[58, 231]
CD166	IgG_1	Becton Dickinson
Human Stromal Cell (STRO-1)	IgM	[12, 54]
TNSALP (STRO-3)	IgG_1	[75]
Hsp90β (STRO-4)	IgG_1	Gronthos, 2009 #694}
Goat anti Mouse IgG PE		Southern Biotech
Goat anti Mouse IgM PE		Southern Biotech
Streptavidin PE		Caltag Laboratories

[1]All primary antibodies and isotype matched controls were used at a concentration of 20 µg/mL with the exception of STRO-1 and 1A6.12 which were used as neat supernatant. Secondary detection antibodies were used at 10 µg/mL.

2.4. Gene Expression Profiling

2.4.1. Preparation of Total RNA

The collection and preparation of total cellular RNA was accomplished using TRIzol (Life Technologies, Carlsbad, Canada). Up to 1 x 10^6 cells were lysed in 1mL of TRIzol, directly in wells or, if grown in a flask, removed from flask using 0.05% trypsin/EDTA

digestion prior to being lysed in TRIzol. Chloroform (200µL per mL) (Ajax Finechem, Taren Point, NSW, Australia) was added to this solution and tubes were shaken vigorously for 15 seconds followed by a 3 minute incubation at room temperature. Centrifugation of this susension at 12,000 x *g* for 15 minutes at 4^{o}C resulted in phase separation. The upper aqueous phase was transferred to a fresh tube and total RNA was precipitated out of solution using isopropanol (500µL per mL) and glycogen (1µL per mL) (Sigma-Aldrich, St. Louis, MO, USA). This preparation was incubated for 1 hour on ice to ensure maximum RNA precipitation. To pellet RNA, cells were centrifuged at 12,000 x *g* for 10 minutes at 4^{o}C. Supernatant was removed and the pellets washed in 1 mL of 75% ethanol before being centrifuged at 7,500 x *g* for 5 minutes at 4^{o}C. Once most of the ethanol was removed, RNA was allowed to air dry for approximately 10 minutes. The dried RNA was then dissolved in RNAse free water (Promega, Madison, WI, USA) at room temperature for 10 minutes before being analysed using a NanoDrop Mass spectrometer (NanoDrop ND-1000 Spectrophotometer, Biolabgroup, Clayton, VIC, Australia) and stored at -20^{o}C. The RNA was purified using column chromatography (RNeasy® MinElute Cleanup Kit, Qiagen, Doncaster, VIC, Australia) according to the manufacturer's instructions.

2.4.2. Quantification and Purity Analysis of RNA

The NanoDrop Mass spectrometer was used for quantification and purity analysis of RNA samples. 1.5 µL of the sample was added to the stage of the NanoDrop. Absorbance at 260 nm was measured to determine the quantity of RNA and purity was measured by the ratio of A_{260}:A_{280}. Common ratios were between 1.85 and 1.95. Samples with values within this range were considered to be of high purity and were either used immediately to generate cDNA or stored at -20^{o}C for future use.

2.4.3. Microarray Analysis

2.4.3.1. Affymetrix® U133 Platform

Microarray analysis was performed on a commercial Affymetrix platform, containing 30,000 in situ synthesised probe sets made using photolithographic technology. Samples of 6 µg total RNA at a concentration of 2 µg/µl were provided for labelling, hybridisation, scanning and statistical analysis to be performed by Rosalie Kenyon and Mark Van Der Hoek at Microarray Facility, University of Adelaide / Hanson Institute, South Australia.

Statistical analysis was performed using Partek Genomics Suite software (Partek Inc. St. Louis, MI, USA) .

2.4.3.2. Illumina® WG-6 Platform

Microarray analysis was performed using a commercial Illumina WG-6 platform (San Diego, CA, USA), containing bead chips targeting 48,000 human transcripts. Samples of 1 µg of total RNA at a concentration of 100 ng/µL were used for labelling, hybridization, scanning and analysis which were performed by Dr. Stephen Wilcox at the Australian Genome Research Facility (AGRF, VIC, Australia). The data obtained were normalised by quantile normalisation method using lumi package in R statistical software [232, 233] and were subsequently imported into GeneSpring GX (Agilent Technologies, Forest Hill, VIC, Australia) for further statistical analysis.

2.4.4. Complementary DNA (cDNA) Synthesis

Complementary cDNA was generated using the SuperScript III Reverse Transcriptase kit (Invitrogen, Carlsbad, Canada). Briefly, 1 µL of oligo(dT) (50 µM, Invitrogen, Carlsbad, Canada), 1µL of dNTP mix (10 mM dideoxynucleotide triphopshates, Fisher Biotec, Wembley, WA, Australia), 1µg of total RNA and distilled water to a total volume of 13µL was added to each microcentrifuge tube. This mixture was heated to 70^{o}C for 5 minutes and then incubated on ice for at least 1 minute in order to denature the RNA. The tubes were then briefly centrifuged before adding 4 µL of 5X first-strand buffer (250 mM Tris-HCl, 375 mM KCl, 15 mM $MgCl_2$) (Invitrogen, Carlsbad, Canada) 2 µL of 0.1M DTT (Dithiothreitol, Invitrogen, Carlsbad, Canada) and 1 µL of SuperScript III RT (200 units / µL) (Invitrogen, Carlsbad, Canada) with gentle pippetting before being incubated at 42^{o}C for 1 hour to allow for primer extension and first strand synthesis. The reactions were stopped by incubating at 70^{o}C for 15 minutes leading to deactivation of the reverse transcriptase enzyme. The cDNA was diluted 1:5 in RNAse free water and used as a template for PCR reactions and stored at -20^{o}C.

2.4.5. Real-Time PCR

Using cDNA generated by the method described in **Section 2.4.4.** PCR was conducted to assess the levels of mRNA expression. Beta-actin (β-actin) was used as a housekeeping control gene and samples were normalized against this control. A reaction mixture

containing 2 µL of sample cDNA, 7.5 µL SYBR Green (RT^2 RealTime™ SYBR Grren/Rox PCR master mix, SA Biosciences, MD, USA), 0.75 µL (10µM) mixed primer pairs (Geneworks, SA, Australia) and 4.75 µL DEPC water was mixed to generate a 15 µL reaction for each tube of a 72 tube rotor of a Rotor Gene RG-6000 Realtime PCR machine (Corbett Research, Sydney, NSW, Australia). Cycling parameters that were used include the following steps; for activation - hold 1 to 15 minutes at 95°C, 15 seconds at 95°C, for cycling (40 cycles) of 25 seconds at 60°C, for 10 seconds at 72°C, for final extension, hold 2 to 3 minutes at 72°C, and melt Curve for 90 seconds pre melt, 5 second steps, 1 degree per step, 72°C to 99°C. The primer pairs used in this thesis are described in **Table 2.2**.

Table 2.2 Primer Set Sequences for RT-PCR

Gene	Gene Acc	Forward 5'-3'	Reverse 5'-3'
β ACTIN	NM 001101	GATCATTGCTCCTCCTGAGC	GTCATAGTCCGCCTAGAAGCAT
RUNX2	NM 004348	GTGGACGAGGCAAGAGTTCA	CATCAAGCTTCTGTCTGTGCC
BMP2	NM 001200	TCAAGCCAAACACAAACAGC	ACGTCTGAACAATGGCATGA
OPN	NM 001040060	ACATCCAGTACCCTGATGCTACAG	GTGGGTTTCAGCACTCTGGT
BSP	NM 004967	ATGGCCTGTGCTTTCTCAATG	AGGATAAAAGTAGGCATGCTTG
PPARγ2	U63415	CTCCTATTGACCCAGAAAGC	TCAAAGGAGTGGGAGTGGTC
LEPTIN	NM 000230	GGCTTTGGCCCTATCTTTTC	ACCGGTGACTTTCTGTTTGG
ADIPSIN	NM 001928	GACACCATCGACCACGAC	CCACGTCGCAGAGAGTTC
AGGRECAN	NM 001135	CTGCTTCCGAGGCATTTC	GCTCGGTGGTGAACTCTAGG
COL II	NM 001844.3	GCCTGGTGTCATGGGTTT	GTCCCTTCTCACCAGCTTTG
COLX	NM 000493	AATGCCCACAGGCATAAAAG	AGGACTTCCGTAGCCTGGTT
ASPM	NM 018136	CAGACTACGTCGTGCAGCAT	ACCAATTCGAAGCCACAAAG
AURKB	NM 004217	GGGAGAGCTGAAGATTGCTG	GGCGATAGGTCTCGTTGTGT
CCNB2	NM 004701	TTGCAGTCCATAAACCCACA	ACTTGGAAGCCAAGAGCAGA
CDC2	NM 001786	CTTTTCCATGGGGATTCAGA	CCATTTTGCCAGAAATTCGT
CDC20	NM 001255	CCTCTGGTCTCCCCATTACA	CAACTCAAAACAGCGCCATA
CENPF	NM 016343	GTCAGCGACAAAATGCAGAA	TGCATATTCTTGGCTTGCTG
CEP55	NM 018131	CAGTTGTCTGCTGCAACCTC	GAGCAGCTGTTTCCGTTTTC
CHEK1	NM 001274	CAGGGGTGGTTTATCTGCAT	TCCACAGGACCAAACATCAA
CIT	NM 007174	AAGTCTCAGCCCAGCACCTA	CCAGGGATCTGATCTTGGAA
CKS2	NM 001827	CACTACGAGTACCGGCATGTT	ATGTGGTTCTGGCTCATGAAT
DLG7	NM 014750	GTCTCACTACTGAATGCCACCTT	GTCTGGCATGTTCTTGATGTCT
E2F2	NM 004091	AGGCCAAGAACAACATCCAGT	CACATAGGCCAGCCTCTTGTT
GINS2	NM 016095	AGACAGAAATGTCGCCTGCT	AGCAGACACTCGGAGTTTGG
LDB2	NM001290	AAGGCAACCAACAACCAAAC	TTGGCTCTCCTACCACCATC
MAD2L1	NM 002358	CTTCTCATTCGGCATCAACA	CCAGGACCTCACCACTTTC

Gene	Gene Acc	Forward 5'-3'	Reverse 5'-3'
NCAPG	NM 022346	TACCGCACGATGGATGATAA	CACTGCATTGCTGTTTGCTT
PBK	NM 018492	CAGCCAAGATCCTTTTCCAG	TGCCAATGTAACAAGCCTCA
POLQ	NM 199420	GGCACAGATGGAGGAGAGAG	CTGCAATGCTCCTGAAAACA
PTTG1	NM 004219	GGGTCTGGACCTTCAATCAA	GGCAGGAACAGAGCTTTTTG
RPA3	NM 002847	AAGCCTGTCTGCTTCGTAGG	TTGGCGGTTACTCTTCCAAC
RRM2	NM 001034	ACAGAAGCCCGCTGTTTCTA	CCCAGTCTGCCTTCTTCTTG
TOP2A	NM 001067	AATCTCAGAGCTTCCCGTCA	TGCCTCTGCCAGTTTTTCTT
TWIST1	NM000474	TCTTACGAGGAGCTGCAGACGCA	ATCTTGGAGTCCAGCTCGTCGCT
UBE2C	NM007019	CTCGCTAGAGTTCCCCAGTG	AAAAGCTGTGGGGTTTTTCC

2.5. Generation of TWIST-1 Over-expressing MSC Lines

2.5.1. Heat Shock Transformation

This work was performed in accordance with the SA Pathology/IMVS biosafety committee licence number PC1NLRD116/2009. The pRUF-IRES-GFP vector was a kind donation by Mr. Paul Moretti (Hanson Institue, Adelaide, SA, Australia). Retroviral vectors pRUF-IRES-GFP **(Figure 2.1A)**, pRUF-IRES-GFP-TWIST-1 (**Figure 2.1B**), VSVG and pGP (SBI System Biosciences) were transformed into chemically competent JM109 (ATCC, Manassas, VA, USA) cells for amplification. Ampoules of JM109 cells cryopreserved at -80^{o}C were removed from the freezer and thawed on ice for 10 minutes. Transformation involved incubating the cells on ice for 30 minutes after the addition of 500 – 1000 ng DNA from one of the plasmids to be amplified. Cells were then incubated at 42^{o}C for 90 seconds before being cooled on ice for a further 2 minutes. At this time, 200 µL of SOC media was added and the mixture was incubated for 45 minutes at 37^{o}C. Following this incubation, 5 µL of cell suspension was plated onto ampicillin (50 µg/mL) agar plates in order to generate single colonies. SOC media was used as it contains protein precursors essential for the rapid repair of cell walls damaged by heat shock transformation.

2.5.2. Maxiprep Plasmid Preparation

As described in **Section 1.5.1**, transformed JM109 cells were cultured on ampicillin agar plates and incubated overnight at 37^{o}C. Single colonies were selected and starter cultures were generated in 5 mL of LB media and cultured overnight at 37^{o}C. Following this, 1 mL of starter culture was transferred to 500 mL LB media and amplified overnight at 37^{o}C.

Figure 2.1 Mammalian Expression Vectors Used in Retroviral Transduction Over-Expression Studies

DPSC and PDLSC lines were stably transduced with (**A**) the pRUF-IRES-GFP expression vector to create vector control cell lines and (**B**) the pRUF-IRES-GFP-TWIST-1 expression vector to create TWIST-1 over-expressing MSC lines.

Figure 2.1

A

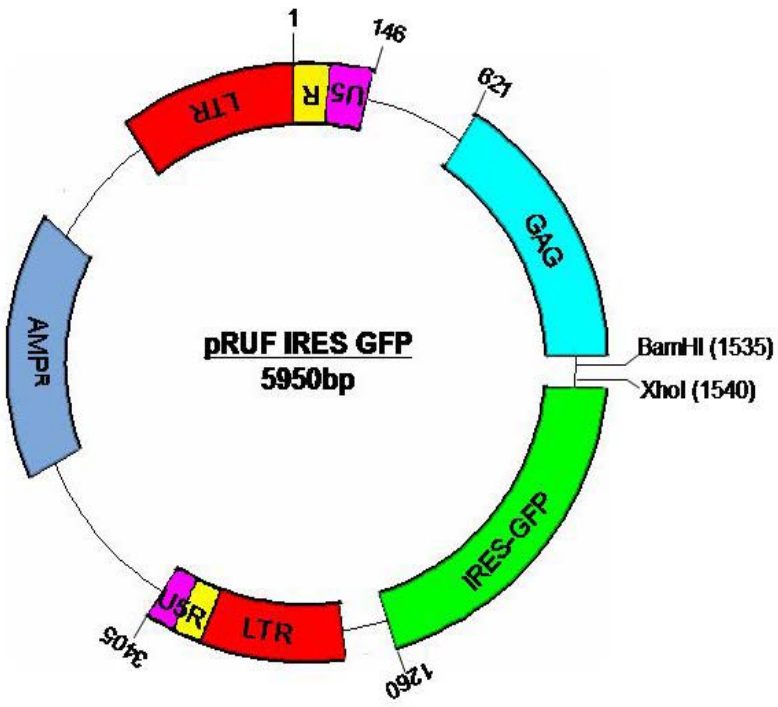
1
146
621
LTR
R
U5
GAG
AMPR
pRUF IRES GFP
5950bp
BamHI (1535)
XhoI (1540)
IRES-GFP
U5
LTR
3405
1260

B

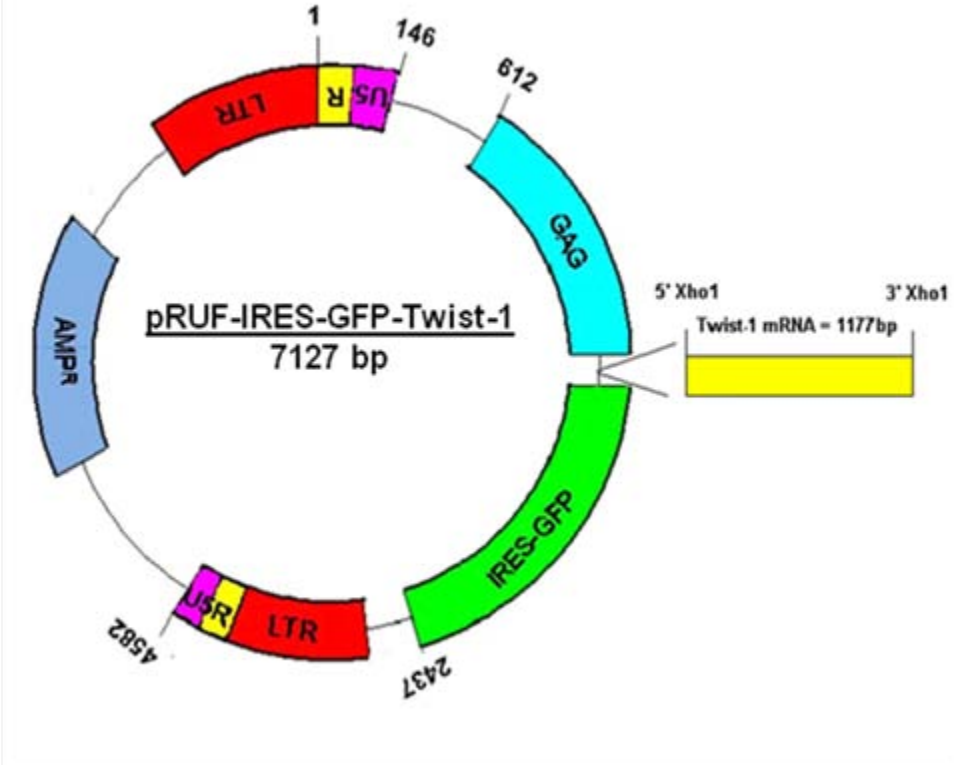
1
146
612
LTR
R
U5
GAG
AMPR
pRUF-IRES-GFP-Twist-1
7127 bp
5' Xho1
3' Xho1
Twist-1 mRNA = 1177bp
IRES-GFP
U5
LTR
4582
2437

The remaining 4 mL of starter culture was stored at 4^{o}C. The reaction that produced the highest yield was diluted 1:1 into 80% glycerol and preserved at -80^{o}C for future plasmid amplification. A maxiprep of each culture was then conducted using the QIAGEN® Midi or Maxi preparation following the protocol in the QIAGEN® Plasmid Purification Handbook (Qiagen, Doncaster, VIC, Australia). Cultures were centrifuged at 6,000 x *g* for 15 minutes at 4^{o}C to harvest the bacterial cells. The bacterial pellet was then resuspended in resuspension buffer P1 (50 mM Tris-Cl, pH 8.0, 10 mM EDTA, 100 µg/mL RNase A) and once resuspended, lysis buffer P2 (200 mM NaOH and 1% SDS (w/v)) was added and the suspension was mixed vigorously. Following a 5 minute incubation, neutralisation buffer P3 (3.0 M potassium acetate, pH 5.5) was added, the samples were mixed thoroughly and transferred into QIAfilter cartridges (Qiagen, Doncaster, VIC, Australia). Following a 10 minute incubation at room temperature, cell lysates were filtered through previously equilibrated Qiagen tips. The tips were equilibrated by applying equilibration buffer QBT (750 mM NaCl, 50 mM MOPS, pH 7.0 and 15% ispropanol (v/v, 0.15% Triton® X-100 (v/v)). This cell lysates were allowed to enter the resin by gravity flow. The QIAGEN-tip was then washed with 2 x 30 mL of wash buffer QC (1.0 M NaCl, 50 mM MOPS, pH 7.0, 15% isopropanol (v/v)). Following the washes DNA was eluted by the addition of 15 mL of elution buffer QF (1.25 M NaCl, 50 mM Tris-Cl, pH 8.5, 15% ispropanol) to ensure maximum DNA yield. To precipitate the DNA, 5 mL of isopropanol was added to the mixture and spun at 15,000 x *g* for 30 minutes at 4^{o}C. The supernatant was then discarded and the DNA pellet was resuspended using a combination of 400 µL TE buffer (10 mM Tris-HCL pH 7.4, 1 mM EDTA), 25 µL 3 M sodium acetate (Sigma Aldrich, St Louis, MO, USA) and 1 mL of 100% ethanol (this is an in house modification to the original Qiagen protocol). The mixture was inverted and centrifuged at 13,000 rpm for 5 minutes in a 1.7 mL Eppendorf tube. The pellet was washed twice in 75% ethanol for 2 minutes and then allowed to air dry in a cell culture biohazard laminar flow hood. Once the pellet was air dried, 200 µL of TE buffer (Qiagen, Doncaster, Victoria, Australia) was added to resuspend the DNA. Each sample was then analysed using a NanoDrop Mass spectrometer (NanoDrop ND-1000 Spectrophotometer, Biolabgroup, Clayton, VIC, Australia) to determine the concentration and purity of DNA (described in **Section 1.4.2**).

2.5.3. Retroviral Supernatant Preparation

HEK293-T cells were grown to confluence in a T^{75} culture flask before being plated to 6 cm culture dishes at a density of 9 x 10^5 cells per dish. These cells were incubated overnight at 37^{o}C to ensure adherence. On the following day, mixtures of 5 µg retroviral GFP plasmid, 4 µg pGP plasmid, 4µg of VSV-G plasmid and 500 µl of DMEM + additives were incubated for 5 minutes at room temperature before adding 20 µL of Lipofectamine 2000 (Invitrogen, Carlsbad, Canada) in 500 µL DMEM + additives. This combined mixture was then incubated at room temperature for 20 minutes before being added drop wise to HEK 293-T cells. Cells were allowed to incubate for 48 hours at 37^{o}C in 5% CO_2. Successful transfection was assessed by examining the cells for green fluorescence using a UV fluorescent microscope (Olympus, Tokyo, Japan).

2.5.4. Retroviral Infection

Once transfection of the producer cells was verified at greater than 80% using a fluorescent microscope **(Figure 2.2A)**, supernatant, containing viral particles, was removed from HEK 293-T cells using a cannula attached to a 20 mL syringe This solution was then filtered through a 0.45µm low protein binding syringe filter (Nalgene, Interpath, Heidelberg West, VIC, Australia) to remove any cellular debris or cells. Filtered viral supernatant was diluted 1:1 with α-MEM + additives supplemented with polybrene (4 µg/mL) (Sigma-Aldrich, St. Louis, MO, USA) and subsequently used to transduce the target MSC populations for 48 hours. After this, GFP expression was verified using a UV microscope. Cells were then reinfected in the same manner described to increase the number of infected cells. After a further 48 hours the viral supernatant was removed and replaced with appropriate growth media, α-MEM + additives.

2.5.5. Selection of Stably Transduced Cell Lines by FACS

Infected MSCs were cell sorted based on GFP expression for all vectors used. To prepare samples for sorting, cells (not more than 75% confluent) were washed with HBSS and liberated using 0.05% trypsin/EDTA digestion. Trypsin was inactivated using HFF buffer and cells were transferred to 14 mL spin tubes. Cells were then centrifuged at 800 *g* for 10 minutes at 4^{o}C. Supernatant was removed and the cell pellets were resuspended and washed in HBSS/ 3% FCS. After the first wash, cells were resuspended in HBSS/3% FCS and filtered through a 40 µm cell strainer (BD Biosciences, Erembodegem, Belgium). This filtered cell suspension was centrifuged under the same conditions and resuspended in 1

Figure 2.2 Enforcement of TWIST-1 Expression in DPSC and PDLSC Populations

Retroviral packaging cell line, HEK 293-T was used in transduction of DPSC and PDLSC populations. Representative micrographs demonstrate (**A**) the transfection efficiency of HEK 293-T cells (scale bar = 50µm) and (**B**) the transduction efficiency of TWIST-1 over-expressing MSC populations (scale bar = 50µ).

Figure 2.2

A

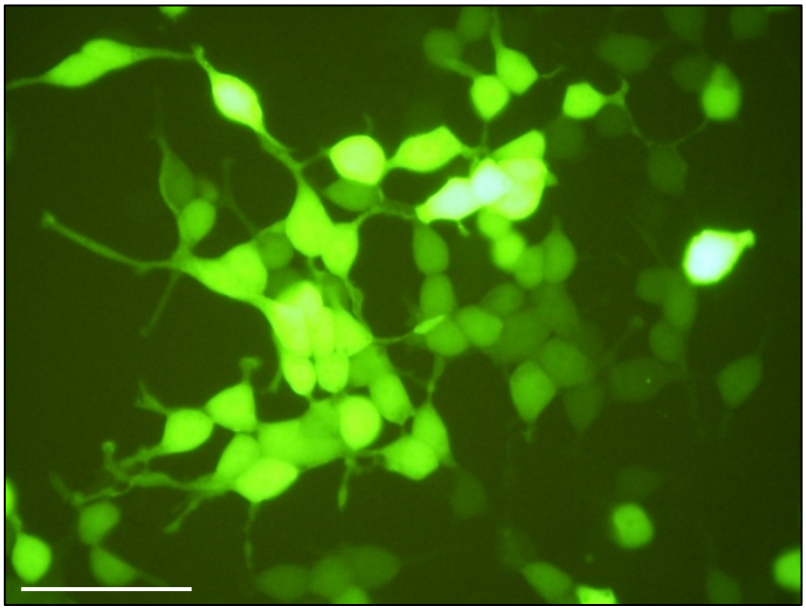

B

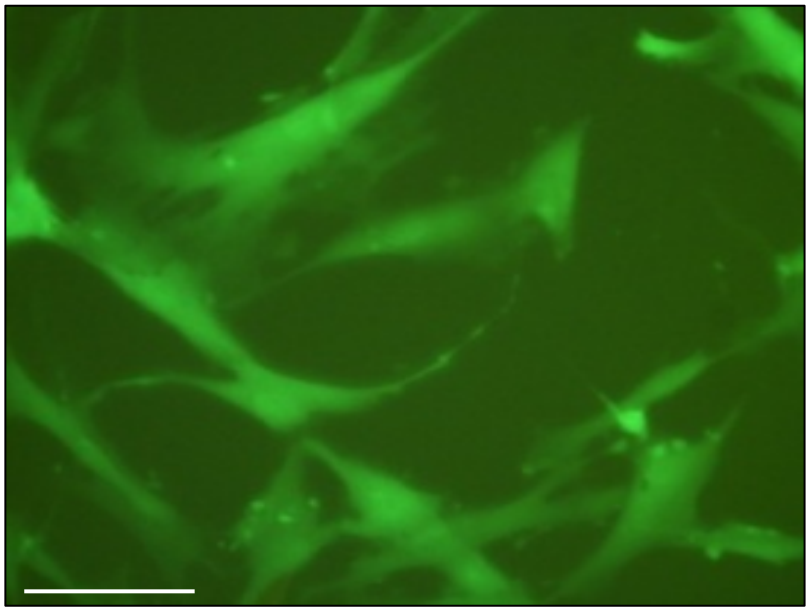

mL HBSS/ 3% FCS before being transferred to a 5 mL polypropylene round bottom tube (Becton Dickinson, Franklin Lakes, NJ, USA). The cells were then sorted using an Epics Altra HyPer Sort FACS machine (Beckman Coulter, Miami, Florida, USA). The brightest 30% of cells in the positive fraction of the population **(Figure 2.2B)** were selected using Expo 32 Multi-comp software (Software version 1.2B). This selected portion of the population was collected in pre-prepared 5 mL polypropylene collection tubes containing 2 mL of α-MEM + additives. These cells were then centrifuged at 1500 *g* for 2 minutes at room temperature, resuspended in α-MEM + additives and plated at 8 x 10^3 cells/cm^2.

2.6. Protein Techniques

2.6.1. Preparation of Protein Lysates

Whole cell lysates were prepared on ice from one confluent 10 cm dish (approximately 3 x 10^6 cells). Cells were washed once with 10 mL of ice cold 1xPBS before 400 µL of lysis buffer was added and cells were scraped off the dish using a cell scraper. The constituents of lysis buffer were dissolved in RO water and at their final concentrations included 20 mM Tris-HCl pH 7.4, 2 mM EDTA, 150 mM NaCl, 1% Triton-X100, 2 mM Sodium Vanadate, 2 mM Sodium Fluoride, 0.1% SDS, 2 mM PMSF, 10 mM Sodium Pyrophosphate and 10% Glycerol in RO water. Cells were then transferred to an eppendorf tube and vortexed. This preparation mixture was incubated on ice for approximately 30 minutes and sonicated for 10 seconds on setting 3 of a Microson ultrasonic cell disruptor (XL2007, Misonix Inc., Farmingdale, NY, USA). Cell lysate was then centrifuged for 30 minutes at 16,000 x *g* at 4^{o}C. This centrifugation was enough to separate the out the nuclear proteins and other cellular debris which formed a pellet at the bottom of the tube. The supernatant was transferred to a new tube and stored at –80^{o}C.

2.6.2. RCDC Protein Assay

The protein concentration of all cell extracts was determined usind the RCDC Protein Assay Kit (BioRad, Hercules, CA, USA) according to the manufacturer's instructions. Serial dilutions of BSA (Bovine Serum Albumin, 2mg/mL, JRH Bioscience) at 1.5 mg/mL, 1 mg/mL, 0.75 mg/mL 0.5 mg/mL 0.2mg/mL and were used to create a standard curve.

2.6.3. Western Immunoblotting

Prior to loading onto gels for poly acrylamide gel electrophoresis (PAGE), protein lysate sample were boiled at 100^{o}C for 5 minutes and then centrifuged at maximum speed for 5 minutes at 4^{o}C.

The stacking layer gel was made by mixing 5.6 mL of MillQ water, 8.0 mL of 30% Bis-acrylamide (BioRad, Gladesville, NSW, Australia), 5.0 mL of 1.5 M Tris (Sigma-Aldrich, St. Louis, MO, USA), 200 µL 10% SDS (Merck, Kilsyth, VIC, Australia), 200 µL 10% of APS (BioRad, Gladesville, NSW, Australia) and 20 µL of TEMED. The separating layer gel was made by mixing 5.061 mL of MillQ water, 1.5 mL of 30% Bis-acrylamide (BioRad, Gladesville, NSW, Australia), 2.25 mL of 0.5 M Tris (Sigma-Aldrich, St. Louis, MO, USA), 90 µL 10% SDS (Merck, Kilsyth, VIC, Australia), 90 µL 10% of APS (BioRad, Gladesville, NSW, Australia) and 9 µL of TEMED. 50µg of protein per lane was transferred to a 12% PAGE gel, and run in SDS running buffer (0.3% (w/v) Tris-HCL, 1.44% (w/v) Glycine, 0.1% (w/v) SDS in water) at 15mA per gel for the stacking layer and 30mA per gel for the separating layer.

The gels were then transferred to a Hybond-P 0.45µm PVDF membrane (Amesham Bioscience UK Limited, Little Chalfont, UK) using the SEMI-PHOR^{TM} Hoefer Semi Dry blotter (Hoefer Scientific Instruments, San Fransisco, CA, USA). The membranes were washed three times with TBS-T (Tris buffered saline/0.1% Tween 20) (Sigma Aldrich, St Louis, MO, USA) and blocked with 50 mL blocking buffer overnight at 4^{o}C. Blocking buffer is made up of 5% Amersham block (Amersham Biosciences UK Limited, Little Chalfont, UK) in TBS-T. After blocking, the membranes were washed three times using TBS-T to remove any residual blocking buffer solids.

The membrane was then ready to be probed with primary antibodies. For the purpose of identification of Twist-1 overexpression at the protein level, the mouse monoclonal Twist antibody (Twist2C1a, IgG1; sc81417) (Santa Cruz Biotechnology, Santa Cruz, CA, USA) was used. This antibody was diluted 1 in 200 into 5% BSA/TBS-T. The membrane and antibody were incubated overnight at 4^{o}C on a rocker. The membrane was then washed three times in TBS-T. Following the final wash, the membrane was probed with a secondary antibody (goat anti-mouse Ig affinity isolated alkaline phosphotase conjugated, P326A) (Chemicon, Melbourne, VIC, Australia) diluted 1 in 2000 into 5%BSA/TBS-T. The secondary antibody was incubated with the membrane for 1 hour at room temperature

on a rocker. The membrane was then washed a further three times with TBS-T rinsed three times with TBS. Antibody binding was visualised by enhanced chemiluminescence using 1mL ECF substrate (GE Healthcare, Europa Bio Products, RPN5785) using a Typhoon 9410 (Amersham, UK) using 488 nm excitation.

2.7. Cell Imaging

Images were taken using an Olympus CKX41 microscope with attached Olympus U-RFLT50 UV light and DP20 camera (Olympus, Tokyo, Japan). Cells were placed on microscope stage and microscope was manually adjusted to correct focal point.

2.8. Statistical Analysis

Data analysis was carried out using Microsoft Excel 2007 (software version 12.0.4518.1014, Microsoft, Redmund, WA, USA). Data points are reported as the mean ± standard deviation (SD) and statistical significance of (*) $p \leq 0.05$ was determined using the unpaired Student t-test.

Chapter 3:

Functional Characterisation of Clonal Populations of BMSC, DPSC and PDLSC

3. Functional Characterisation of Clonal BMSC, DPSC and PDLSC Populations

The defining features of adult MSCs include their ability to undergo extensive proliferation, express an appropriate immunophenotype and demonstrate a capacity for multi-directional differentiation [38, 234]. These properties account for the role that the MSC-like populations play in maintenance, repair and regeneration of the tissues that they are derived from. Due to the complexity of processes involved in tissue maintenance, it is reasonable to consider that MSC-like populations present in different tissues contain subpopulations of cells at various stages of development and exhibit various levels of differentiation and proliferation potentials [12, 53, 235]. It was initially demonstrated by Friedenstein and colleagues that rodent bone marrow derived CFU-F colonies arise from single cells [11, 236] and this finding was later confirmed for cell populations isolated from human bone marrow [237]. The individual cells that possessed the capacity to give rise to CFU-F and their progeny were later termed and classified as MSCs [36]. Analysis of MSC populations at a clonal level allows for the unique opportunity to characterise the progeny of a single progenitor cell within the isolated population.

Numerous research groups have addressed the issue of heterogeneity within MSC populations, and have conducted studies to assess the differences exhibited by clonal populations in terms of cell size, morphology, growth and developmental potentials and, more recently, genomic and proteomic profiles. Owen *et al* observed that whilst all the colonies grown from individual cells isolated from rabbit bone marrow showed the potential to self renew, they demonstrated differences in size and morphology as well as variations of expression of Alkaline Phosphatase (marker of osteogenic differentiation) activity [235]. In a clonal analysis study of human BMSCs, Kuznetsov *et al* demonstrated variability in proliferation and differentiation capacities of single cell derived populations. They showed that approximately 60% of the clones tested had the ability to undergo osteogenesis *in vivo* whilst the remainder failed to form bone when transplanted into immunodeficient mice. The transplants presented with a variable degree of bone development and formation of haematopoietic tissue was identified in transplants where bone production was abundant. They hypothesised that the cells with the ability to form abundant bone and a haematopoietic microenvironment are more immature in their nature

in comparison to potentially lineage committed progenitors that failed to differentiate *in vivo* [53]. Muraglia and colleagues, characterised the differentiation potential of clonaly expanded human BMSCs, and found that the populations contained uni-, bi- and tri-potential clones in terms of their osteogenic, chondrogenic and adipogenic differentiation [238]. As the clones proliferated and progressed towards senescence they lost lineage differentiation potential. Clones that initially exhibited osteo-chondro-adipogenic differentiation potential were compared to clones of initial osteo-chondrogenic potential to determine the maintenance of their differentiation potential through mitotic divisions. These results indicated that adipogenic potential is lost first in the tri-potential clones and that chondrogenic potential was lost earlier in the bi-potential clones. Hence, these data indicate that an osteogenic lineage is the default linage of BMSCs. Accordingly, Muraglia *et al* hypothesised that the reasons for this predisposition include possible intrinsic commitment of BMSC or favourable osteogenic differentiation conditions during *in vitro* culture [238]. This study clearly described the presence of hierarchy in terms of differentiation amongst clonal bone marrow derived CFU-F.

Characterisation of prospectively isolated clones derived from a subpopulation of BMSCs, selected on their cell surface expression of VCAM-1 (CD106) and STRO-1, demonstrated that high proliferative clonal populations exhibit the capacity to undergo osteogenic, adipogenic and chondrogenic differentiation *in vitro* [12]. In this study all of the assessed high proliferating clones were able to undergo mineralisation and chondrogenesis *in vitro*, whilst 95% of tested clones exhibited adipogenic differentiation potential. A little over half of the clones translated their osteogenic potential *in vivo*, and were able to form organised bone tissue when ectopically transplanted in mice. This work highlights the limitations of cellular characterisation as it shows that a functional profile of MSC populations, obtained through *in vitro* studies, does not necessarily indicate the functional capacity of these cells in an *in vivo* setting [12].

Many other studies have focused on clonal analysis of MSC-like populations in order to characterise the differentiation hierarchy present in the stromal system [239-246]. Moreover, analysis of MSC-like clones has been performed on cells isolated from tissues other than the bone marrow, including dental pulp [97, 247], dermal tissue [248], synovium [249] and periosteum [250].

The heterogeneity within MSC populations presents a major obstacle in the use of these cells in therapeutic applications as it potentially results in cell preparations of undefined properties and unpredictable potential. This highlights the importance of cellular characterisation of MSCs at a clonal level as it gives an opportunity to determine specific stages of development and identify unique markers that could be used for the isolation and expansion of high proliferative, multi-potential MSC subpopulations. In the present study we aimed to characterise clonally derived MSC populations present within bulk cultures of BMSCs, DPSCs and PDLSCs, by comparing their growth and differentiation potentials. The findings of these experiments identified subpopulations of short-lived and long-lived /multi-potential clones within bone marrow, dental pulp and periodontal ligament derived MSCs.

3.1. Results

3.1.1. Differential Growth Potential of BMSC, DPSC and PDLSC Clones *in vitro*

Immunomagnetic selection was used to isolate STRO-1^+ human bone marrow, dental pulp and periodontal ligament clonal MSCs. The STRO-1^+ cells from each tissue were plated at low density and individual plastic-adherent MSC-like colonies were isolated using cloning rings as previously described [12, 97].

A total of 260 colonies obtained from 9 BM donors were expanded in continuous subculture until cellular senescence was achieved. A small proportion of clones (31/260; 12%) exhibited high growth potential which exceeded 20 population doublings (mean generation time of 0.48 PD per day ± 0.05 SD). However, the majority of clones (179/260; 69%) exhibited a limited to moderate proliferation potential and were unable to expand beyond 20 population doublings with a mean generation time of 0.29 PD per day ± 0.03 SD (**Figures 3.1A, 3.2A)**.

Similar studies were performed for clonogenic DPSCs and PDLSCs, previously reported to have higher proliferative potentials and life spans compared to their bone marrow counterparts [41, 110]. A total of 24 clones obtained from 4 dental pulp donors were serially passaged until they had reached cellular senescence. The majority of clones (16/24; 67%) exhibited high growth potential, ranging from 25 to 45 population doublings

Figure 3.1 Differential Growth Potential of MSC-like Clonal Populations.

Clonal cell populations of BMSCs, DPSCs and PDLSCs exhibit varying growth potentials as determined by the population doublings for each clone. The bar graphs depict population doubling values for individual clones of high and low growth potential within the (**A**) BMSC, (**B**) DPSC and (**C**) PDLSC populations.

Figure 3.1

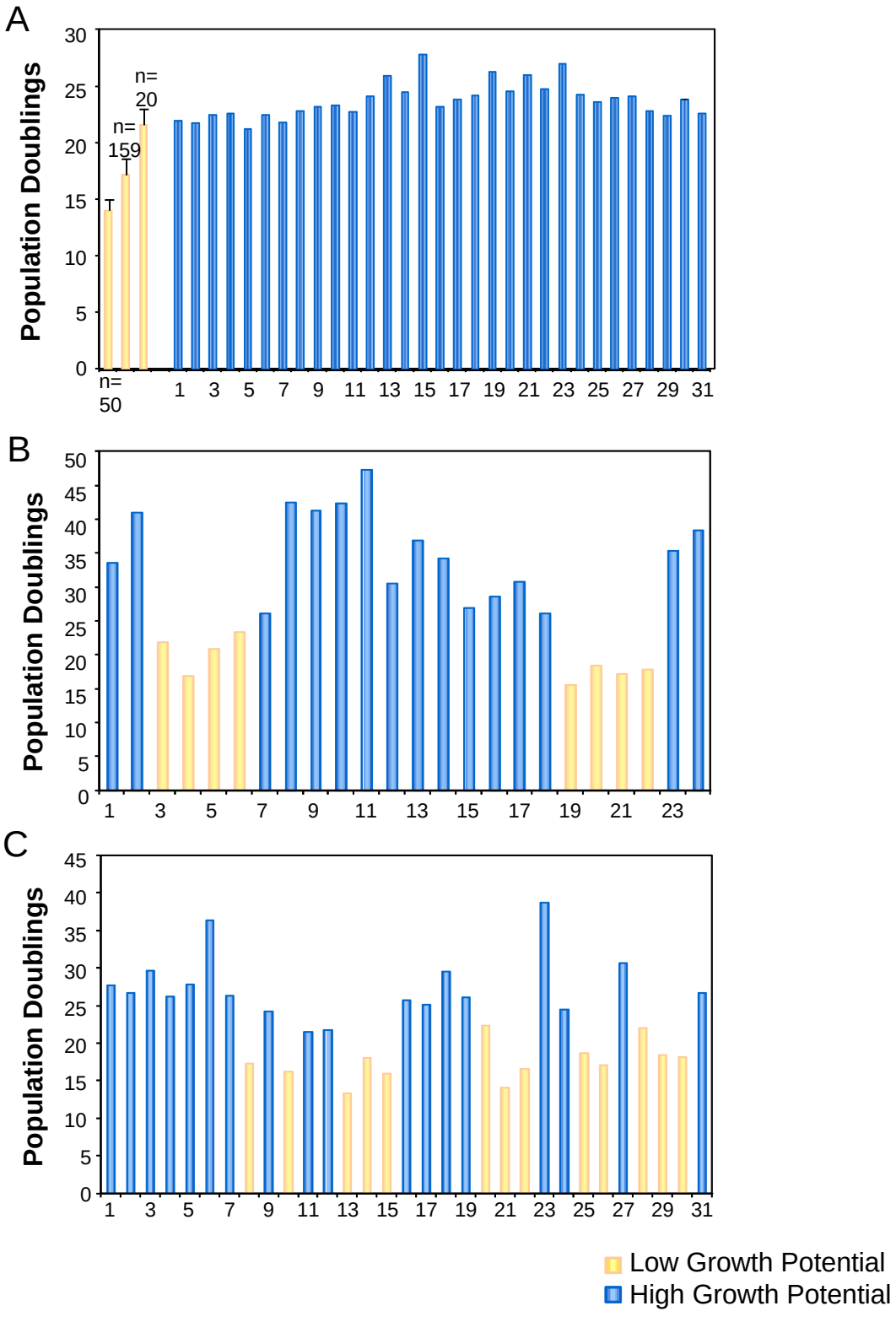
A
Population Doublings
n= 50
n= 159
n= 20
B
Population Doublings
C
Population Doublings
Low Growth Potential
High Growth Potential

Figure 3.2 Differential Growth Potential of MSC-like Clonal Populations.

(**A**) The bar graph shows average population doubling values for clonal cell populations of high growth potential in comparison to cell clones exhibiting low growth potential within the BMSC, DPSC and PDLSC populations. (**B**) Representative micrographs indicate the differences in cellular proliferation and morphology in BMSC, DPSC and PDLSC clones of low and high growth potential (scale bar = 200μm).

Figure 3.2

A

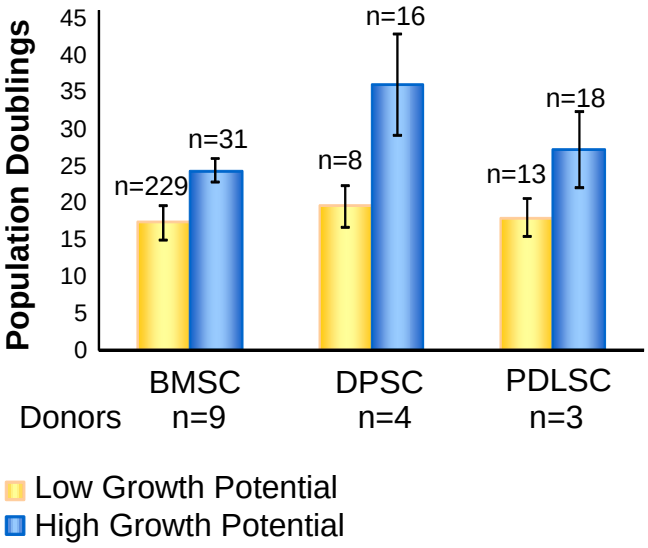
Population Doublings
45
40
35
30
25
20
15
10
5
0
n=229
n=31
n=8
n=16
n=13
n=18
BMSC
n=9
DPSC
n=4
PDLSC
n=3
Donors
Low Growth Potential
High Growth Potential

B

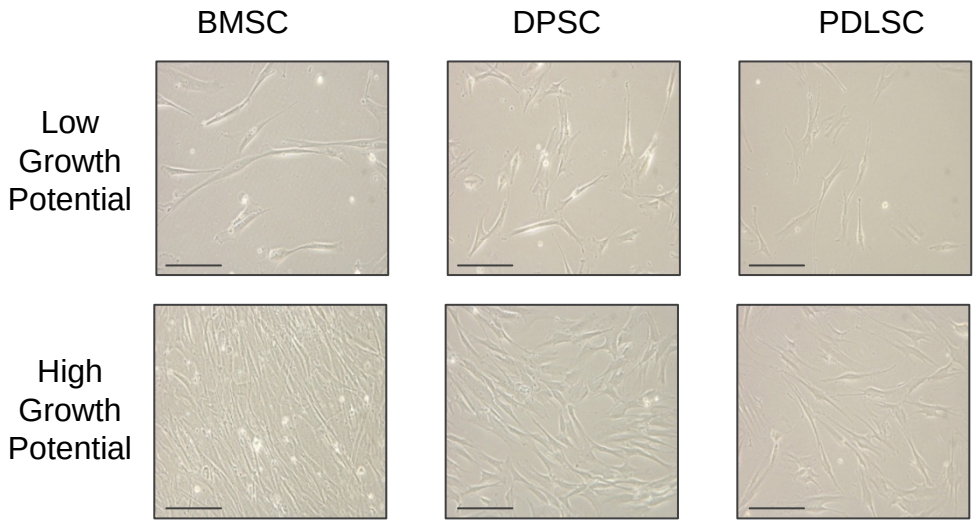
BMSC
DPSC
PDLSC
Low Growth Potential
High Growth Potential

(mean generation time 1.07 PD per day ± 0.25 SD). However, the remainder of the colonies (8/24; 33%) were found to possess low growth potential with a mean generation time of 0.29 PD per day ± 0.01 SD (**Figures 3.1B, 3.2A)**.

Similarly, a total of 31 cell clones obtained from three periodontal ligament donors were expanded in culture to the point of senescence. Approximately 58% (18/31) of the clones exhibited high levels of growth ranging from 21 to 37 population doublings (mean generation time 0.69 PD per day ± 0.13 SD), while the remaining clones demonstrated low growth potential (13/31; 42%) with a mean generation time of 0.30 PD per day ± 0.01 SD (**Figures 3.1C, 3.2A).**

3.1.2. Differential Potential of Long Lived BMSC, DPSC and PDLSC Clones *in vitro*

The majority of low proliferative clones, particularly for BM derived MSC, exhibited a life-span of 15 to 18 population doublings or approximately 30,000 to 300,000 cells per clone, respectively. Therefore, due to limited cell numbers, we were unable to perform functional analyses to assess the differentiation potential of the low growth potential MSC clones. However, these clones were used for the isolation of total RNA for retrospective microarray studies and confirmatory Real-Time PCR analyses in **Chapter 4**. BMSC, DPSC and PDLSC clones that exhibited high levels of growth (greater than 20 population doublings) were subsequently assessed for their potential to differentiate into cells of osteogenic, adipogenic and chondrogenic lineages. After four weeks of osteoinduction, all of the BMSC clones assessed (31/31, 100%) produced Alizarin Red staining mineralized nodules (**Figure 3.3A(i)**) [12, 55]. Furthermore, 90% of the clones (28/31) also exhibited adipogenic differentiation potential, indicated by the formation of Oil Red O positive lipid clusters (**Figure 3.3A(ii)**). Qualitative analyses of the osteogenic differentiation potential were further confirmed by the expression of markers associated with osteogenesis, including bone morphogenetic protein (BMP), bone sialoprotein (BSP), osteoblast associated genes osteopontin (OPN) and RUNX-2, an early osteogenic transcription factor, compared to uninduced control cultures (**Figure 3.3B(i))**. Adipogenic differentiation potential of BMSCs was further confirmed by elevated levels of expression of adipocyte related markers, ADIPSIN and LEPTIN and perixosome proliferator-activated receptor gamma 2 (PPARγ2), a key transcription factor involved in regulation of adipogenesis, compared to uninduced control cultures (**Figure 3.3B(ii))**.

Figure 3.3 Osteogenic and Adipogenic Differentiation Potential of Long Lived Clones within the BMSC Population.

Individual clonal cell populations of long lived BMSCs exhibit varying levels of mineralisation and adipogenic differentiation potential. (**A**)(**i**) Alizarin Red (scale bar = 200μm) and (**ii**) Oil Red O (scale bar = 50μm) staining of clonal BMSC populations cultured under inductive osteogenic and adipogenic conditions, identified the presence of mineral nodules and lipid globules, respectively. All of BMSC clones tested (31 out of 31) showed the potential to form mineral, whilst majority of clones (28 out of 31) showed the potential to form lipid. (**B**) Real-Time PCR analysis demonstrated increased levels of expression of markers of (**i**) osteogenesis, BMP, BSP, OPN and RUNX2 and (**ii**) and adipogenesis, ADIPSIN, LEPTIN and PPARγ2, in BMSC clones treated with induction media in comparison to their controls. The data represent the mean values ± standard deviations of triplicate experiments normalized to the house keeping β-actin gene. Statistical significance of (*) of $p<0.05$ was determined by the unpaired t-test.

Figure 3.3

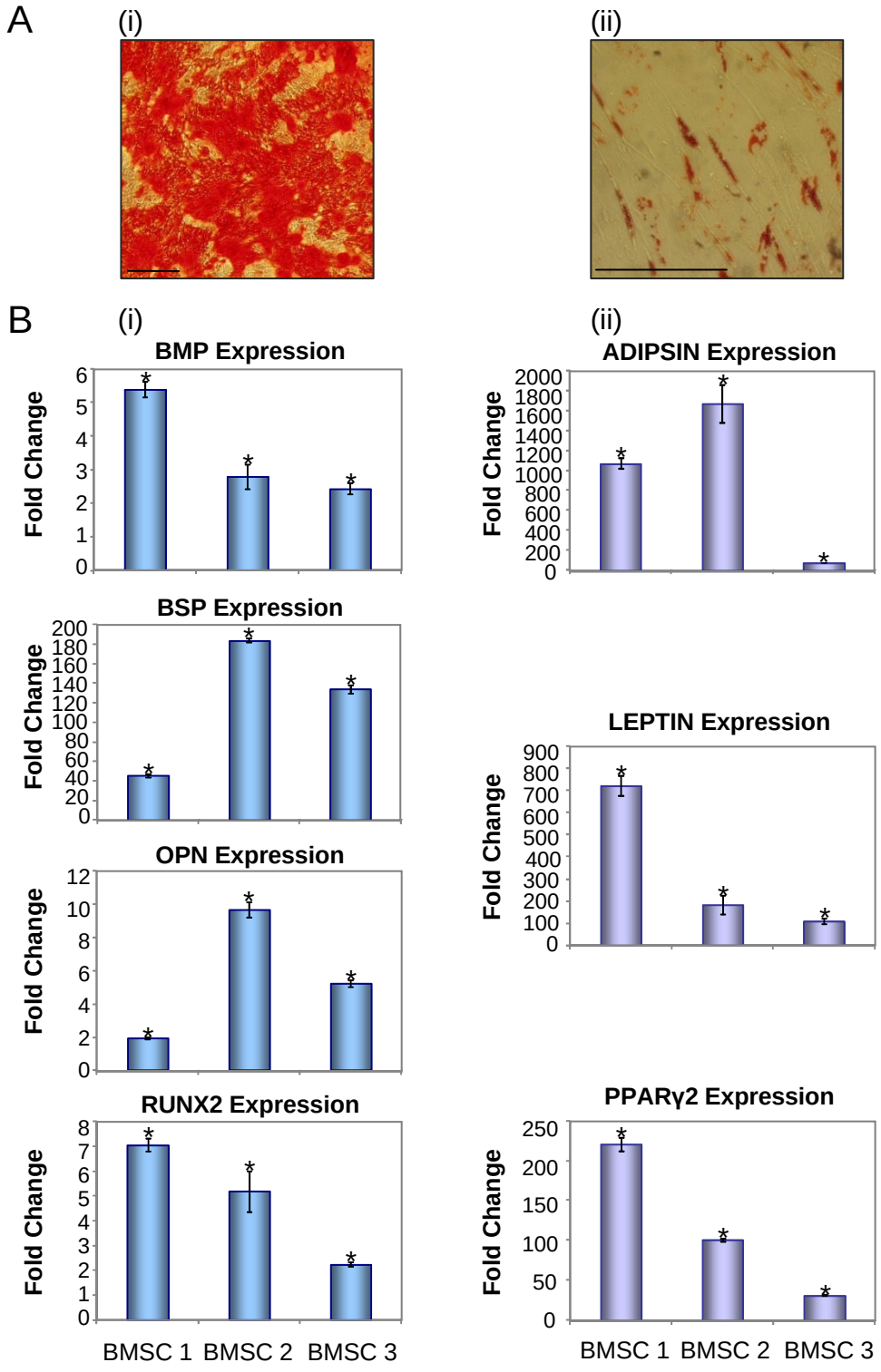
A
(i)
(ii)
B
(i)
(ii)
BMP Expression
ADIPSIN Expression
BSP Expression
LEPTIN Expression
OPN Expression
RUNX2 Expression
PPARγ2 Expression
Fold Change
BMSC 1
BMSC 2
BMSC 3

In parallel studies, 16 high proliferative DPSC clones exhibited the capacity to form Alizarin Red positive mineralized nodules (**Figure 3.4A(i))**, whilst 31% (5/16) also displayed the ability to form Oil Red O positive lipid laden globules (**Figure 3.4A(ii))**. These results were confirmed using Real-Time PCR to determine the levels of expression of BMP, BSP, OPN and RUNX-2, markers involved in osteogenic differentiation (**Figure 3.4B(i))**, and adipogenic markers, ADIPSIN, LEPTIN and PPARγ2 (**Figure 3.4B(ii))**, compared to uninduced control cultures. All of the PDLSC clones (18/18; 100%) demonstrated potential to form mineralized deposits (**Figure 3.5A(i))**, while 37% (7/18) of these clonal lines also formed adipocytes (**Figure 3.5A(ii))**. These findings were associated with an increase in expression levels of osteogenic markers in all of the PDLSC clones (**Figure 3.5B(i))**, and an elevation of ADIPSIN, LEPTIN and PPARγ2 expression in clones that exhibited adipogenic differentiation capacity (**Figure 3.5B(ii))**, in comparison to uninduced control cultures.

Upon identification of their differentiation potential into cells of osteogenic and adipogenic lineages, three bi-potential clones were selected from each of the three tissue types and assessed for their chondrogenic differentiation potential. Selected cell clones, when cultured under inductive conditions, showed capacity to differentiate into cells of the chondrogenic lineage indicated by immunohistochemical staining of cell pellets with anti-collagen type II antibody (**Figures 3.6A, 3.7A, 3.8A**). Quantitative assessment of glycosaminoglycan synthesis confirmed an increase in the production of the polysaccharide by the selected BMSC, DPSC and PDLSC clones (**Figures 3.6B, 3.7B, 3.8B)**. Furthermore, results obtained from Real-Time PCR analysis, showed an up-regulation of expression of markers associated with chondrogenesis, COLLAGEN II, COLLAGEN X and AGGRECAN in cell pellets of selected clones, compared to the corresponding uninduced cultures (**Figures 3.6C, 3.7C, 3.8C).** These clones were designated as high growth and multi-differentiation potential.

3.1.3. Immunophenotypic Profiles of Long Lived, Multi-Potential BMSC, DPSC and PDLSC Clones

To assess the expression profile of cell surface antigens present on long-lived, multi-potential BMSC, DPSC and PDLSC clones, we used a panel of mesenchymal and

Figure 3.4 Osteogenic and Adipogenic Differentiation Potential of Long Lived Clones within the DPSC Population.

Individual clonal cell populations of long lived DPSC exhibit varying levels of mineralization and adipogenic differentiation potential. (**A**)(**i**) Alizarin Red (scale bar = 200μm) and (**ii**) Oil Red O (scale bar = 50μm) staining of clonal DPSC populations cultured under inductive osteogenic and adipogenic conditions, identified the presence of mineral nodules and lipid globules, respectively. 17 out of 17 DPSC clones tested exhibited capacity to form mineral, and 8 out of 17 clones showed potential to form lipid. (**B**) Real-Time PCR analysis demonstrated increased levels of expression of markers of (**i**) osteogenesis, BMP, BSP, OPN and RUNX2, and (**ii**) adipogenesis, ADIPSIN, LEPTIN and PPARγ2, in DPSC clones treated with induction media in comparison to their controls. The data represent the mean values ± standard deviations of triplicate experiments normalized to the house keeping β-actin gene. Statistical significance of (*) of $p<0.05$ was determined by an unpaired t-test.

Figure 3.4

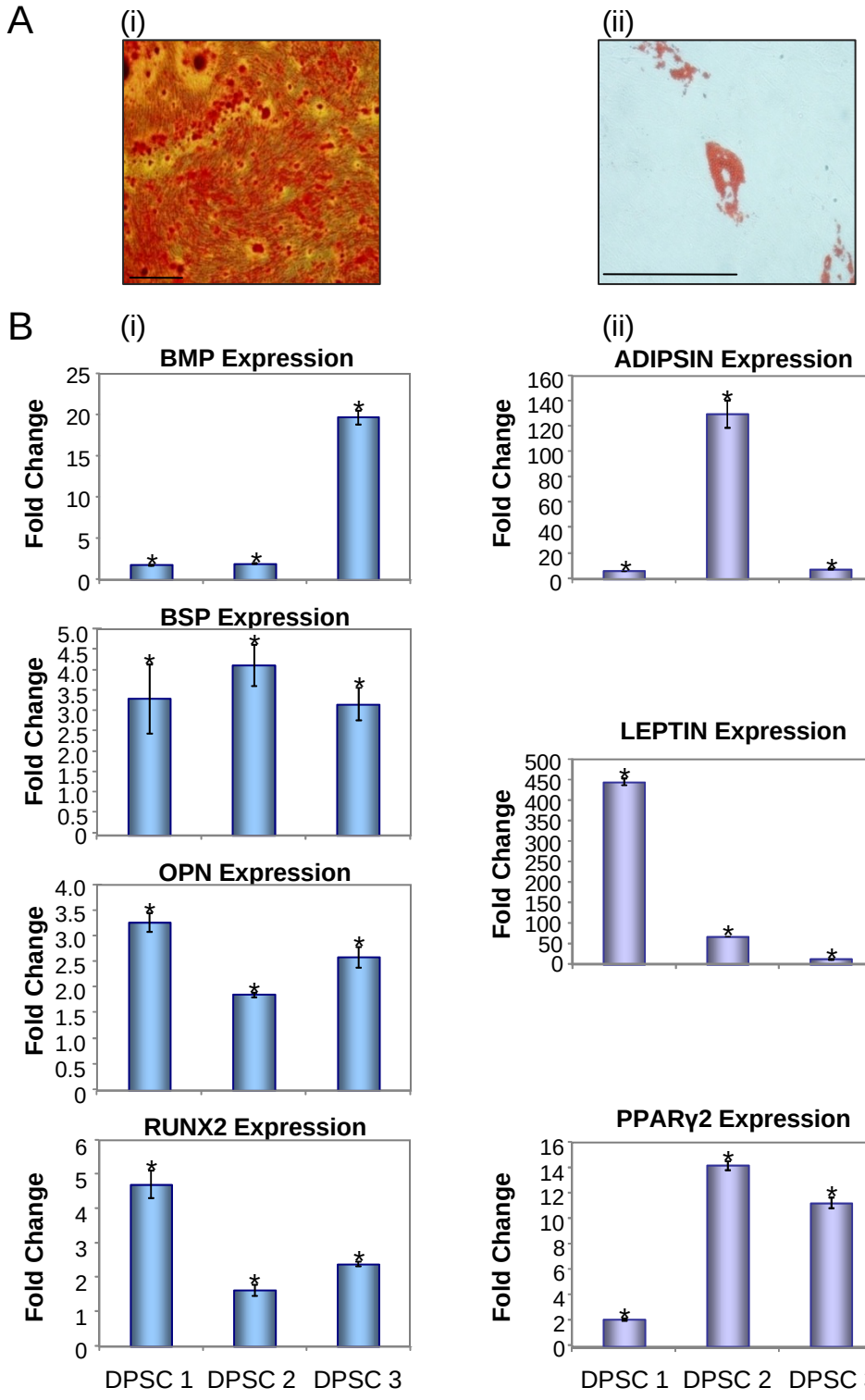
A
(i)
(ii)
B
(i)
(ii)
BMP Expression
ADIPSIN Expression
BSP Expression
LEPTIN Expression
OPN Expression
RUNX2 Expression
PPARγ2 Expression
Fold Change
DPSC 1
DPSC 2
DPSC 3

Figure 3.5 Osteogenic and Adipogenic Differentiation Potential of Long Lived Clones within the PDLSC Population.

Individual clonal cell populations of long lived PDLSC exhibit varying levels of mineralisation and adipogenic differentiation potential. (**A**)(**i**) Alizarin Red (scale bar = 200μm) and (**ii**) Oil Red O (scale bar = 50μm) staining of clonal BMSC, DPSC and PDLSC populations cultured under inductive osteogenic and adipogenic conditions, identified the presence of mineral nodules and lipid globules, respectively. 16 out of 16 PDLSC clones tested showed capacity to form mineral and 5 out of 16 PDLSC clones exhibited potential to form lipid. (**B**) Real-Time PCR analysis demonstrated increased levels of expression of markers of (**i**) osteogenesis, BMP, BSP, OPN and RUNX2, and (**ii**) adipogenesis, ADIPSIN, LEPTIN and PPARγ2, in PDLSC clones treated with induction media in comparison to their controls. The data represent the mean values ± standard deviations of triplicate experiments normalized to the house keeping β-actin gene. Statistical significance of (*) of $p<0.05$ was determined by the unpaired t-test.

Figure 3.5

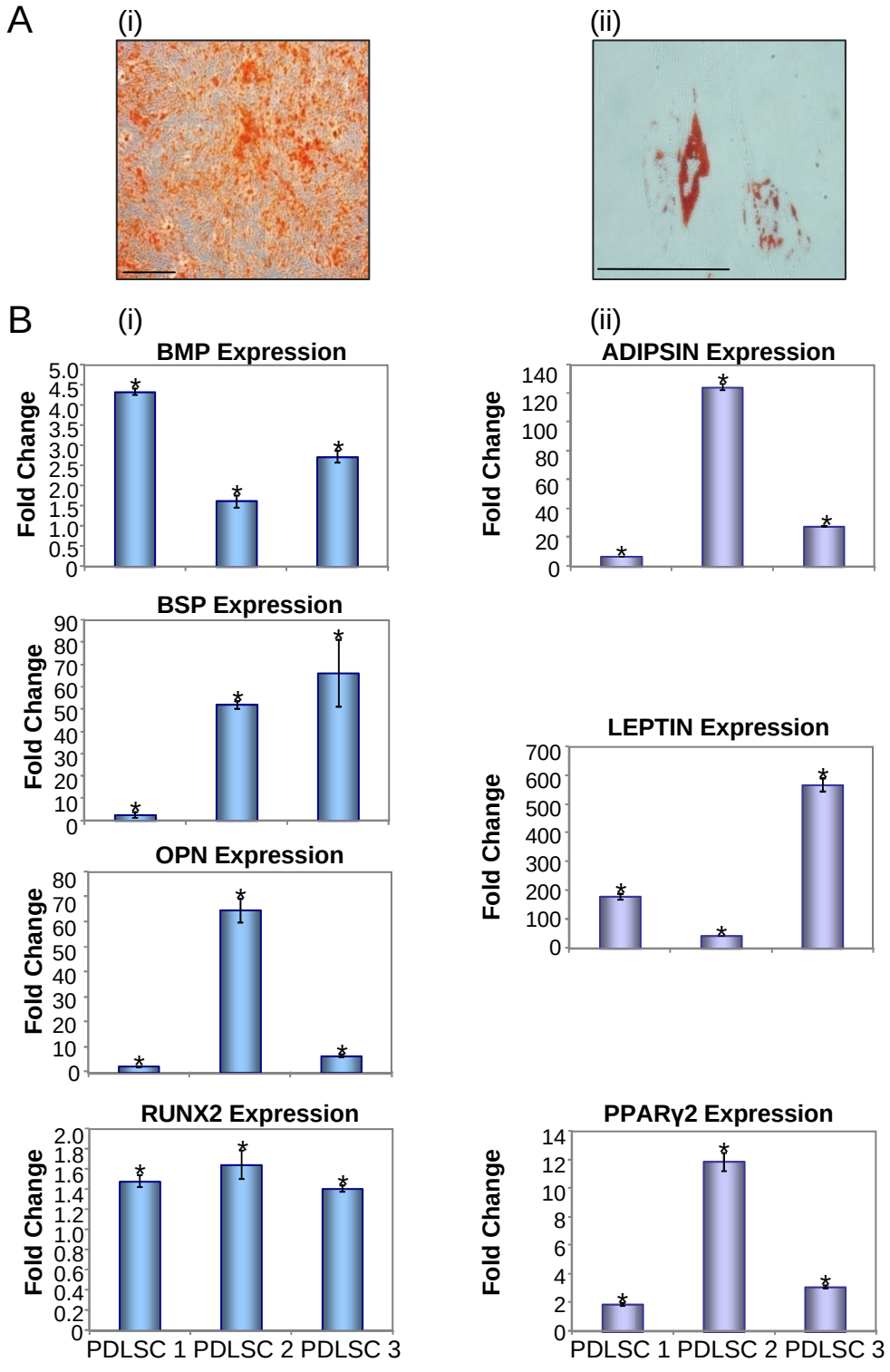
A
(i)
(ii)
B
(i)
(ii)
BMP Expression
ADIPSIN Expression
BSP Expression
LEPTIN Expression
OPN Expression
RUNX2 Expression
PPARγ2 Expression
Fold Change
PDLSC 1 PDLSC 2 PDLSC 3

Figure 3.6 Chondrogenic Differentiation Potential of Long Lived BMSC Population.

Chondrogenic differentiation potential was assessed by immunohistochemical staining of chondrocyte pellets with (**A**) anti-collagen type II antibody (**i**) (scale bar =500 µm), and (**ii**) (scale bar = 50 µm). Haematoxylin and Eosin staining was performed to assess cellular morphology (**iii**) (scale bar =500 µm), and (**iv**) (scale bar = 50 µm). All of the selected BMSC clones showed the capacity to differentiate into cells of chondrogenic lineage. (**B**) Glycosaminoglycan synthesis was measured and normalized to DNA content per well following induction with chondrogenic inductive media. The data represents the mean values ± standard deviation generated from three selected BMSC clones of high growth potential cultured under chondrogenic inductive conditions ± TGFβ1. Statistical significance of (*) of $p<0.05$ was determined using the unpaired t-test. (**C**) Real-Time PCR analysis confirms an increase in expression of markers of chondrogenesis COLLAGEN II, COLLAGEN X and AGGRECAN, in BMSC cultured under inductive conditions in comparison to their controls. The data represent the mean values ± standard deviations of triplicate experiments normalized to the house keeping β-actin gene. Statistical significance of (*) of $p<0.05$ was determined using the unpaired t-test.

Figure 3.6

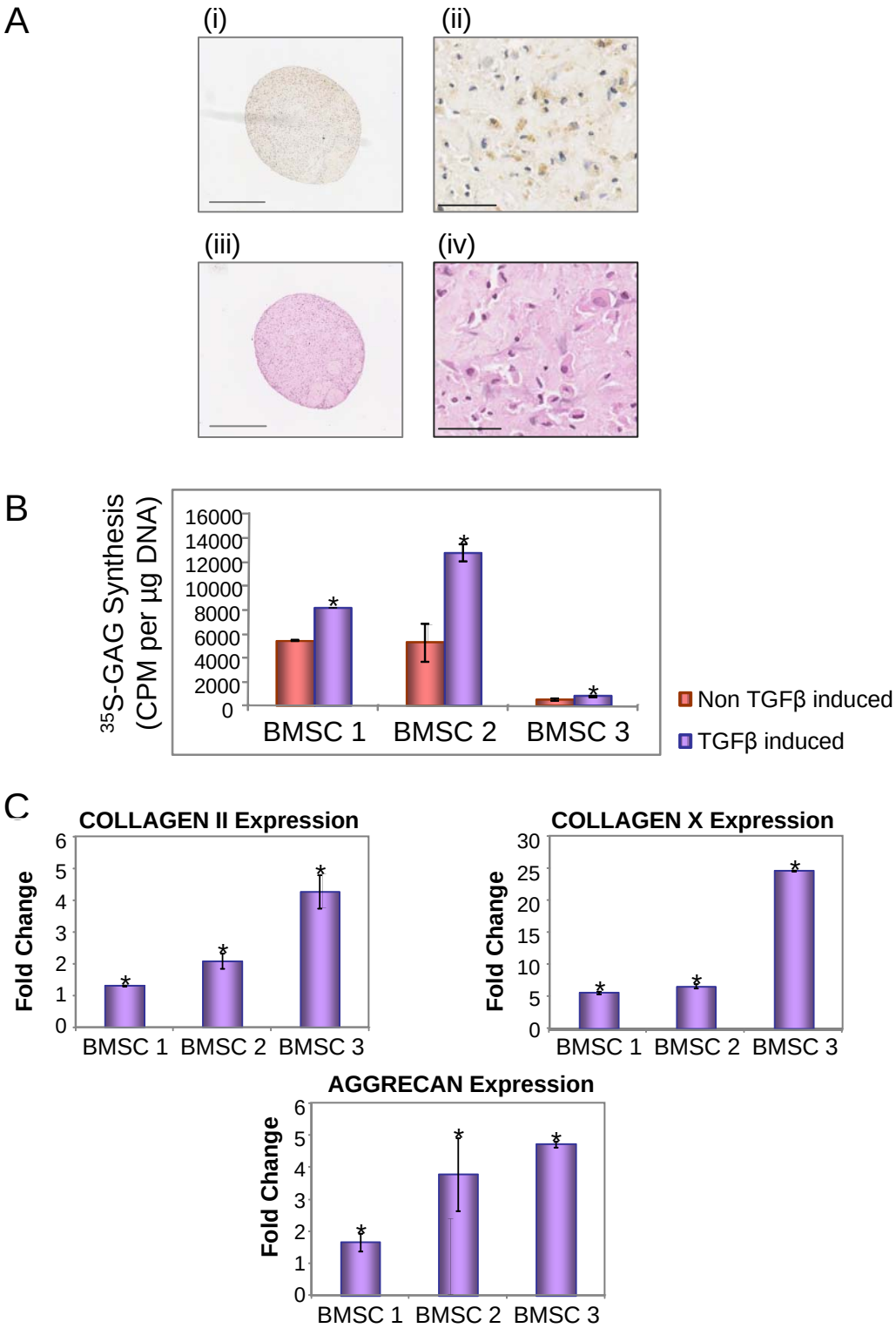
A
(i)
(ii)
(iii)
(iv)
B
35S-GAG Synthesis (CPM per µg DNA)
16000
14000
12000
10000
8000
6000
4000
2000
0
BMSC 1
BMSC 2
BMSC 3
Non TGFβ induced
TGFβ induced
C
COLLAGEN II Expression
Fold Change
6
5
4
3
2
1
0
BMSC 1
BMSC 2
BMSC 3
COLLAGEN X Expression
Fold Change
30
25
20
15
10
5
0
BMSC 1
BMSC 2
BMSC 3
AGGRECAN Expression
Fold Change
6
5
4
3
2
1
0
BMSC 1
BMSC 2
BMSC 3

Figure 3.7 Chondrogenic Differentiation Potential of Long Lived DPSC Population.

Chondrogenic differentiation potential was assessed by immunohistochemical staining of chondrocyte pellets with (**A**) anti-collagen type II antibody (**i**) (scale bar =500 µm), and (**ii**) (scale bar = 50 µm). Haematoxylin and Eosin staining was performed to assess cellular morphology (**iii**) (scale bar =500 µm), and (**iv**) (scale bar = 50 µm). All of the selected DPSC clones showed the capacity to differentiate into cells of chondrogenic lineage. (**B**) Glycosaminoglycan synthesis was measured and normalized to DNA content per well following induction with chondrogenic inductive media. The data represents the mean values ± standard deviation generated from three DPSC clones of high growth potential, cultured under chondrogenic inductive conditions ± TGFβ1. Statistical significance of (*) of $p<0.05$ was determined using the unpaired t-test. (**C**) Real-Time PCR analysis confirms an increase in expression of markers of chondrogenesis COLLAGEN II, COLLAGEN X and AGGRECAN, in DPSC cultured under inductive conditions in comparison to their controls. The data represent the mean values ± standard deviations of triplicate experiments normalized to the house keeping β-actin gene. Statistical significance of (*) of $p<0.05$ was determined using the unpaired t-test.

Figure 3.7

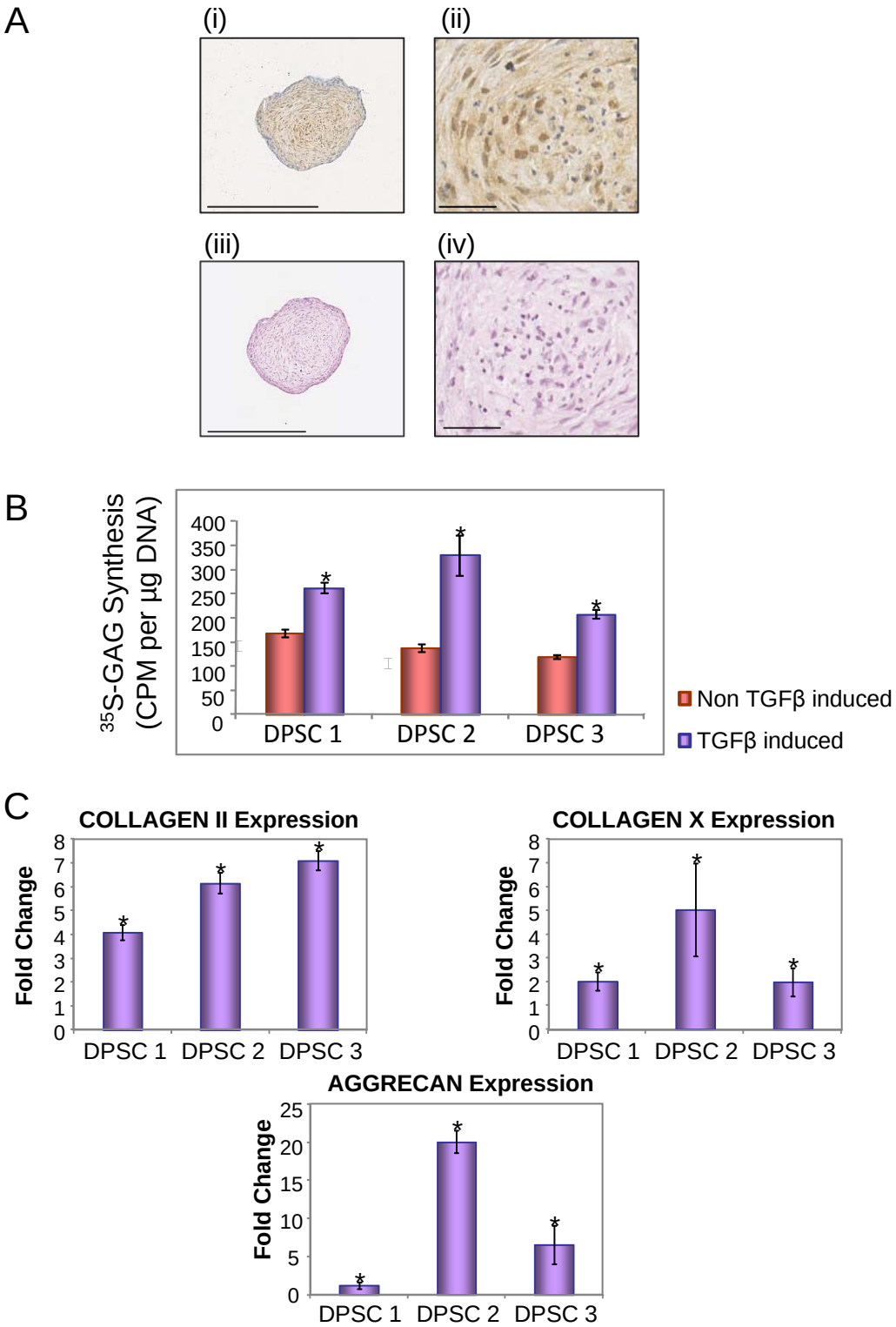
A
(i)
(ii)
(iii)
(iv)
B
35S-GAG Synthesis (CPM per µg DNA)
400
350
300
250
200
150
100
50
0
DPSC 1
DPSC 2
DPSC 3
Non TGFβ induced
TGFβ induced
C
COLLAGEN II Expression
Fold Change
8
7
6
5
4
3
2
1
0
DPSC 1
DPSC 2
DPSC 3
COLLAGEN X Expression
Fold Change
8
7
6
5
4
3
2
1
0
DPSC 1
DPSC 2
DPSC 3
AGGRECAN Expression
Fold Change
25
20
15
10
5
0
DPSC 1
DPSC 2
DPSC 3

Figure 3.8 Chondrogenic Differentiation Potential of Long Lived PDLSC Population.

Chondrogenic differentiation potential was assessed by immunohistochemical staining of chondrocyte pellets with (**A**) anti-collagen type II antibody (**i**) (scale bar =500 µm), and (**ii**) (scale bar = 50 µm). Haematoxylin and Eosin staining was performed to assess cellular morphology (**iii**) (scale bar =500 µm), and (**iv**) (scale bar = 50 µm).All of the selected PDLSC clones showed the capacity to differentiate into cells of chondrogenic lineage. (**B**) Glycosaminoglycan synthesis was measured and normalized to DNA content per well following induction with chondrogenic inductive media. The data represents the mean values ± standard deviation generated from three PDLSC clones of high growth potential, cultured under chondrogenic inductive conditions ± TGFβ1. Statistical significance of (*) of $p<0.05$ was determined using the unpaired t-test. (**C**) Real-Time PCR analysis confirms an increase in expression of markers of chondrogenesis COLLAGEN II, COLLAGEN X and AGGRECAN, in PDLSC cultured under inductive conditions in comparison to their controls. The data represent the mean values ± standard deviations of triplicate experiments normalized to the house keeping β-actin gene. Statistical significance of (*) of $p<0.05$ was determined using the unpaired t-test.

Figure 3.8

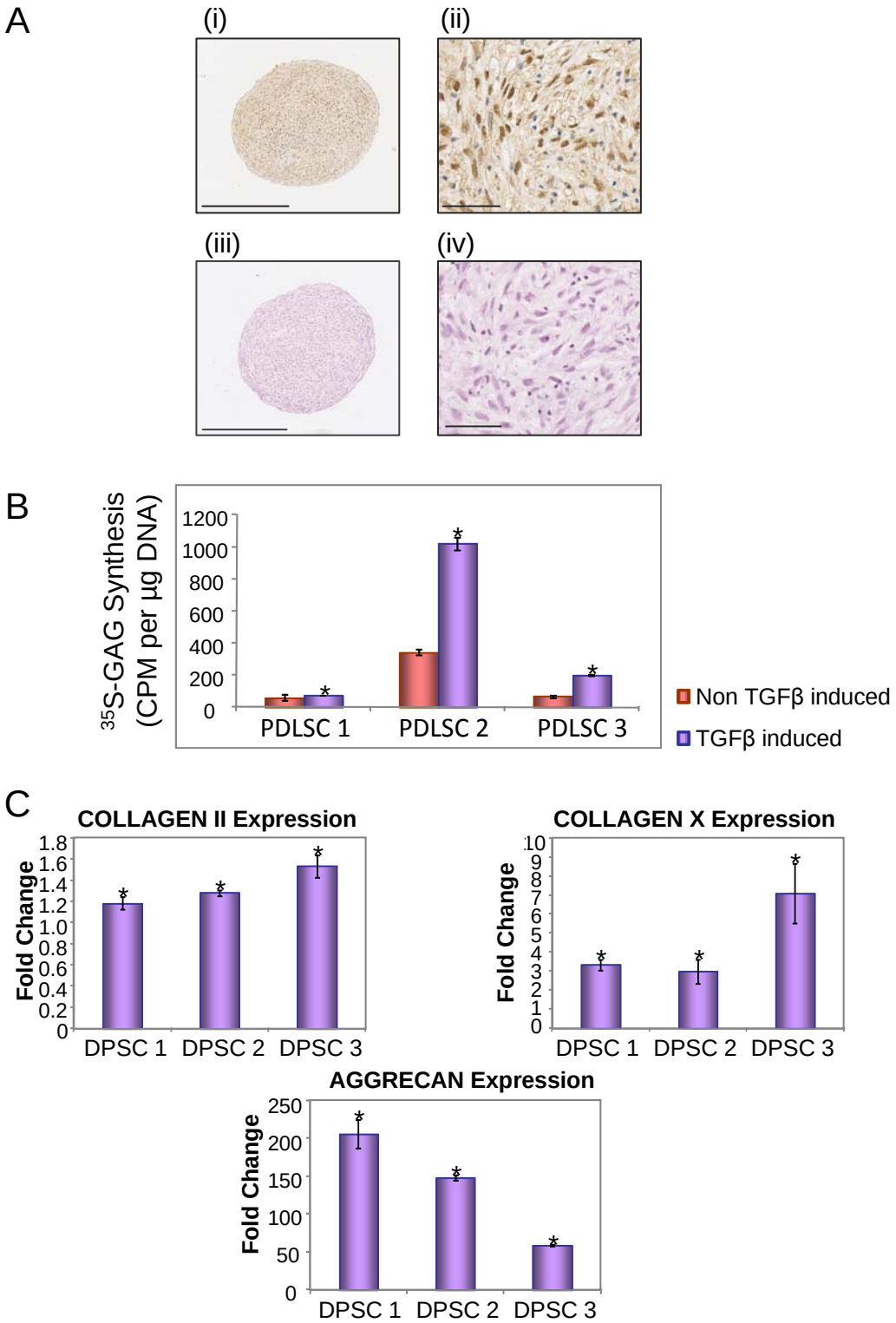
A
(i)
(ii)
(iii)
(iv)
B
35S-GAG Synthesis (CPM per µg DNA)
1200
1000
800
600
400
200
0
PDLSC 1
PDLSC 2
PDLSC 3
Non TGFβ induced
TGFβ induced
C
COLLAGEN II Expression
Fold Change
1.8
1.6
1.4
1.2
1.0
0.8
0.6
0.4
0.2
0
DPSC 1
DPSC 2
DPSC 3
COLLAGEN X Expression
Fold Change
10
9
8
7
6
5
4
3
2
1
0
DPSC 1
DPSC 2
DPSC 3
AGGRECAN Expression
Fold Change
250
200
150
100
50
0
DPSC 1
DPSC 2
DPSC 3

haematopoietic associated markers (**Table 3.1**). All selected cell clones lacked the expression of monocyte/macrophage marker CD14, haematopoietic stem/progenitor cell marker CD34, and the leukocyte marker CD45, whilst expressing higher levels of mesenchymal stem cell associated markers CD44, CD73, CD90, CD105, CD106, CD146 and CD166. Furthermore, we determined the expression of antigens identified by STRO-1, STRO-3 and STRO-4, antibodies that identify clonogenic MSCs of high proliferation and multi-differentiation potential. Expectedly, all of the assessed MSC populations demonstrated high reactivity to STRO-4, however, selected clones exhibited variable levels of reactivity to STRO-1 and STRO-3 (**Figures 3.9 – 3.14**).

3.2. DISCUSSION

The present study focused on characterising the differentiation and proliferation potentials of clonally expanded cell lines isolated from three different tissues, bone marrow, dental pulp and periodontal ligament. STRO-1 was used in prospective immunoselection of cell populations obtained from these tissues, as this antibody identifies MSCs of high clonogenic capacity and multi-differentiation potential [12, 54, 58]. In addition to a number of studies that focused on the characterisation of STRO-1^+ MSC populations, more recently, Psaltis and colleagues performed a comparison of biological and functional properties of STRO-1 selected and plastic-adherence selected MSC populations from human bone marrow [251]. Their findings illustrated that enrichment of MSCs based on STRO-1 expression resulted in a population that contained a high proportion of immature cells with an enhanced clonogenic efficiency, growth potential and enhanced functional properties [251].

In accord with previous findings, functional studies performed in these experiments clearly illustrated the heterogeneity in the proliferation potentials of clonal MSC-like cells residing in the bone marrow, dental pulp and periodontal ligament tissues [12, 41, 53, 110]. Our data suggest that only a small fraction of BMSC exhibit high proliferative potential capable of undergoing more than 20 population doublings. In contrast, approximately 2/3 of the DPSCs and PDLSCs exhibited an extensive proliferation capacity and an ability to exceed 20 population doublings. The extent of difference in growth potential within different MSC population may partially be accounted for by the limitations present in current isolation procedures and *in vitro* culture conditions used for

Table 3.1 Cell Surface Expression Profile of Mesenchymal and Non-Mesenchymal Precursor Markers of BMSC, DPSC and PDLSC Clones of High Proliferation and Multi-Differentiation Potential (n=3).

	BMSC		DPSC		PDLSC	
	Median (%)	Range (%)	Median (%)	Range (%)	Median (%)	Range (%)
CD14	0.03	0.2-1.8	0.5	0.4-0.8	0.0	0.0-0.2
CD34	0.2	0.1-0.6	0.3	0.0-0.5	0.8	0.1-0.8
CD45	1.0	0.5-2.5	0.4	0.3-1.8	0.4	0.2-1.5
CD44	95.8	94.8-97.3	100	93.0-100	99.8	99.8-100
CD73	91.7	82.2-95.5	100	100	99.9	99.8-100
CD90	86.6	63.1-92.5	67.8	12.3-80.8	96.8	96.5-98.4
CD105	85.0	77.8-93.5	100	100	99.9	99.8-100
CD106	9.9	5.8-31.1	96.6	1.2-97.9	99.6	80.8-99.8
CD146	52.1	46.6-69.0	99.9	98.9-100	53.2	34.6-99.9
CD166	84.4	73.1-95.7	99.8	99.7-100	99.9	99.7-100
STRO-1	5.8	3.5-19.0	8.3	2.6-18.9	29.3	28.6-47.5
STRO-3	2.0	1.3-7.8	26.3	7.2-100	40.7	32.4-100
STRO-4	73.1	59.8-81.8	99.9	99.6-100	100	100

Figure 3.9 Expression of MSC Surface Markers in Long Lived Multi-Potential BMSC Clones

Flow-cytometric analysis was employed to asses cell surface expression of MSC markers in long lived, multi-potential clonal populations of BMSCs. The data is presented as the median value of percentage of cells positive for the selected markers for the three clones tested. Solid, red histograms represent the expression of test markers and open histograms show the expression of negative isotype controls.

Figure 3.9

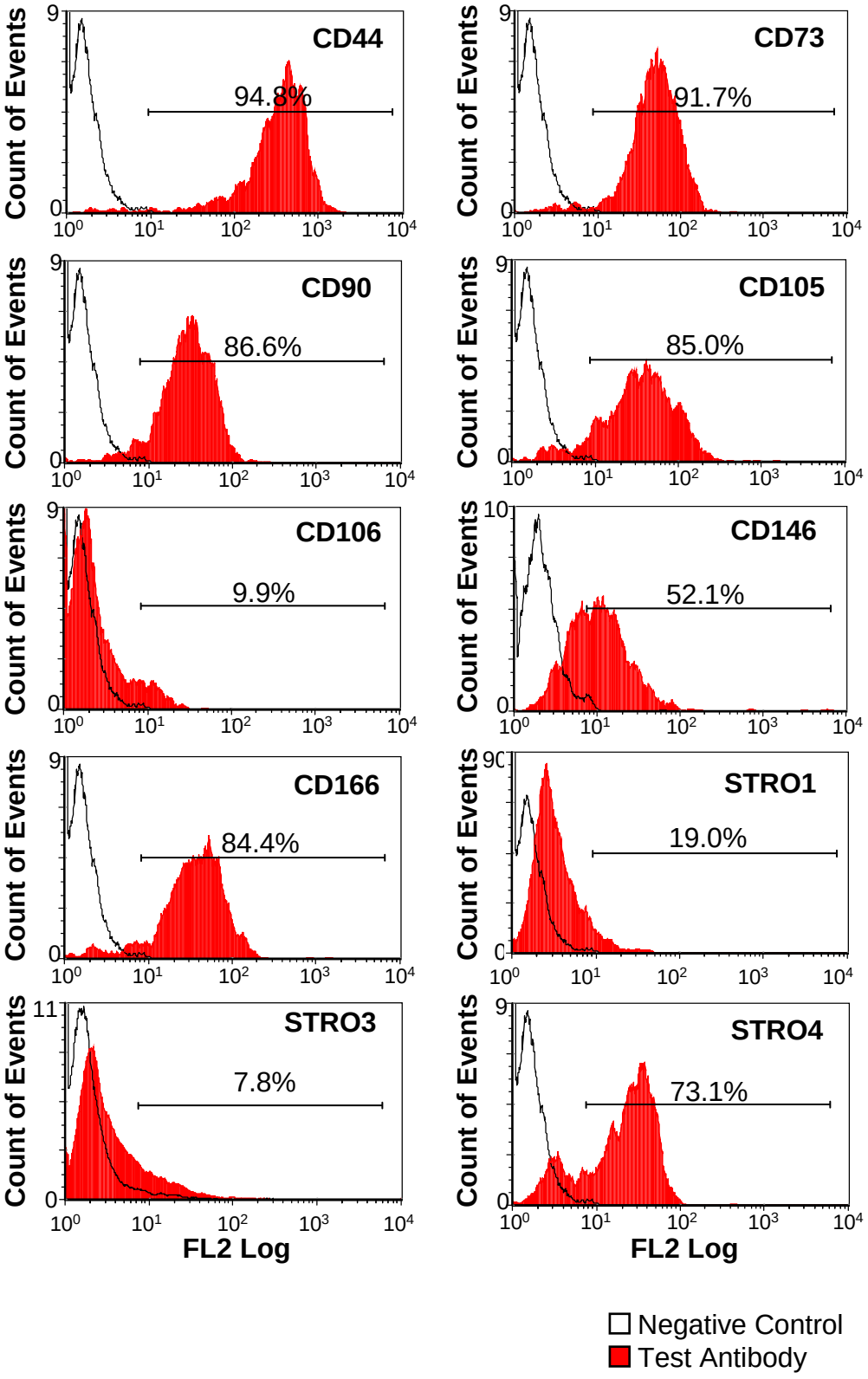
CD44
94.8%
CD73
91.7%
CD90
86.6%
CD105
85.0%
CD106
9.9%
CD146
52.1%
CD166
84.4%
STRO1
19.0%
STRO3
7.8%
STRO4
73.1%
Count of Events
FL2 Log
Negative Control
Test Antibody

Figure 3.10 Expression of Non-MSC Surface Markers in Long Lived Multi-Potential BMSC Clones

Flow-cytometric analysis was employed to asses cell surface expression of non-MSC markers in long lived, multi-potential clonal populations of BMSCs. The data is presented as the median value of percentage of cells positive for the selected markers for the three clones tested. Solid, red histograms represent the expression of test markers and open histograms show the expression of negative isotype controls.

Figure 3.10

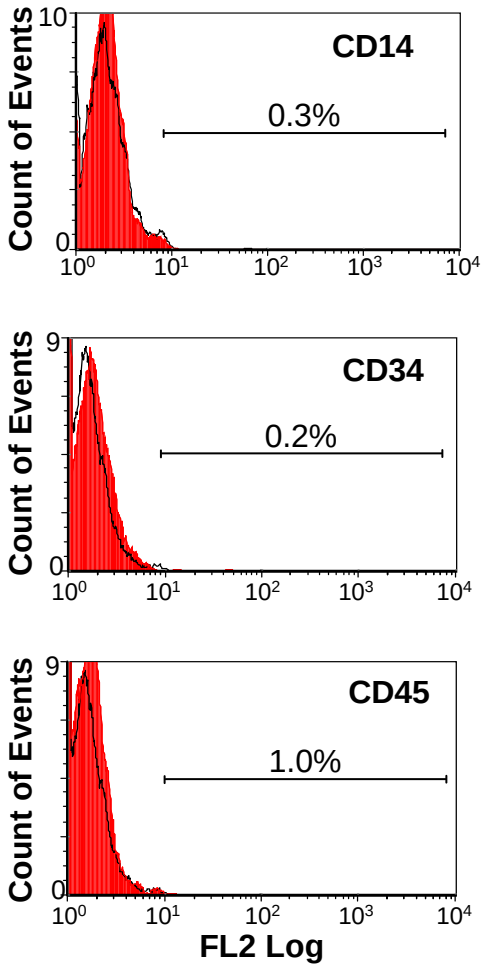

Negative Control
Test Antibody

Figure 3.11 Expression of MSC Surface Markers in Long Lived, Multi-Potential DPSC Clones

Flow-cytometric analysis was employed to asses cell surface expression of MSC markers in long lived, multi-potential clonal populations of DPSCs. The data is presented as the median value of percentage of cells positive for the selected markers for the three clones tested. Solid, red histograms represent the expression of test markers and open histograms show the expression of negative isotype controls.

Figure 3.11

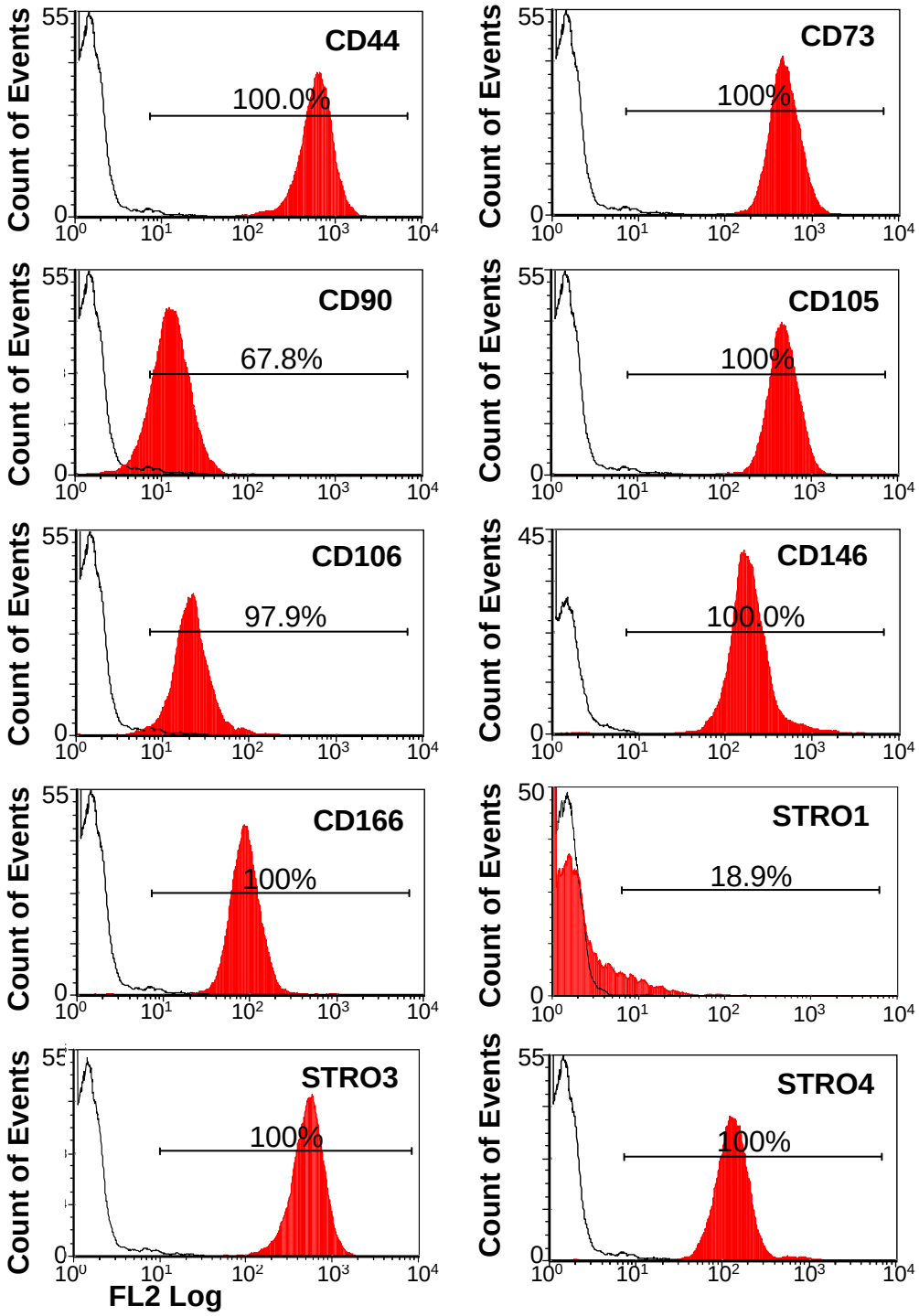
CD44
100.0%
CD73
100%
CD90
67.8%
CD105
100%
CD106
97.9%
CD146
100.0%
CD166
100%
STRO1
18.9%
STRO3
100%
STRO4
100%
Count of Events
FL2 Log
Negative Control
Test Antibody

Figure 3.12 Expression of Non-MSC Surface Markers in Long Lived Multi-Potential DPSC Clones

Flow-cytometric analysis was employed to asses cell surface expression of non-MSC markers in long lived, multi-potential clonal populations of DPSCs. The data is presented as the median value of percentage of cells positive for the selected markers for the three clones tested. Solid, red histograms represent the expression of test markers and open histograms show the expression of negative isotype controls.

Figure 3.12

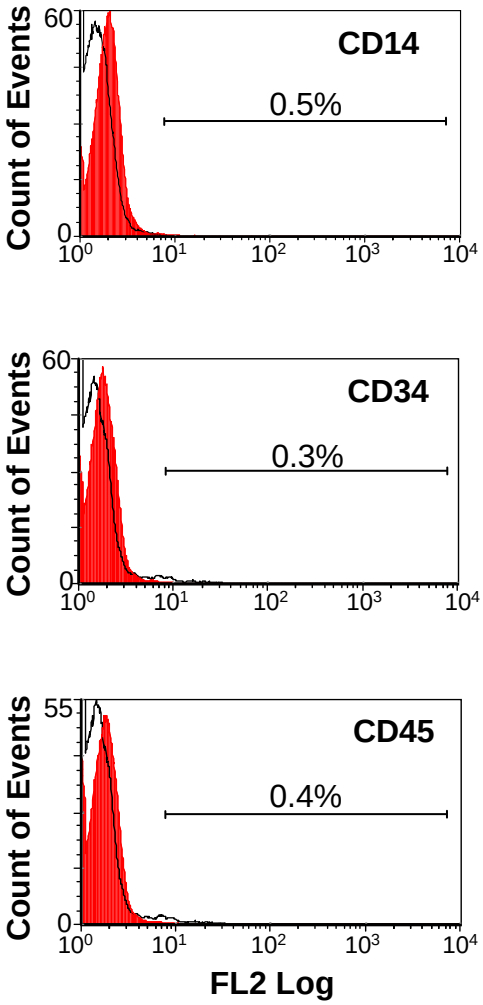
CD14
0.5%
CD34
0.3%
CD45
0.4%
Count of Events
60
55
0
10^0
10^1
10^2
10^3
10^4
FL2 Log
Negative Control
Test Antibody

Figure 3.13 Expression of MSC Surface Markers in Long Lived, Multi-Potential PDLSC Clones

Flow-cytometric analysis was employed to asses cell surface expression of MSC markers in long lived, multi-potential clonal populations of PDLSCs. The data is presented as the median value of percentage of cells positive for the selected markers for the three clones tested. Solid, red histograms represent the expression of test markers and open histograms show the expression of negative isotype controls.

Figure 3.13

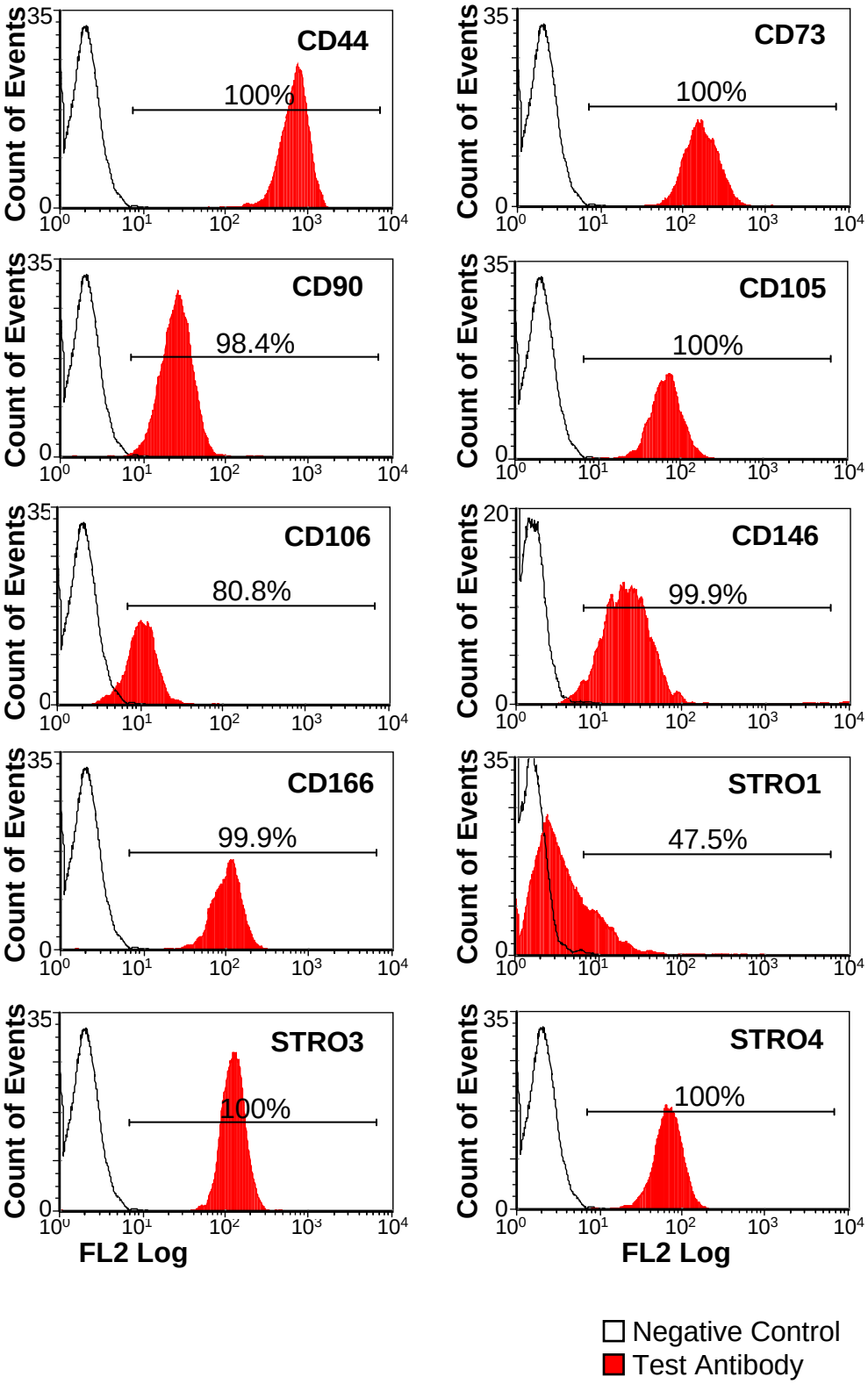
CD44
100%
CD73
100%
CD90
98.4%
CD105
100%
CD106
80.8%
CD146
99.9%
CD166
99.9%
STRO1
47.5%
STRO3
100%
STRO4
100%
Count of Events
FL2 Log
Negative Control
Test Antibody

Figure 3.14 Expression of Non-MSC Surface Markers in Long Lived Multi-Potential PDLSC Clones

Flow-cytometric analysis was employed to asses cell surface expression of non-MSC markers in long lived, multi-potential clonal populations of PDLSCs. The data is presented as the median value of percentage of cells positive for the selected markers for the three clones tested. Solid, red histograms represent the expression of test markers and open histograms show the expression of negative isotype controls.

Figure 3.14

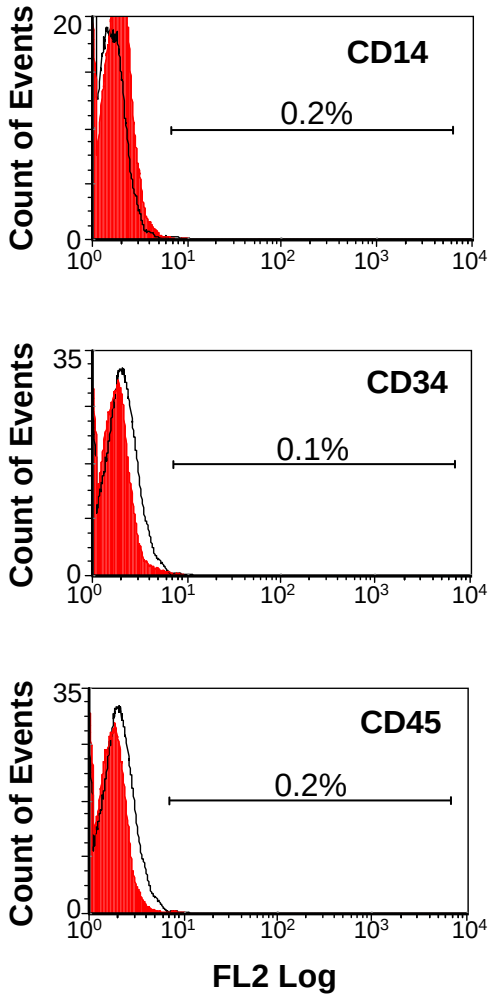

Negative Control
Test Antibody

maintenance and expansion of MSC. These conditions could selectively favour expansion and support growth of specific MSC populations. Furthermore, the differences observed in growth potential across the three MSC-like populations may be associated with their different developmental origins. The determining factors that arise during the development of mesodermally derived BMSCs and the dental MSCs, derived from the ectomesenchyme [252, 253], may hold a vital role in commitment and establishment of cellular proliferation potential.

In the past, biological and functional comparisons of MSCs derived from different tissues have been documented. Sakaguchi and colleagues performed a comparison of MSCs isolated from the bone marrow, synovium, periosteum, skeletal muscle and adipose tissue [254]. Their studies initially indicated that colony forming efficiency was ~100 fold greater in MSCs derived from all other tissues in comparison to BMSCs. On the other hand, assessment of proliferation potentials, illustrated that BMSCs and periosteum and synovium derived MSC retained their growth capacity at later passages in comparison to MSCs isolated from adipose and muscle tissues [254]. As expected, they showed that the BMSCs and adipose derived MSCs exhibited the greatest adipogenic differentiation capacity, whilst BMSCs and cells derived from the synovium and periosteum demonstrated a superior ability to undergo osteogenic differentiation [254]. In other studies, comparisons of MSC populations derived from the bone marrow, adipose tissue, placenta, thymus and skin concluded that, although the cells presented with comparable levels of gene expression for various MSC associated markers, morphological differences and gene expression variability were noted across the different tissues of origin [255]. In addition they found that adipose tissue contained a higher number of clonogenic MSC-like cells initially present in culture in comparison to other tissues [255]. Comparative characterisation of BMSCs and MSC-like cells derived from the umbilical cord and skin has been conducted to determine the differentiation capacities of these cells [256]. The BMSCs exhibited tri-differentiation potential in terms of adipogenic, osteogenic and chondrogenic lineages, the majority of umbilical cord MSC-like cells exhibited adipogenic and chondrogenic potential and skin derived MSC were most limited in their potential and exhibited the ability to differentiate only into adipocytes [256]. Similarly in the present study, we have shown that clonal populations of BMSC, PDLSC and DPSC exhibit a differential capacity for osteogenic, chondrogenic and adipogenic differentiation. An assessment of transcriptional and proteomic expression patterns identified specific

differences in profiles of BMSCs and MSCs derived from adipose tissue [257]. Although both cell populations are known to differentiate into osteogenic, adipogenic and chondrogenic lineages [258, 259], quantitative analysis elucidated that BMSCs were more prone toward osteogenic and chondrogenic differentiation than adipose-derived MSCs [257]. The above findings suggest that the tissue of origin is a vital factor related to determination of cell lineage commitment, in accord with the findings of the present study. Collectively these studies illustrate that whilst MSC-like cells reside in numerous tissues and meet the minimal MSC defining criteria, these populations exhibit both subtle and pronounced differences present within the boundaries of the MSC paradigm. In characterisation studies such as ours, these differences may be manifested through cellular proliferation and differentiation potentials.

Due to the limitation in cell numbers of low growing clones across BMSC, DPSC and PDLSC populations, further analysis of their multi-lineage differentiation potential was restricted. On the other hand, we were able to demonstrate that essentially all of the BMSC clonal lines that showed evidence of high growth potential exhibited a capacity to differentiate into cells of osteogenic, chondrogenic and adipogenic lineages. This frequency of multi-potential BMSC clones was higher than that observed for DPSCs and PDLSCs, where only 50% of the highly proliferative DPSC and PDLSC clones also exhibited multi-potential differentiation potential. These results support the earlier findings of Muraglia and colleagues who proposed that BMSC are predisposed to osteogenic differentiation and that adipogenic lineage is the first to diverge from the differentiation pathway, whilst osteogenic and chondrogenic pathways proceed together to separate at a later stage [238]. Moreover, the findings of the present study further confirm this pattern of lineage commitment within dental pulp and periodontal ligament derived MSC. Further characterisation of the developmental potential of BMSCs, DPSCs and PDLSCs would have given more insight into their functional capabilities and, based on the results, would have further subdivided these clonal populations. The ability of MSCs to undergo myogenic and neurogenic differentiation has been previously documented [97, 145, 260, 261] and whilst it would have been insightful to analyse the potential of BMSCs, DPSCs and PDLSCs in relation to these lineages, we were unable to perform the assays due to a limitation in cell number of our populations.

The results obtained from cell surface expression profiling of highly proliferative clones, which exhibited multi-differentiation potential, were consistent with the widely accepted criteria of specific surface antigen expression pattern, characteristic to MSCs [38]. Our findings demonstrated that all of the MSC populations across the three tissues lack the expression of non mesenchymal stem cell markers CD14, CD34 and CD45. On the other hand, these clones exhibited high levels of expression of markers associated with MSCs, including CD44, CD73, CD90, CD105, CD106, CD146 and CD166. In accordance with those findings, the expression of antigens recognised by STRO-1, STRO-3 and STRO-4 was high for the majority of MSC clones, with the exception of variable expression of STRO-1 observed for the BMSC and DPSC populations. Moreover, reduced levels of expression of the antigen recognised by STRO-3 were observed in BMSC populations.

Previous studies have suggested that cell surface expression profiles of MSC may be altered during *ex vivo* expansion and manipulation. Relevant to our findings, progressive loss of expression during cell culture has been recognised for the antigen reactive to STRO-1 [262, 263]. Initial identification of STRO-1, demonstrated that this antibody reacts with an as yet unidentified antigen present on a fraction of BMMNC and selects a population of high proliferative capacity and multi-lineage differentiation potential [54, 55]. It was further recognised that cells present within the STRO-1^{+} population contained all detectable clonogenic CFU-F [54, 55]. STRO-3 recognises a unique epitope present on the extracellular domain of tissue non specific alkaline phosphatise (TNSALP) [75]. This antibody identifies a subpopulation of BMSCs of high proliferative capacity and multi-lineage differentiation potential. Furthermore, STRO-3 was found to bind to BMSCs strongly reactive to STRO-1, and it was indicated that STRO-1^{bright}/STRO-3^{+} selection of BMMNC led to greater than 410- fold enrichment in CFU-F in comparison to unselected BMMNC population [75]. Variable reactivity to STRO-1 has been documented in MSC populations derived from the bone marrow [176, 264] as well as different tissues [254, 265, 266]. These studies support the suggestion that the expression of the antigen identified by STRO-1 is highly sensitive to *ex vivo* culture conditions and susceptible to developmental progression of MSCs. It has been demonstrated that STRO-1 antigen is present on immature precursors of cells of the osteoblast lineage and is lost during differentiation toward functional osteoblasts [262, 263]. This previously recognised feature of MSCs may have accounted for variations of STRO-1 and STRO-3 reactivity in populations assessed in this study.

Data obtained from functional analyses performed on different clonal populations isolated from the bone marrow, dental pulp and periodontal ligament confirm the general hypothesis that *ex vivo* expanded CFU-F from different tissues contain a heterogeneous mix of cells with varying differentiation and proliferation potentials and supports previous assumptions of the hierarchical nature of stromal populations from different tissues [267]. This study provides the basis for further characterisation of identified clonal populations in **Chapters 4 and 5**.